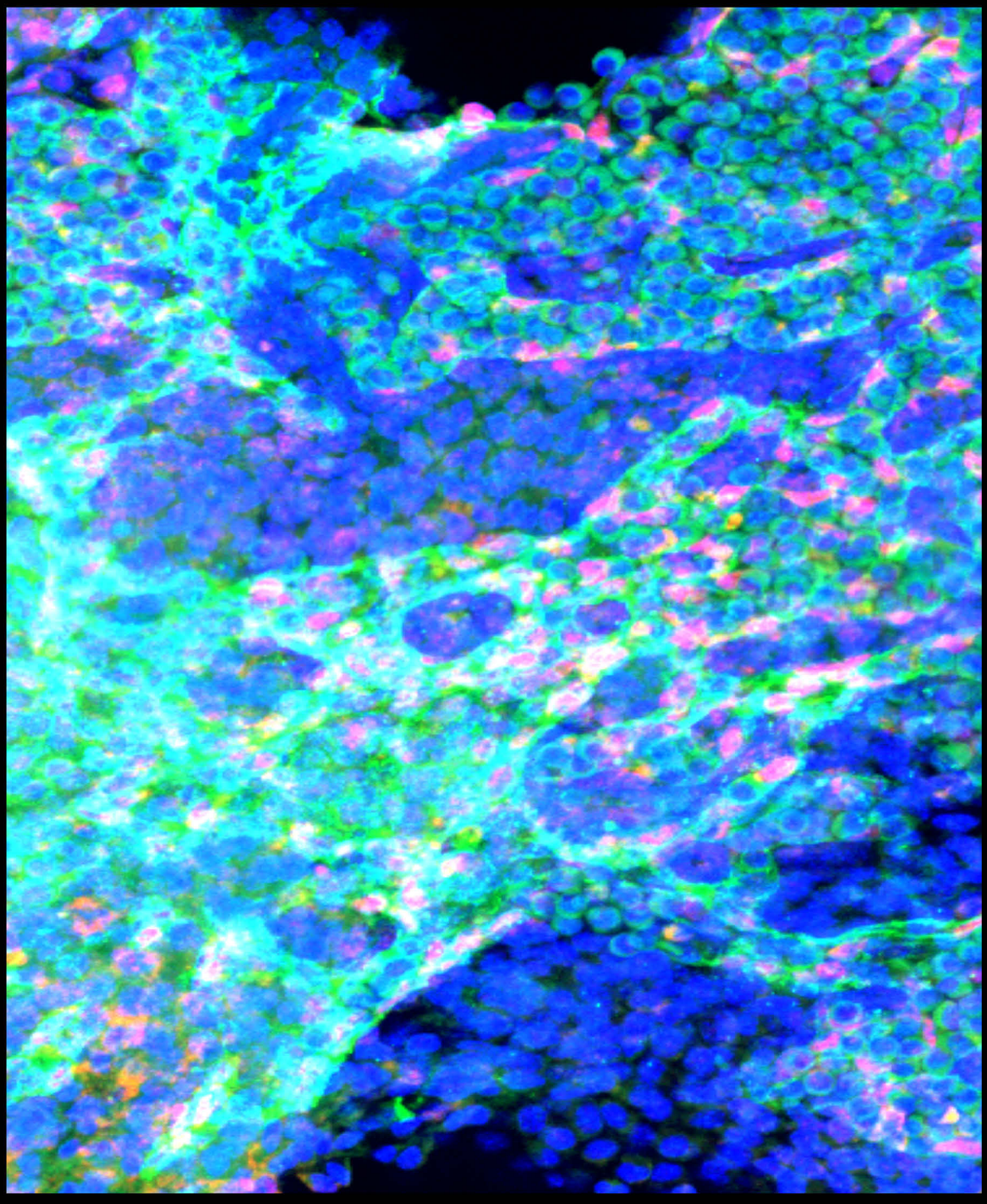
Universidad Autónoma de Madrid
Programa de doctorado en Biociencias Moleculares

# Role of Notch signaling in coronary vessel angiogenesis and remodelling



Stanislao Igor Travisano

Madrid, 2018

Programa de Doctorado en Biociencias Moleculares
Departamento de Biología Molecular
Facultad de Ciencias

Universidad Autónoma de Madrid

# Role of Notch signaling in coronary vessel angiogenesis and remodelling

Doctoral thesis

Stanislao Igor Travisano
Graduated in Biology
Madrid 2018

Tutor: Susana Cadenas
Directores: José Luis de la Pompa Mínguez y Donal MacGrogan
Centro Nacional de Investigaciones Cardiovasculares Carlos III (CNIC)

Alla mia famiglia

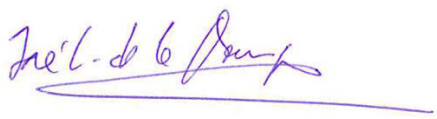
This work was performed in Dr. José Luis de la Pompa Mínguez´s laboratory in the Cardiovascular Developmental Biology and Repair Department at the National Center for Cardiovascular Research (CNIC-ISCIII) in Madrid.

Stanislao Igor Travisano was supported by a PhD fellowship from the Spanish Ministry of Economy and Competitiveness SAF2010-17555 and CB16/11/00399 (CIBER CV).

We hereby certify that Stanislao Igor Travisano has carried out the experimental work leading to his PhD thesis entitled "*Role of Notch signaling in coronary vessel angiogenesis and remodelling*" under our supervision at the Centro Nacional de Investigaciones Cardiovasculares-CNIC in Madrid.

We also declare that the work presented is novel and of great importance in the field, and of sufficient quality to merit to be presented in order to obtain a PhD degree by the Universidad Autónoma de Madrid.

José Luis de la Pompa Mínguez



Donal MacGrogan



## Acknowledgment

I thank all who in one way or another contributed to the completion of this thesis. I would like to express my sincere gratitude to everyone who has supported me and has been always by my side these past years.

A special thanks to the CNIC technical units and to the members of the laboratory.

Epistola *de modo studendi*

Quia qaesivisti a me qualiter te studere oporteat in thesauro scientiae aquirendo, tale a me tibi super hoc traditur consilium:
ut per rivulos, non statim in mare, eligas introire, quia per faciliora ad difficiliora oportet devenire.
Haec est ergo monitio mea et instructio tua.
Tardiloquum te esse jubeo et tarde ad locutorium accedentem.
Conscientiae puritatem amplectere.
Orationi vacare non desinas.
Cellam frequenter diligas.
Omnibus te amabilem exibe.
Nihil quaere penitus de factis aliorum.
Nemini te multum familiarem ostendas, quia nimia familiaritas parit contemptum et subtractionis a studio materiam subministrat.
De verbis et factis saecularium nullatenus te intromittas.
Discursus super omnia fugias.
Sanctorum et bonorum imitari vestigia non omittas.
Non respicias a quo audias, sed quidquid boni dicatur, memoriae recommenda.
Et quidquid poteris in armariolo mentis reponere satage.
Altiora te ne quaesieris.
Ista sequens vestigia, frondes et fructus in vinea Domini quandiu vitam habueris, proferes et produces.
Haec si sectatus fueris, ad id pertingere poteris, quod affectas. Vale.

# Summary/ Resumen

## Summary/Resumen


Summary

Coronary vessels supply the myocardium with nutrients and oxygen and are crucial for heart development and function. Coronary development defects result in coronary disease, a major cause of morbidity and mortality worldwide. The Notch signaling pathway is a highly conserved pathway, crucial for the regulation of cell specification and proliferation in specific tissue and organs. Specifically, the Notch pathway regulates the processes leading to the formation of the ventricular chambers; trabeculation, coronary vessel formation and trabecular compaction.

To gain insight into coronary development, the roles of Notch ligands Jag1 and Dll4 were examined as well as the Notch-ligand modulator Mfng and a downstream target, Efnb2. By using loss function murine models of endocardial *Jag1*, *Dll4* and *Efnb2* and endothelial gain of function of *Mfng* and *Dll4* in combination with *ex vivo* ventricular explant assays, we find that Notch is required at different stages of coronary development. Conditional inactivation of Jag1 during the early phase of coronary development results in the arrest of sinus venosus (SV) sprouting whereas loss of Dll4 results in excessive sprouting. Later induced loss of Jag1 or Dll4 or gain of Dll4 or MFng leads to defective arterial specification, vascular malformations and aberrant coronary arterial patterning. Loss of Ephrinb2 phenocopies loss Jag1, and Ephrinb2 can rescue defective angiogenesis of Jag1- and Dll4-inactivated ventricular explants, identifying Ephrinb2 as a target of both ligands during coronary artery formation. Thus, Jag1 and Dll4/MFng have early opposing roles and late cooperative roles in coronary formation and the downstream direct target Ephrinb2 in endothelium and endocardium is a key effector molecule for the coronary arterial morphogenesis.

Comparative transcriptome profiling of the different loss and gain of function mutant hearts revealed hypoxic, oxidative stress and cell death pathways and the activation of immune-inflammatory responses suggestive of ischaemic cell death. Thus perturbation of endocardial/endothelial Notch signaling severely disrupts coronary development and consequently myocardium proliferation and compaction, resulting in embryonic lethality. This implies that development of the coronary vessels and growth and maturation of the ventricles are two interlinked Notch-dependent processes.

## Resumen

Los vasos coronarios son cruciales para el desarrollo y la función del corazón. Defectos en el desarrollo de estos vasos resultan en enfermedades coronarias, siendo una importante causa de mortalidad en todo el mundo. La vía de señalización de Notch es una vía altamente conservada basada en una cascada proteolítica que produce la liberación de su dominio intracelular, que se transloca al núcleo y activa la transcripción de genes diana, siendo una vía clave en la regulación de la diferenciación y la proliferación celular en ciertos tejidos y órganos. Además, la vía de Notch regula los procesos implicados en el desarrollo de las cámaras ventriculares: la trabeculación, la formación de vasos coronarios y la compactación trabecular.

Para estudiar el desarrollo coronario, se examinaron las funciones de los ligandos de Notch, Jag1 y Dll4, así como del modulador de la activación de Notch mediada por los ligandos, MFng, y de la diana directa, Ephrinb2. En este trabajo, mediante el uso de modelos murinos de pérdida de función específica de endocardio de Jag1, Dll4 y Efnb2 y ganancia de función de Mfng y Dll4, junto con ensayos de explantes ventriculares *ex vivo*, se observó un nuevo mecanismo mediante el que la activación de Notch1 controla el desarrollo de vasos coronarios. La señalización a Notch1 a través de Jag1 y Dll4 en el seno venoso embrionario es crucial para coordinar la angiogénesis y las conexiones arteriovenosas que contribuyen a suministrar nutrientes y oxígeno al miocardio compacto. Fallos en este proceso conducen a malformaciónes arteriovenosas (AVM) y de los vasos coronarios, a una alterada diferenciación arterial y a la activación de vías de hipoxia, estrés oxidativo y muerte celular.

Los resultados conseguidos sugieren que Jag1 y Dll4/MFng tienen funciones opuestas pero complementarias en el desarrollo coronario y que la diana directa, Ephrinb2, juega un papel clave en el endotelio y el endocardio para la remodelación angiogénica y postangiogénica de los vasos. Un análisis comparativo de expresión génica mediante Rnaseq sugirió la existencia de una respuesta inmune mediada por interferones tipo I y tipo II, junto con muerte celular isquémica, lo cual sugiere que el desarrollo de unos vasos coronarios funcionales y la maduración de los ventrículos son dos procesos interconectados y dependientes de Notch. La alteración de la vía de señalización de Notch altera gravemente el desarrollo coronario y, en consecuencia, la proliferación y compactación del miocardio.

# Index of contents

Pag.


Acknowledgment 7

**Summary** 9

Index 13

Abbreviations 17

**Introduction** 19

**1**. Brief overview of heart development 21

**2**. Ventricular trabeculation 22

**3.1** Notch Pathway 24

**3.2** Ephrin-Eph signaling 27

**4.1** Coronary development 27

**4.2** Coronary Artery Anomalies 28

**5.** Origin of the coronary endothelium:

**5.1** ST/Proepicardium 31

**5.2** Sinus Venosus endocardium 32

**5.3** Chamber endocardium 33

**6.** Angiogenesis and Vasculogenesis 34

**7.** Role of Notch in ECs 35

**Objectives** 37

**Methods** 41

Mouse strains and genotyping 43

4-hydroxy-tamoxifen (4-OHT) induction 44

Harry´s Haematoxilin/Eosin staining and LacZ staining 45

In situ Hybridization 45

N1ICD (V1744) 45

RNA-Seq 47

Ultrasound 48

Resection Model 49

Staining of Whole-Mount Tissues 49

Mounting Heart on Slide **50**
Immunohistochemistry, EdU incorporation and detection **50**
Quantification of immunochemistry **50**
Quantification of compact myocardium thickness **50**
Mouse ventricular explant culture **51**
IF on explants **51**
Lentiviral production **52**
Statistics **52**

**Results** **53**

Jag1, Dll4, and MFng are co-expressed in SV and sub-epicardial vessels **56**
Most ventricular free-wall coronary vessels derive from Nfatc1$^{+}$ progenitors **56**

Endocardial *Jag1* inactivation arrests SV sprouting, whereas *Dll4* deletion causes excessive SV sprouting **60**

Jag1 and Dll4 are regulating proliferation of the endothelium from the SV while myocardial patterning is maintained **62**

Arrested myocardial growth in endocardial *Jag1* or *Dll4* mutants is due to a global hypoxic and metabolic stress response **62**

Defective coronary remodelling and maturation in endothelial *Jag1* and *Dll4* mutants **67**

Forced endothelial *Dll4* expression disrupts coronary vascular remodelling **71**

Forced endothelial *MFng* expression phenocopies *Dll4* gain-of-function in coronaries **73**

*Efnb2* is required for coronary arteriogenesis and vessel branching **76**
Notch mutants display arterio-venous malformations **80**

Comparative transcriptome profiling reveals a common hypoxia-dependent gene signature in endocardial/endothelial Notch mutants **82**

*Efnb2* is required for coronary arterial vessel branching **85**

Myocardial *Mib1* inactivation results in aberrant coronary arterial patterning **85**

**Discussion** **89**

**Conclusions** **101**

**Bibliography** **105**

## Index of figures and tables

### Figures

Figure 1. Heart development 22
Figure 2.1. Notch Pathway 24
Figure 2.2. Structure of Notch receptors and ligands 25
Figure 3. Resection Model 41
Figure 4. Mouse ventricular explant culture 44
Figure 5. Jag1, Dll4 and Manic Fringe expression in the SV of control hearts at E11.5 55
Figure 6. Jag1, Dll4 and Manic Fringe expression between E13.5-E17.5 56
Figure 7. Nfatc1$^{+}$ progenitors give rise to the majority of coronary vessels 58
Figure 8. Nfatc1 include early arterial progenitors 59
Figure 9. Endocardial *Jag1* or *Dll4* inactivation disrupts coronary plexus formation 61
Figure 10. Endocardial *Jag1* or *Dll4* deletion disrupts endothelial proliferation 63
Figure 11. Comparative gene expression profiling 65
Figure 12. Gene profiling analysis of E12.5 hearts 67
Figure 13. Late endothelial *Jag1* or *Dll4* inactivation disrupt coronary plexus remodelling 69
Figure 14. Induced endothelial *Jag1* or *Dll4* deletion disrupts myocardial growth and arterial differentiation 70
Figure 15. Forced *Dll4* or *MFng* expression leads to early SV sprouting defects 72
Figure 16. Forced *MFng* and *Dll4* expression impair left coronary development 73
Figure 17. Forced endothelial *Dll4* or *MFng* expression disrupts coronary arteriovenous differentiation and remodelling 75
Figure 18. Endocardial *Efnb2* deletion causes thin myocardium and decreased compact myocardium (CM) proliferation 76
Figure 19. Endocardial *Efnb2* inactivation disrupts coronary artery differentiation and remodelling 78
Figure 20. Endocardial deletion of *Efnb2* causes arteriovenous fistulae and disrupts arterial endothelial integrity 79
Figure 21. Endocardial *Efnb2* deletion leads to VSD and arrhythmias but heart function is unaffected 80

Figure 22. Coronary vessels of Notch pathway and Notch effector mutants display vascular malformations 81
Figure 23. Comparative analysis of HALLMARK and KEGG gene sets 83
Figure 24. Efnb2 rescues disrupted arterial branching in endocardial *Jag1* and *Dll4* mutant explants 84
Figure 25. Myocardial inactivation of *Mib1* distrupta coronary artery differentiation and remodelling 87
Figure 26. Sequential antagonistic and complementary roles of Jag1 and Dll4 in coronary vessel development 98

**Tables**

Table 1. - Incidence of Coronary Anomalies and Patterns, as Observed in a Continuous Series of 1950 Angiograms 29
Table 2. - PCR primers and conditions for genotyping 44
Table 3. - List of primary antibody used for the IHC 46

**Supplementary** RNA-seq data**,** IPA, GSEA and Source data are provided in the digital format of the thesis.

# Abbreviations

**AV**: Arterovenous
**AVC**: Atrio Ventricular Canal
**AVM:** Artero Venous Malformation
**ALGS:** Alagille syndrome
**β-Gal:** beta-galactosidase
**CADASIL**: Cerebral Autosomal Dominant Arteriopathy with Subcortical Infarcts and Leukoencephalopathy
**CA**: Coronary Artery
**CAA**: Coronary Artery Anomalie
**CAVF**: Coronary Arterovenous Fistula
**CBF1**: Cp-binding factor 1
**CSL**: CBF1/Su(H)/Lag-1
**CV**: Coronary Vein
**DAPI**: "4',6-DiAmidino-2-PhenylIndole"
**Dll4:** Delta like 4
**DSL:** Delta/Serrate/Lin12 domain
**EdU:** 5-Ethynyl-2´-deoxyuridine
**EGF:** Epidermal Growth Factor
**EMT:** Ephitelial-to mesenchyme transition
**EPDC:** Epicardial Derived Cells
**FHF:** First heart field
**IHC:**Immunohistochemistry
**ISH:** *In Situ* Hybridization
**Ivs:** Interventricular septum
**Jag1:** Jagged1
**LCA:** Left Coronary Artery
**Lv:** Left ventricle
**Mam:** Mastermind
**MFng:** Manic-Fringe
**Mib1:** Mind bomb-1
**NECD:** Notch Extracellular Domain
**NICD:** Notch Intracellular Domain
**NLS:** Nuclear localization signal
**Nrg1:** Neuregulin-1
**OFT:** Outflow tract
**PEST:** Proline, glutamic acid, serine and treonined enriched-domain
**POFUT-1:** Protein O-Fucosyltransferase 1
**Ra:** Right atria
**RBPJ:** Recombination Signal-Binding Protein 1 for J-Kappa sequence (CBF1 in mammals)
**RCA:** Right Coronaty Artery
**Rv:** Right ventricle
**SHF:** Secondary Heart Field
**SMA:** Smooth muscle actin
**SV:** Sinus Venosus

**SV40:** Simian vacuolating virus
**TAD:** Transcriptional activation domain
**TOF:** Tetralogy of Fallot
**VEGF:** Vascular Endothelial Growth Factor
**VEGFR2:** Vascular Endothelial Growth Factor Receptor 2 (Flk-1)
**VSD:** Ventricular septal defect
**WT:** Wild type

# Introduction

## 1. Brief overview of heart development

In vertebrates, the heart is the first organ to form and function during development. The cardiac progenitors are specified during gastrulation, at embryonic day (E) E7.5 in mouse in response to signals from the embryonic endoderm. Once specified, the cardiac progenitors emerge from the primitive streak and move anterior and laterally into the lateral plate mesoderm (Moorman and Christoffels 2003; Buckingham *et al*., 2005). The cells in the cephalo-medial region will form a cardiac crescent and consist of two populations of cardiac progenitors cells, the first and second heart fields (respectively FHF and SHF) that include progenitors of the first cardiac tissues, the myocardium and endocardium (de la Pompa and Epstein, 2012; Moorman and Christoffels, 2003).

At E8.0 the cardiogenic progenitors form two bilateral tubes that, as development proceeds, fuse in the middle region of the embryo forming a single tube called primitive heart tube. The primitive heart consists of two layers, an inner endocardium and outer myocardium, separated by an extracellular matrix (ECM) termed cardiac jelly (de la Pompa and Epstein, 2012). The primitive tube then elongates and undergoes a rightward looping in which the initial anterior-posterior polarity transforms into a right-left, a process known as R-looping (Moorman and Christoffels, 2003).

At E9.5 the heart consists of four anatomically and molecularly distinct regions, the atrium, AVC, OFT and ventricle, covered by a single layer of epicardial cells (Moorman and Christoffels, 2003). After E9.5 the three principal cardiac cell types comprise the endocardium that forms the endothelial lining of the heart, the myocardium or cardiac muscle cells, and the epicardium that is the source of cardiac fibroblasts. The epicardium develops from a transient, extracardiac structure called the septum transversum/proepicardium (ST/PE), a group of coelomic progenitors located at the venous pole of the embryonic heart ( Pérez-Pomares and de la Pompa, 2011, Cano *et al*., 2016).

## 2. Ventricular trabeculation

During heart development, the myocardium differentiates into two layers, the outer compact zone and the inner trabeculated zone, both of them characterized by a distinct set of marker genes. During this process, the trabecular myocytes are intimately associated

with the developing endocardium, and cross-talk between these two tissues is essential for trabeculation (High and Epstein, 2008).

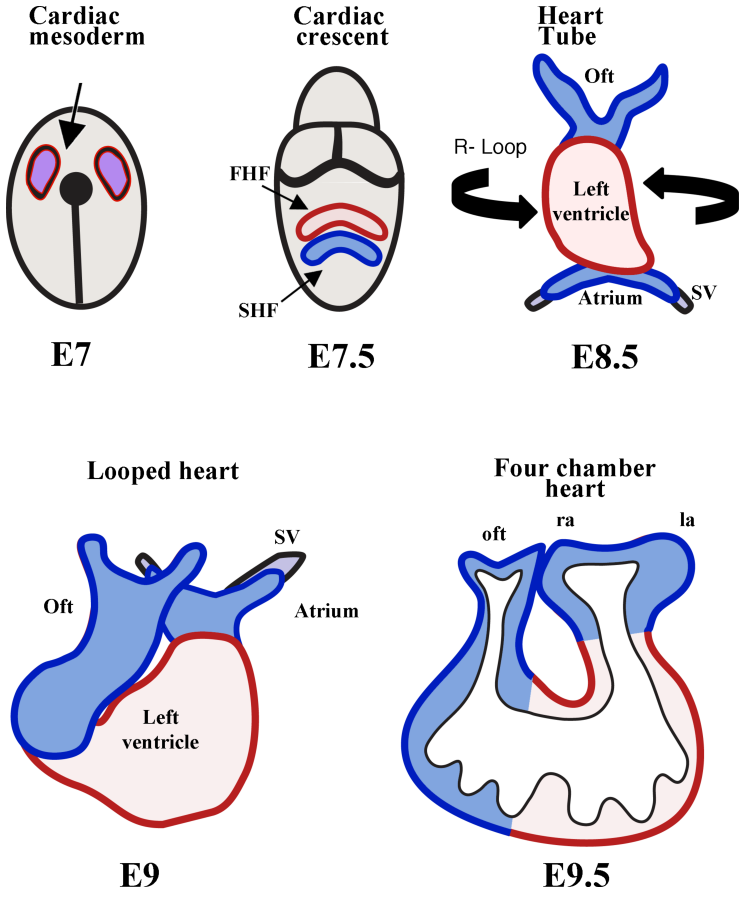



**Figure 1. Heart development**
Ventral view of the developing mouse embryo. At E7.0, cardiac mesodermal progenitors (red) migrate to the center of the embryo to form the cardiac crescent. At E7.5, two cardiac fields can be distinguished: the first heart field (red) and the second heart field (blue). At E8.0-E8.5, the cardiac tube consists of two layers: endocardium and myocardium. At this stage the heart undergoes a characteristic R-loop to form a looped heart. Transversal section depicting an E9.5 heart which consists of distinct regions: right atrium(ra), left atrium (la), ventricle and outflow tract (OFT) and a common ventricle.

At E9.5 trabecular formation has been shown to be dependent on EphrinB2 (*efnb2*) and its receptor EphB4 (Wang *et al*., 1998), neuregulin (Nrg1) and its receptors erythroblastic leukaemia viral oncogene homologues 2 and 4 ERBB2 and ERBB4 (Meyer and Birchmeier, 1995) and BMP10 (Chen *et al*., 2004). Apart from enhancing contractility, the trabeculations are also important in coordinating intra-ventricular conduction, and in compartmentalizing the blood in the heart prior to its septation (Sedmera *et al*., 2003). Between E10.5 and E14.5 dynamic morphological change are occurring in the remodelling of the OFT, which in turn generates a differential distribution of blood flow. The cylindrical OFT is transformed into the base of the

ascending aorta and pulmonary trunk (outlet of the right ventricle) concomitant with atrio-ventricular septation and aortic arch artery remodelling (Yashiro *et al*., 2007). Trabeculae increase the myocardial mass and facilitate oxygen and nutrient exchange in the heart muscle prior to coronary vascularization (Sedmera *et al*., 2000). High proliferative activity was evident in the outer layer (ventricular compact layer) compared to the inner region (trabeculae) between E9.5–14.5 (Sedmera *et al*., 2003). Moreover metabolic compartmentalization of the embryonic heart with an enhanced glycolytic program in the compact myocardium contrasting with a more oxidative metabolic signature in the trabeculae was described at this stage of chamber development (Menendez-Montes *et al*., 2016). As ventricular volume increases, trabeculae become compressed within the ventricular wall resulting in significant increase of proportion and thickness of the compact myocardium. In this process, termed compaction, the majority of trabeculae have become compacted by E14.5 in the mouse contributing to the formation of a thicker, compact ventricular wall (Sedmera *et al*., 2000).

### 3.1 The Notch pathway

Recently endocardial Notch signaling has been assiociated with several morphogenetic processes during cardiac development (de la Pompa and Epstein 2012 ; High and Epstein 2008). Conditional inactivation of myocardial Mib1 gene causes a phenotype strongly reminiscent of LVNC. Abrogation of Mib1-dependent signaling disrupts trabecular maturation and patterning, arresting the development of chamber myocardium (Luxán *et al*., 2013). Furthermore myocardial inactivation of Jag1 and Jag2 also causes LVNC, suggesting that both ligands are Mib1 substrates in the myocardium (D'Amato *et al*., 2016a).

Notch is an evolutionarily conserved signaling pathway that regulates cell-fate specification, differentiation, and patterning. In mammals there are four Notch receptor homologs (Notch1–Notch4) and five Notch ligands: Jagged (Jag1 and Jag2) and Delta-like (Dll1,Dll3 and Dll4). Notch signaling is initiated upon binding of the Notch ligand to the Notch receptor, leading to a cascade of events that ultimately culminates in the cleavage of the Notch intracellular domain (NICD) by γ-secretase. NICD then translocates to the nucleus, where it regulates transcription of target genes (Jarriault *et al*., 1995). The Notch extracellular domain (NECD) consists of up to 36 tandem EGF-like repeats, including those that interact directly with ligands (Wharton *et al*., 1985; Luca *et*

*al*., 2015) whereas the ECD of the Jagged family contains 16 EGF repeats and the Delta family contains 6–8, followed by a DSL (Delta/Serrate/Lin12) domain.

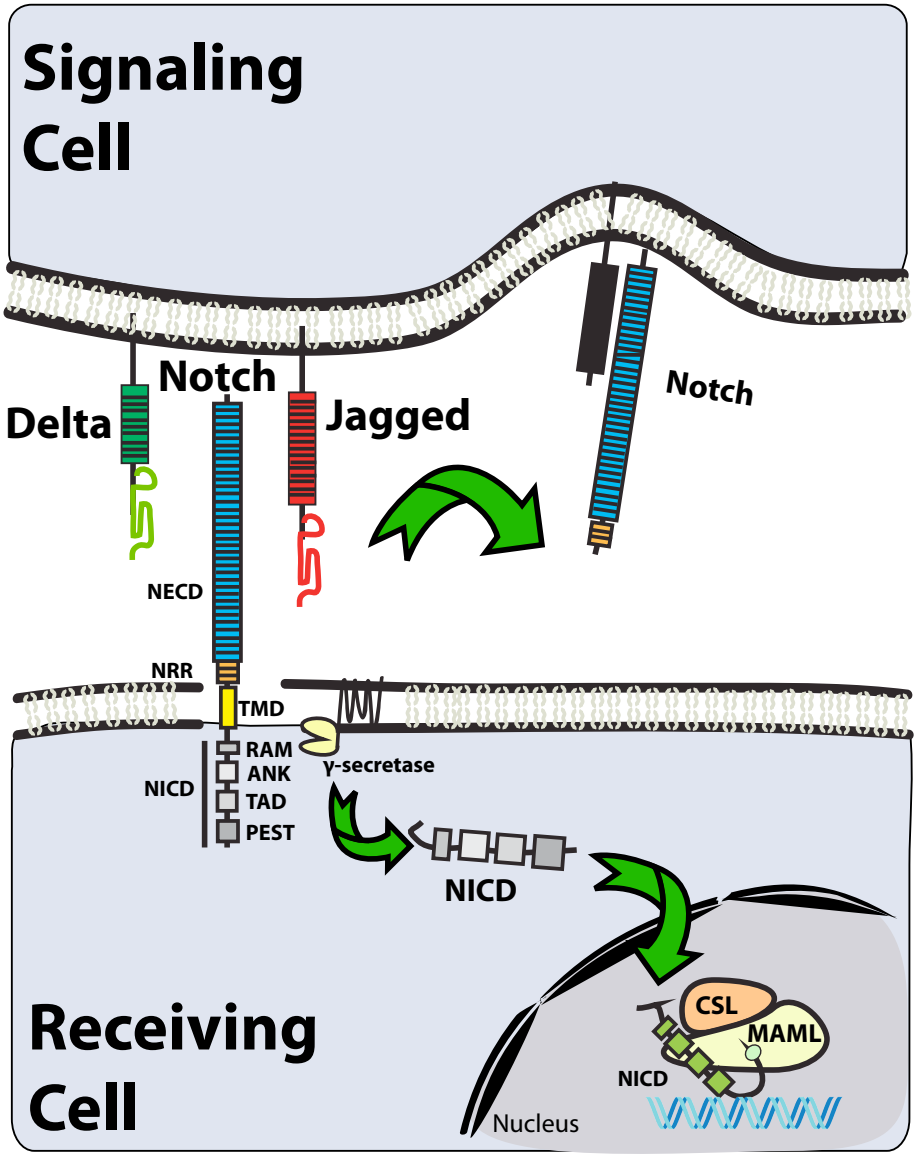



**Figure 2.2.** Notch signaling pathway.
In canonical Notch signaling, ligands bind to Notch receptors on the adjacent mammalian cell surface. Ligand binding exerts a force on the receptor which displaces the Lin12/Notch repeats (LNRs) in the NRR, exposing the site for cleavage by ADAM10. This cleavage renders the residual transmembrane Notch fragment as a substrate for proteolysis by the γ-secretase complex, to release the NICD. The Notch intracellular domain (NICD) can travel to the nucleus where interacts with the DNA-binding protein CBF1–Suppressor of Hairless–LAG1 (CSL) and the co-activator Mastermind (MAM) to promote gene transcription.

EGF-like repeats of the Notch receptor with appropriate consensus sequences are post-translationally modified with O-glycans, initiated by O-fucose, O-glucose, or O-

GlcNAc (Moloney *et al*., 2000A; Matsuura *et al*., 2008). Pofut1,a member of the glycosyltransferase O-Fuc family, is responsible for the transfer of O-fucose to EGF repeats with an O-fucose consensus sequence and is an essential component of Notch signaling in all contexts examined to date (Shi & Stanley 2003). Members of the Fringe family of enzymes extend the O-fucose modification by adding GlcNAc to further regulate Notch activity (Moloney *et al*., 2000B ; Brückner *et al*., 2000). Fringe modifications at EGF8 and EGF12 enhance Notch1 activation in response to DLL1 directly by increasing binding (Kakuda *et al*., 2017) but incorporation of GDP-fucose analogs intracellularly, substrates of Pofut1, at EGF8 is predicted to cause a steric hindrance with Delta-like, but not Jag ligands (Schneider *et al*., 2017).

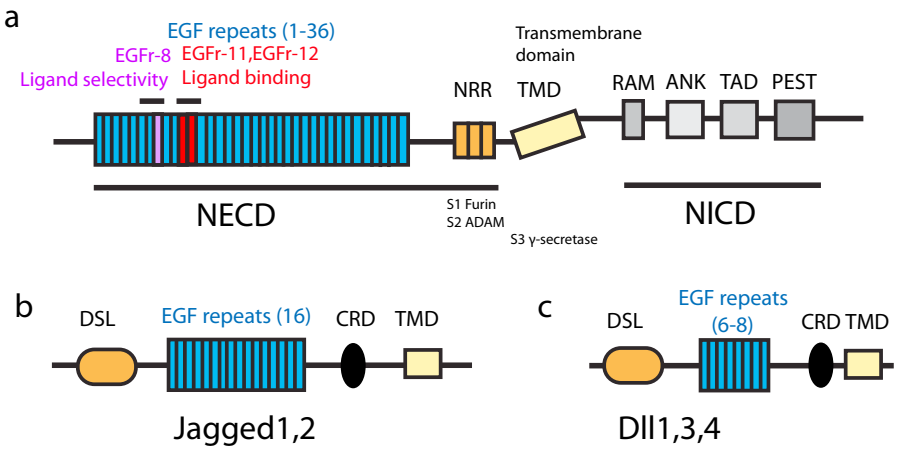



**Figure 2.2.** Structure of Notch receptors and ligands. In mammals there are four Notch receptors (Notch1-4). Notch proteins reside on the cell surface as heterodimers formed by a transmembrane domain (NECD) and an intracellular domain (NICD) (**a**). The NECD comprise of a variable number of EGF-like repeats. Repeats 11-12 (red squares) mediate the binding with ligands expressed in the neighbouring cell (trans-activation) and EGF-like repeat 8 modification is crucial for the ligand selectivity (purple square). The EGF-like domain is followed by negative regulatory region (NRR) that contains 3 Lin12/Notch repeats and a heterodimerization domain that flanks the S1 cleavage. Notch also contains a transmembrane domain (TMD), a RAM (RBPjκ association module) domain, nuclear localization sequences (NLSs), a seven ankyrin repeats (ANK) domain, and a transactivation domain (TAD) that habors conserved proline/glutamic acid/serine/threonine-rich motifs (PEST). Notch receptors interact with two types of ligands (**b**), Delta (Delta1, 3 and 4) and Serrate (Jagged1-2) that are also transmembrane proteins with a long extracellular domain composed of a variable number of EGF-like repeats depending on the ligand and a DSL domain, and a short intracellular domain related with their recycling. The Serrate family also presents a cysteine-enriched domain (CR).

Notch plays a critical role in tissue development and maintenance of many organs. Functional studies in vertebrates demonstrate that Notch is required for cardiovascular development (Kokubo *et al*., 2005; Niessen and Karsan, 2008; MacGrogan *et al*., 2010). Mutations of Notch ligands and receptors are implicated in

numerous congenital and acquired human diseases (Garg *et al*., 2006; Chabriat *et al*., 2009). Mutations in Notch signaling components have been implicated in several forms of congenital cardiovascular disease, including cardiac outflow tract defects (*JAG1*, *NOTCH2*), aortic valve disease (*NOTCH1*), cardiomyopathy (*PSEN1* and *PSEN2*), and cerebral arteriopathy (*NOTCH3*) (High and Epstein, 2008). Mutations identified in several studies, for the *Jagged1* gene *(JAG1),* have been implicated in ALGS (Oda, Elkahloun *et al*., 1997) and Tetralogy of Fallot (Krantz, Smith *et al*., 1999). Mutation for the *Notch3* gene are known to be responsible for CADASIL (Joutel, Corpechot *et al*., 1996), moreover mutations in *Notch1* have been found in family with Aortic Valve anomalies (Garg, Muth *et al*., 2005) and more recently others for *Mib1 gene* in family with LVNC (Luxán *et al*. 2013).

The Notch pathway is involved in multiple aspects of vascular development, including arterial-venous differentiation (Swift and Weinstein 2009), as well as lymphatic vessel development (Fatima *et al*., 2014). Notch stimulation instructively induces arterial characteristics in endothelial cells (EC), moreover forced expression of Notch intracellular domain (NICD, activated form of Notch) induced mRNA expression for a subset of arterial-specific markers such as ephrinB2, connexin40, and HERP1 only in EC (Iso *et al*., 2006). Embryos with endothelial cell-specific Notch1 gene deletion have vascular defects, and exhibit decreased diameter of the dorsal aortae and form arteriovenous malformations distinctly different from the Notch1 gain of function mutants. Moreover, embryos homozygous for mutations of the EphrinB/EphB pathway Ephrinb2 and Ephb4 exhibit vascular defects and arteriovenous malformations that phenocopy the Notch1 gain of function mutants (Krebs *et al*., 2010).

### 3.3 Ephrin/Eph signaling

Eph proteins belong to the superfamily of transmembrane Tyr kinase receptors. Eph proteins allow short-distance cell–cell communication by binding their membrane tethered ephrin ligands. This activates direct signaling pathways that affect the cellular cytoskeleton, leading primarily to cell repulsion but also in some instances to cell adhesion, cell proliferation, tissue boundary formation, cell migration and axon guidance, among others. Eph receptors have been classified into EphA or EphB subfamilies depending on whether they preferentially bind to membrane-anchored (glycophosphatidylinositol (GPI)-linked) or transmembrane ephrin ligands, referred to as

ephrin-As and ephrin-Bs, respectively (Kania, A. and Klein, R. 2016).

The development of blood vessels (angiogenesis) depends on a single ligand–receptor pair: ephrin-B2 and EphB4. Ephrin-B2 and its intracellular interactors, the clathrin-associated protein disabled 2 (Dab2) and the cell polarity regulator PAR-3, promote clathrin-dependent VEGF receptor internalization and thereby downstream signaling, inducing sprouting (Wang, Y. *et al*. 2010; Nakayama M. *et al*. 2013). The expression of ephrin-B2 in arterial territories and of EphB4 in venous territories may help to establish borders between these two compartments, and their absence in mice causes severe defects in blood vessel growth and remodelling (Pitulescu & Adams 2010). Formation of the two earliest major vessels, the dorsal aorta and the cardinal vein, requires ephrin-B2:EphB4 repulsive signaling in endothelial cells (Kania, A. and Klein, R. 2016)**.** The EphrinB2/EphB4 membrane-bound ligand/receptor system is required for cardiovascular development, including trabeculation (Wang *et al*., 1998; Gerety *et al*., 1999). Both *EfnB2* (Wang *et al*., 1998) and *EphB4* (Gerety *et al*., 1999) are expressed throughout the endocardium. Notch is required for endocardial EphrinB2 and EphB4 expression; ephrinB2 expression is drastically reduced in *RBPJk* mutants (Grego-Bessa *et al*., 2007), whereas EphB4 expression is increased. During vascular development, EphrinB2 marks arterial and EphB4 vein endothelium (Wang *et al*., 1998). The observation that Notch mutants show loss of *Efnb2* and increased *EphB4* expression suggests that the endocardial default phenotype, like that of endothelium, would be "vein" (Grego-Bessa *et al*., 2007). Shear stress increases expression of the arterial endothelial marker EphrinB2 in murine ES cells via the VEGF-Notch signaling pathways (Masumura *et al*., 2009), that suggest a feedback loop between Notch and Ephrin signaling pathways at the early vascular development and angiogenic interactions for the separation of the arteries and veins boundaries in vascular remodelling (Wang *et al*., 1998).

### 4.1 Coronary Development

Until the late 1980s, the development of the coronaries was proposed to work as a simple *angiogenic* process, based on anatomical view, in which the endothelium of the aorta was sprouting out from the aortic root to cover epicardially the heart, and this theory was proposed as the "outgrowth theory" (The PI of CASS and Their Associates. The National Heart, Lung, and Blood Institute 1983).

Now we know that the working theory for the coronary development is the "ingrowth theory" (Bogers *et al*., 1989). In their study, Bogers and coworkers demonstrated that the major coronary arteries could be identified in the walls of the aortic sinuses before the emergence of coronary arterial orifices, thus suggesting ingrowth rather than outgrowth of the arterial channels. Coronary artery endothelium from a peritruncal coronary plexus invade the aortic root through a process of *vasculogenesis*. This latter process imply a tiny regulation of two different processes, *angiogenesis* and *vasculogenesis* that are regulated by the VEGF pathway.

### 4.2 Coronary Arteries Anomalies

The incidence of CA anomalies in the normal human population were addressed in autopsied patients and coronary angiography populations (Angelini P., 1999). Classification criteria for CA anomalies have been used by considering all possible coronary anatomic variations. The definition of a normal coronary artery (and, hence, an anomaly) is a disputed point originating from the high spectrum of morphological variation. Base on coronary embryonic developmental mechanisms and CA congenital anomalies, three main group were identified: Anomalies of CA connection, Anomalies of intrinsic CA anatomy, Anomalous myocardial/CA interaction (Pérez-Pomares *et al*. 2016). In a series of 1950 patients studied by coronary angiography, was found that CAAs had a global incidence of 5.64%, which is much higher than usually reported (Angelini P., 2007). Particularly noteworthy were the 0.92% incidence of anomalous origination of the RCA from the left sinus, the 0.87% diagnosis of fistulas and the 0.67% with the absent of the left main coronary artery (Angelini P., 2007).

- **Fistulas**

CAVF are rare anatomical conditions present in 0.002% of the general population (Dodge-Khatami *et al*., 2000). Communications between the coronary arteries and the cardiac chambers (coronary-cameral fistulas) or low-pressure veins (coronary arterio-venous malformations) are most often congenital in nature (Liberthson *et al*., 1979). Coronary artery fistula (CAF) or coronary arterio-venous fistula (CAVF) is an abnormal connection between a coronary artery and any of the 4 chambers of the heart or any of the great vessels (superior vena cava, pulmonary artery, pulmonary veins, or coronary sinus)

(Sommer *et al*., 2008). Treatment for these malformations include surgical ligation, either isolated or in association with CA bypass grafting, and interventional closure with occlusion coils, umbrellas, vascular plugs, and covered stents (Mangukia *et al*., 2012).

- **Myocardial Bridges**

Myocardial bridging is a congenital variant of a coronary artery in which a portion of an epicardial coronary artery (most frequently the middle segment of the left anterior descending [LAD] artery) takes an intramuscular course In several mammals and in birds, most of the coronary arteries are intramyocardial, apparently without having adverse functional consequences (Angelini *et al*. 2002). Hypertrophic cardiomyopathy has been found to have a high prevalence of myocardial bridging, with reported rates of up to 80% on angiography (Navarro-Lopez *et al*. 1986).

**Table 1.** Incidence of Coronary Anomalies and Patterns, as Observed in a Continuous Series of 1950 Angiograms

| Variable | N (%) Coronary anomalies (total) 110 (5.64) |
|---|---|
| Split RCA | 24 (1.23) |
| Ectopic RCA (right sinus) | 22 (1.13) |
| Ectopic RCA (left sinus) | 18 (0.92) |
| Fistulas | 17 (0.87) |
| Absent left main coronary artery | 13 (0.67) |
| Circumflex arising from right sinus | 13 (0.67) |
| LCA arising from right sinus | 3 (0.15) |
| Low origination of RCA | 2 (0.1) |
| Other anomalies | 3 (0.27) |
| Coronary dominance patterns | |
| Dominant RCA | 1641 (89.1) |
| Dominant LCA (circumflex) | 164 (8.4) |
| Codominant arteries (RCA, circumflex) | 48 (2.5) |

LCA indicates left coronary artery. Adapted from Angelini P *et al* with permission from Lippincott, Williams & Wilkins. Copyright 1999.

## 5. Origin of the coronary endothelium

Although it's widely known that the ECs have a mesodermal origin (Ishii Y. *et al*., 2009), several sources have been suggested to give rise to coronary endothelium independently: the endocardium lining the ventricular trabeculae (Viragh S *et al*., 1981), the aortic root endothelium (Ogden *et al*., 1998), the liver sinusoids (Poelmann *et al*., 1993) and the epicardium (Pèrez-Pomares *et al*., 1998; Katz *et al*., 2012).

The origin of cardiac ECs has been the subject of intense study in recent years as its developmental mechanism is incompletely understood. Genetic lineage tracing on mouse has demonstrated that at least three different sources contribute to mammalian

coronary endothelium: ST/Proepicardium, that in avian coronary vascular system consists of the proepicardium (PE) derivatives (Mikawa & Fischman, 1992; Perez-Pomares *et al*., 1998; Manner, 1999; Guadix *et al*., 2006; Nesbitt *et al*., 2006) and shows less contribution to the murine CA endothelium, the SV endocardium, that mostly provides the sprouting of coronary veins (Red-horse *et al*., 2010) and the Ventricular endocardial sprouts which are trapped into the coronary arteries of the murine compact myocardium during compaction (Wu *et al*.,2012). Although none of the previous studies primarily intended to establish a single origin for coronary endothelium, it is frequent to find these and other works quoted to support the hypothesis of embryonic coronary intimal layer being formed from one endothelial population only (Red-Horse *et al*., 2010; Tian *et al*., 2015). In accordance to all these observations, the identification of the origin of coronary endothelium has been controversial due to the limitations of the Cre lines used in these studies (Red-Horse *et al*., 2010; Wu *et al*., 2012; Tian *et al*., 2015; Perez-Pomares *et al*., 2016). Careful analysis of recent publications in the field reveals that such controversy is often based in the assumption that all coronary endothelium derives from a single endothelial cell progenitor pool (Zhang & Pu, 2013; Tian *et al*., 2015; Perez-Pomares *et al*., 2016). Such interpretation relies in results derived from *in vivo*, Cre/LoxP-based cell lineage tracing of murine coronary endothelium (Zhou & Pu, 2012; Wu *et al*., 2012; Cano *et al*., 2016).

### 5.1 Septum Transversum/Proepicardium

At E9.5 proepicardial derivatives consist mainly of EPDCs and contribute to the majority, if not all, of the interstitial fibroblasts found later in the embryonic myocardium. As development progresses the epicardially derived fibroblasts eventually become the predominant cell type in the leaflets that derive from these lateral cushions (Wessel *et al*., 2012). Other studies show extensive myocardial staining seen (Cai *et al*., 2008; Zhou *et al*., 2008), open to the possibility that a subset of myocardial cells may share a common progenitor with the epicardium or may actually be epicardially derived. Although in vivo cell tracing and in vitro culture of avian PE cells clearly shows that PE cells can differentiate into coronary endothelium (Mikawa *et al*., 1992; Guadix *et al*., 2006) studies in mammals claimed the contribution of PE to coronary endothelium is minor (Cai *et al*., 2008; Zhou *et al*., 2008). The so-called “epicardial” Cre constructs used in these studies are based on the expression of genes such as Gata5, Tbx18, or Wilms’ tumor suppressor

(Wt1) all of which are expressed by both PE and ST cells.

Regarding the origins of coronary endothelial cells, it has been shown elsewhere that extra-cardiac (proepicardial) endothelial contribution to coronary formation is quite extensive, while studies in mouse embryos restrict the proepicardial contribution to a rough 20% of coronary endothelial cells (Palmquist-Gomes *et al*., 2017). PE comprises several cell compartments, identified by either Scleraxis or Semaphorin3D gene that provides evidence on the contribution of a subset of epicardial progenitors (proepicardial cells) to the murine coronary endothelium (Katz *et al*., 2012). The ST/PE-derived component of coronary endothelium is mechanistically related to CA rather than to CV, revealing a functional role for these cells in transmural arterio–venous patterning of the coronary vascular tree (Cano *et al*., 2016).

### 5.2 Sinus Venosus Endocardium

Two endocardial populations have been reported to participate in the building of the embryonic coronary vascular system. The first derivates from the sinus venosus endocardium, which sprouts to give rise to the nascent Apelin$^{+}$ coronary vasculature (Red-Horse *et al*., 2010) . The Sinus Venosus (SV) is a transient stucture in cardiovascular development that receives venous blood from the vitelline vein, umbilical vein, and common cardinal vein and returns it to the atrium (Vrancken Peeters *et al*.1997) . The Sinus Venosus endocardium, which is able to vascularize sub-epicardially, is made of differentiated venous endothelial cells , which sprout onto the developing heart under the guidance of Vegf-c at E10.5 (Chen *et al*., 2014) . There they start to dedifferentiate and spread to form the coronary plexus, and subsequently re-differentiate and remodel into coronary arteries, capillaries, and veins (Red-Horse *et al*., 2010). Recent studies claimed the SV source implies that cells that were originally venous endothelium become reprogrammed to an arterial fate, and subsequently invade the ventricle wall in an epicardium-to-endocardium direction to form coronary arteries, which are found in an intra-myocardial location in the heart wall (Zhang *et al*., 2016). In this view, coronary arteries and veins share a common developmental origin from the SV and seem to be the main if not the only source for coronary endothelium. A recent study (Sharma *et al*., 2017) show that loss of the Apelin$^{+}$ population do not impair the later development of either CA and CV demonstrating that the embryonic heart is made of different sources of

coronary endothelium with a high plasticity.

### 5.3 Chamber endocardium

Endocardial cells are molecularly distinct from cells that comprise the vascular endothelium of blood vessels. For example, expression of the transcription factor nuclear factor of activated T cells (Nfatc) is restricted to endothelial cells of the endocardium; moreover, detection of Nfatc in murine precardiac mesoderm at E7.5 (de la Pompa *et al*., 1998) suggests that Nfatc expression marks specified endocardial cells, similar to the pattern of Nkx-2.5 in specified cardiac myocytes. Nfatc-null mice fail also to develop normal cardiac valves and septa, structures that contain the progeny of endocardial endothelial cells (de la Pompa *et al*., 1998, Ranger *et al*., 1998).

Nfatc1 is also expressed in cells of the proepicardium (PE) and is required for EPDCs and then for invasion into myocardium. Moreover conditional loss of Nfatc1 expression in EPDCs in mice causes reduced coronary vessel and fibrous matrix in myocardium (Combs *et al*., 2011).

A second major source of coronary endothelium has been identified in the ventricular endocardium ($Nfatc1^{+}$ lineage), which contributes massively to coronary arterial endothelium by angiogenesis through myocardial-endocardial VEGF signaling (Wu *et al*., 2012). However, more recently, using another endocardial line marking the $Npr3^{+}$ lineage, it was shown that the chamber endocardium contribute only to a small number of coronary arteries in the septum (Zhang *et al*., 2016A). Moreover endocardial plasticity has been validated by Nfatc1 lineage tracing proving that endocardial cells can differentiate also into hematopoietic cell, cushion mesenchyme, coronary, liver vascular endothelial cell (Zhang *et al*. 2018).

Although Nfatc1-Cre has been reported to label only a small part of the endocardium of SV in addition to that of the ventricle (Wu *et al*., 2012), recent report showed that Nfatc1 constitutive recombinase labeled both VE and SV efficiently (Zhang *et al*., 2016A). Furthermore, a detailed characterization of the lineage potential and heterogeneity of endocardial cells during development showed that a component of one organ (endocardium) influences the development of another organ (liver) through direct vascular contribution (Zhang *et al*., 2016B).

## 6. Angiogenesis and Vasculogenesis

In mice, development of coronary arteries begins with the formation of an endothelial plexus by precursor cells arising from ventricular endocardium (Wu *et al*., 2012), sinus venous endocardium (Red-Horse *et al*., 2010), and proepicardium/epicardium (Katz *et al*., 2012). CXCL12/Cxcr4 signaling axis has been reported to be essential for the maturation of the ventricular coronary endothelial plexus and establishment of functional coronary circulation (Cavallero *et al*., 2015; Ivins *et al*., 2015). In mouse prospective coronary veins are known to be located sub-epicardially, and the patterns of the venous sprouts suggest a model in which local signals in the developing heart induce angiogenic outgrowth (Wagner *et al*., 2005; Red-Horse *et al*., 2010; Cano *et al*., 2016). The SV at E9.5 starts to account for the scaffolding of coronary veins which are formed by vascular sprouting (Red-Horse *et al*., 2010). Vegfc is important for the SV-derived pathway, activating vessel migration along the surface of the ventricles (Chen *et al*., 2014). Vegfc binds Vegfr3, a Vegf receptor expressed mainly in lymphatic vessels and in embryonic blood endothelial cells (Tammela *et al*., 2008) which is also important in the endothelial sprouting modulated by Notch (Benedito *et al*., 2012). In its highly processed form, Vegfc also binds Vegfr2 (Joukov *et al*., 1997), a receptor that is expressed by most blood endothelial cells and that strongly stimulates vascular growth upon binding VEGF family members. However, coronary arteries are located intramyocardially, and the mechanism by which they assemble is still under debate. Around E11.5, endocardial precursor cells, through Vegfr-2, respond to Vegf-a signaling from the myocardium and migrate into the myocardium to form coronary plexuses where they mature into arteries, arterioles, and capillaries (Wu *et al*., 2012). Angiogenic precursor cells form vascular plexuses through vasculogenesis and this process is regulated by Notch and Vegfa signaling through a Dll4/Notch1/Vegfa/Vegfr2 signaling axis, as the lack of Pofut1 or Dll4 also results in defective coronary arteriogenesis (Wang *et al*., 2017). Development of the coronary artery endothelium is supported by the nuclear translocation of Notch1 intracellular domain (a well-known arterial endothelium fate determinant) and its downstram targets in both ventricular endocardial and prospective coronary artery endothelium (Del Monte *et al*., 2011). Furthermore activation of the transmembrane receptor Notch1 directly regulates vascular barrier function through a non-canonical, transcription-independent signaling mechanism

that drives assembly of adherens junctions through adhesive and cytoskeletal remodelling. (Polacheck *et al*., 2017). Moreover Jag1/Notch3 signaling is known to be crucial for smooth muscle cell recruitment and differentiation during vascular maturation (High *et al*., 2008; Voltz *et al*., 2015). Taken together, all these data suggest that both processes angiogenesis and vasculogenesis are crucial for coronary development and for the formation of a functional arterial endothelial plexus.

**7. Notch in ECs**

Notch signaling functions as a key regulator of angiogenesis outside of the heart in physiological and pathological conditions (Roca and Adams 2007). In particular Notch guides arterial-venous specification (Swift and Weinstein 2009), tip and stalk cell selection during sprouting angiogenesis (Gerhardt *et al*., 2003), proliferation and survival of endothelial cells (Noseda *et al*., 2004), and smooth muscle recruitment and differentiation (High *et al*., 2008). Expression analyses show that the major components of the Notch pathway in the vascular system consist of three ligands (Dll-4, Jagged-1, and Jagged-2), three receptors (Notch-1, -3, and -4) (Tatsuya *et al*. 2003). The most compelling evidence that *Notch* genes are involved in human vascular disorders comes from an analysis of a human disorder termed CADASIL which is manifested by stroke and vascular dementia and characterized by arteriopathy of cerebral arterioles (Joutel *et al*. 1996).

In mice, the Notch 1, Notch4, Jag1, Jag2, and Dll4 genes are all expressed in arterial but not venous ECs (Villa *et al*., 2001). Mice lacking Notch4 have no major defects in vessel formation, but Notch1 knockout mice exhibit a reduction in size of axial vessel, failure to properly remodel the vasculature, and die during embryonic development. Notch1/Notch4 double mutants show abnormal development in the axial vessels that is more severe than in Notch1 mutants, suggesting that the 2 genes are at least partially functionally overlapping (Krebs *et al*., 2000). Dll4 heterozygous mice also show reduced ephrinB2 expression and increased EphB4 expression, consistent with a failure in arterial differentiation (Duarte *et al*., 2004). *Notch4* gain of function (GOF), in endothelial cells and their progenitors leads to embryonic vascular defects (Uyttendaele *et al*., 2001), furthermore ectopic activation of other Notch pathway receptors such as ectopic *Notch1* activation in endothelial cells ($Notch1^{GOF}$) leads to embryonic vascular remodelling defects and arterio-venous malformations (AVM) that are distinct from

those exhibited by Notch pathway loss of function mutants (Krebs *et al*., 2010). Moreover, *Efnb2* and *Ephb4* loss of function mutants form arteriovenous malformations (Amyere *et al*., 2017), and these arteriovenous malformations phenocopy the arteriovenous malformations present in $Notch1^{GOF}$ embryos (Krebs *et al*., 2010). Taken together, these results implicate Dll4-Notch1/4 and their downstream effectors in proper vessel formation during murine development and suggest that Notch activity is important for promoting arterial cell fate and remodelling of the vasculature.

Angiogenesis requires a tightly coordinated balance between EC sprouting and the maintenance of existing vascular tubes. This equilibrium relies on the selection of the asymmetric cell division in the control of collective cell migration (Costa *et al*., 2016). Endothelial expression of VEGF-A and of the chemokine receptor CXCR4 have been reported as key Notch-dependent processes in the control of vessel growth (Pitulescu *et al*., 2017; Hasan *et al*., 2017). Dll4 expression in a tip cell activates Notch signaling and thereby suppresses sprouting in adjacent ECs. Jagged1 is also a critical component in the process of tip cell selection. In contrast to Dll4, Jagged1 is proangiogenic and functions by downregulating Dll4-Notch signaling (Benedito *et al*., 2009). Given that Dll4 and Jagged1 have opposing roles in endothelial sprouting, upstream signals controlling the expression of one or the other ligand might modulate angiogenesis positively or negatively. While VEGF has been shown to induce the expression of Dll4 in ECs, Jagged1 is absent in tip cells, which are exposed to the highest levels of VEGF, suggesting that the two ligands might be regulated differentially (Benedito *et al*., 2009).

The post-translational modification of the NECD is essential for proper NOTCH ligand–receptor interactions and subsequent signaling (Stanley, Okajima *et al*., 2010) and the expression of Fringe glucosaminyltransferases is highly relevant in the growing vasculature as well as in the control of the tip cell selection. Pofut1 is required for angiogenesis and for vascular development as its inactivation results in defective coronary artery formation (Wang *et al*., 2017) and systemic Fng inactivaion also affects coronary vessel development (D'Amato *et al*., 2016A), both by depressing Dll4/Notch signaling in ECs.

# Objectives

## Objectives

Abnormal Notch signaling can cause a variety of heart malformations. How endocardial Notch1, the most relevant receptor in the heart, regulates coronary development and ventricular trabeculation and compaction is still unknown. Jagged1 and Delta4 are the ligands that regulate Notch1 activity in the endothelium but due to the early embryonic lethality that their inactivation leads to, its role in coronary development has not been elucidated.

The objectives of this thesis are:

- to determine the endothelial progenitor cells where Notch1 activity is required and how this pathway guides endothelial proliferation and fate specification.

- to characterize the spatio-temporal expression of the ligands Jagged1 and Delta4 together with the glycosyltransferase Manic Fringe, and how they modulate Notch1 activity in progenitor cells from the SV.

- to elucidate the role of the Notch1 downstream target EphrinB2 in the endocardium and in the endothelium of the coronary artery, and its requirement for the remodelling and the pruning processes.

- to evaluate the role of the coronaries in chamber compaction and myocardial growth.

- to determine the Notch-dependent functions during coronaries development through transcriptomic analysis of different mutants.

# Methods

### Mouse strains and genotyping

Mouse strains were *CBF:H2B-Venus* (Nowotschin, Xenopoulos *et al*., 2013), *R26R* (Soriano, 1999), *R26R-YFP* (Srinivas, Watanabe *et al*., 2001), *Tie2-Cre* (Kisanuki, Hammer *et al*., 2001), *Nfatc1pan-Cre* (Wu *et al*., 2012), *Cdh5(PAC)-Cre$^{ERT2}$* (Wang, Nakayama *et al*., 2010), *cTnT-Cre* (Jiao, Kulessa *et al*., 2003), *Dll4$^{flox}$*(Koch, Fiorini *et al*., 2008), *Jag1$^{flox}$* (Mancini, Mantei *et al*., 2005), *Efnb2$^{flox}$* (Grunwald, Ilona C. *et al*., 2004) , *Notch1$^{flox}$* (Radtke, Wilson *et al*., 1999), *Mib1$^{flox}$* (Koo, Yoon *et al*., 2007). *Rosa26- MFng*Tg mice (Acc. No. CDB0917K : http://www.cdb.riken.jp/arg/mutant%20mice%20list.html). For the generation of *Rosa26- Dll4$^{GOF}$* Tg mice a cDNA encoding a native form of murine *Delta4* was cloned into a modified version of the *pROSA26-1* vector, preceded by the ubiquitous CAG promoter and a loxP-flanked 'Neo$^{R}$-STOP' cassette and followed by 6x repetition of c-Myc cassette and a bovine polyadenylation sequence. Gene targeting was done with TT2 ES cells and confirmed by Southern blotting. Mice were generated by injection of targeted ES cells into ICR embryos, and were backcrossed with the C57BL/6 strain. In the case of the different mutants analyzed, the WT embryos were the littermates who did not express the Cre-recombinase. To simplify the nomenclature we used the following names to refer the different mutant and transgenic line.

| | |
|---|---|
| *CBF:H2B-Venus* | *CBF:H2BVenus;WT* |
| *R26R-RFP;Nfatc1-Cre* | *R26R$^{RFP/+}$;Nfatc1pan-cre$^{+/-}$* |
| *R26R-YFP;Nfatc1-Cre* | *R26R-$^{YFP/+}$; Nfatc1pan-cre$^{+/-}$* |
| *Dll4flox;Nfatc1-Cre* | *Dll4$^{flox;flox}$/+; Nfatc1pan-cre$^{+/-}$* |
| *Dll4flox;Cdh5-Cre* | *Dll4$^{flox;flox}$;Cdh5-Cre$^{+/-}$* |
| *Notch1flox;Nfatc1-Cre* | *Notch1$^{flox;flox}$; Nfatc1pan-cre$^{+/-}$* |
| *Efnb2flox;Nfatc1-Cre* | *Efnb2$^{flox/flox}$;Nfatc1-Cre$^{+/-}$* |
| *Jag1flox;Nfatc1-Cre* | *Jag1$^{flox/flox}$;Nfatc1-Cre$^{+/-}$* |
| *Mib1$^{flox}$;cTnt-Cre* | *Mib1$^{flox/flox}$;cTnt-Cre$^{+/-}$* |
| *MFng$^{tg}$;Tie2-Cre* | *MFng$^{tg/tg}$;Tie2-Cre$^{+/-}$* |
| *Dll4$^{tg}$;Tie2-Cre* | *Dll4$^{tg/+}$; Tie2-Cre$^{+/-}$* |

Genotyping of the different genes was performed using the primers listed in Table2

**Table 2. PCR primers and conditions for genotyping**

| Gene | Oligos 5' to 3' | Annealing Temp. | Product |
|---|---|---|---|
| Dll4$^{flox}$ | 5′ GTGCTGGGACTGTAGCCACT 3′ | 60 | 455 bp -Flox |
| | 5′ TGTTAGGGATGTCGCTCTCC 3′ | | 408 bp -WT |
| Notch1$^{flox}$ | 5′ CTG ACTTAGTAGGGGGAAAAC 3′ | 60 | 350 bp -Flox |
| | 5′ AGTGGTCCAGGGTGTGAGTGT 3′ | | 300 bp -WT |
| Jag1$^{flox}$ | 5′ AGGTTGGCCACCTCTAAATC 3′ | 60 | 417 bp -Flox |
| | 5′ GCAAGTCTGTCTGCTTTCATC 3′ | | 267 bp -WT |
| MFng$^{tg}$ | 5′ AAAGTCGCTCTGAGTTGTTAT 3′ | 60 | 300 bp -Tg |
| | 5′ GCGAAGAGTTTGTCCTCAACC 3′ | | 650 bp -WT |
| | 5′ AGGCTGCAGAAGGAGCGGGA 3′ | | |
| Dll4$^{Tg}$ | 5′AAAGTCGCTCTGAGTTGTTAT 3′ | 58 | 600 bp-Tg |
| | 5′GGAGCGGGAGAAATGGATATG 3′ | | 427 bp-WT |
| | 5′CGGCCTCTGAGCTATTCCAGA 3′ | | |
| EfnB2 | 5′ CTTCAGCAATATACACAGGATG 3′ | 60 | 370bp -Flox |
| | 5′ TGCTTGATTGAAACGAAGCCCGA 3′ | | 270bp-WT |
| Mib1 | 5′ ACACCCAGAGGAAGCCCT AC 3′ | 60 | 500bp-Flox |
| | 5′ CTCACATCACCAAAGGATTGT 3′ | | 320bp-WT |
| | 5′ CCA GTCATAGCCGAATAGCC 3′ | | |
| Tie2-Cre | 5′ GGGAAGTCGCAAAGTTGTGAGTT 3′ | 60 | 500 bp -Cre |
| | 5′ CTAGAGCCTGTTTTGCACGTTC 3′ | | |
| Nfatc1-Cre | 5′AATAAG CCTGCCGTGGTCACTGG 3′ | 60 | 1000 bp -Cre |
| | 5′ AACCCTGGACGCCTGGGACAC 3′ | | 290 bp -WT |
| | 5′ GAAGCAACTCAT CGATTGATTTACG 3′ | | |
| cTnt-Cre | 5′ TACTCAAGAACTACGGGCTGC 3′ | 57 | 350 bp–Cre |
| | 5′ GCACTCCAGCTTGGTTCCCGA 3′ | | |
| Cdh5-Cre | 5′CTGGGATGCTGAAGGCATCAG 3′ | 55 | 760 bp -Cre |
| | 5′ TTGCGAACCTCATCACTCGTT 3 | | |

**4-hydroxy-tamoxifen (4-OHT) induction**

*Dll4$^{flox/+l}$;Cdh5-Cre$^{ERT/+}$* male mice were crossed with *Dll4$^{flox/flox}$* females and pregnant females were administered with 4-OHT (H6278 Sigma) once by oral gavage at 12.5 days of gestation. Embryos were dissected at E15.5. *Jag1$^{flox/+}$;Cdh5-Cre$^{ERT/+}$* female mice were crossed with *Jag1$^{flox/flox}$* males and pregnant females were administered with 4-OHT (H6278 Sigma) once by oral gavage at 9.5 days of gestation. Embryos were dissected either at E15.5 or E16.5.

### Harry´s Haematoxilin/Eosin staining and LacZ staining

Hematoxylin/eosin (H+E) staining was performed by standard methods. The LacZ staining for *Nfatc1-cre; Rosa26R* mice was performed following the protocol described by (Shalaby *et al*. 1995) .

### *In situ* Hybridization

Whole-mount *in situ* hybridization (WISH) and sectioning were as described (de la Pompa *et al*. 1997). ISH was performed on 7mm sections as described in (Kanzler *et al*. 1998). Details for probes will be provided on request.

### N1ICD (V1744)

Serial 7 μm sections were prepared and mounted on poly-lysine-treated slides. After deparaffinization and rehydration in an ethanol series, antigen was retrieved by boiling samples in a microwave oven for 10 min (twice, 5 min each) in sodium citrate (10 mM, pH 6.0) to avoid evaporation. Slides were allowed to cool to room temperature (RT) and washed in distilled water (4 times, 3 min each) and PBS (3 min). Endogenous peroxidase activity was quenched using 1% $H_2O_2$ in 100% methanol (40 min, RT) followed by 3 washes in PBS (5 min each) and 2 washes in 0.3% Triton/PBS (10 min each). For blocking, samples were incubated (1 h) in histoblock solution (3% BSA, 20 mM MgCl2, 0.3% Tween 20, 5% FBS in PBS) prior to incubation with anti-cleaved Notch1 antibody (V1744 antibody, Cell Signaling; 1:100 dilution in histoblock solution; 4ºC, overnight), followed by washing with PBS (2 washes, 5 min each) and 0.3% Triton X100/PBS (2 washes, 5 min eac

**Table 3**. List of primary antibody used for the IHC.

| Antigen | Cardiac expression | Catalog number | Clone number | Source Ig | IHC dilution | Source |
|---|---|---|---|---|---|---|
| a-SMA-Cy3 | Cardiomyocytes /smooth muscle cells | D3B8 | 1A4 | Mouse | 100 | Sigma-Aldrich |
| BrdU | Proliferating cells | 347580 | B-44 | Mouse | 50 | BD Biosciences |
| CD31/Pecam-1 | Endocardium/coronary endothelium | 550274 | MEC 13.3 | Rat | 100 | BD Biosciences |
| Dll4 | Endocardium/coronary endothelium | sc-28915 | | Rabbit | 100 | Santa Cruz Biotechnology |
| Endomucin | Endocardium | sc-65495 | V.7C7 | Rat | 200 | Santa Cruz Biotechnology |
| GFP | GFP expressing cells | 632381 | JL-8 | Mouse | 200 | Clontech |
| Jag1 | Cardiomyocytes /coronary endothelium | 2620 | 28H8 | Rabbit | 100 | Cell Signaling Technology |
| NFATc1 | Endocardium/coronary endothelium | ALX-804-022-R100 | 7A6 | Mouse | 100 | Enzo Life Sciences |
| Cleaved Notch1 (Val1744) | Endocardium/coronary endothelium | 4147 | D3B8 | Rabbit | 100 | Cell Signaling Technology |
| p27 | p27 expressing cells | K0082-3 | p27 Kip1 | Mouse | 100 | Medical and Biological Laboratories |
| Notch 3 | Pericyte | ab23426 | G00041 | Rabbit | 100 | Abcam |
| ERG | Endothelium | ab110639 | EPR3863 | Rabbit | 100 | Abcam |
| Glut1 | Cell membrane of different cell type | 07-1401 | C00222 | Rabbit | 100 | MERCK Millipore |

Lectin

| Antigen | Cardiac expression | Catalog number | IHC dilution | Source |
|---|---|---|---|---|
| Isolectin IB4-Alexa Fluor 647 | Endocardium/coronary endothelium | I32450 | 300 | Molecular Probes |

Secondary antibodies

| Antigen | Label or Dye | Amplification | Catalog number | IHC dilution | Source |
|---|---|---|---|---|---|
| Anti-rabbit | HRP | TSA Cy3/fluorescein | P0448 | 100 | Dako |
| Anti-goat | HRP | TSA Cy3/fluorescein | P0449 | 100 | Dako |
| Anti-rat | Biotin | TSA Cy3/fluorescein | BA4001 | 100 | Vector laboratories |
| Anti-rabbit | Biotin | TSA Cy3/fluorescein | 111-066-003 | 100 | Jackson |
| Anti-mouse | Alexa Fluor 647 | | 115-606-003 | 200 | Jackson |
| Anti-mouse | Alexa Fluor 488 | | A-11029 | 200 | Invitrogen |
| Anti-rat | Alexa Fluor 488 | | A-11006 | 200 | Invitrogen |

**RNA-Seq**

RNA was isolated at E12.5, from whole hearts, for WT (4 replicate samples, pooling 4 embryos) and *Jag1$^{flox}$;Nfatc1-Cre* embryos (4 replicate samples, pooling 4 embryos), and for WT (4 replicate samples, pooling 4 embryos) and *Dll4$^{flox}$;Nfatc1-Cre* (4 replicate samples, pooling 4 embryos). It was isolated at E15.5, from heart ventricles, for WT (4 replicate samples, pooling 3 embryos) and *Dll4$^{flox}$;Cdh5-Cre$^{ERT2}$* (3 replicate samples, pooling 3 embryos) and for WT (4 replicate samples, pooling 3 embryos) and *Dll4$^{GOF}$;Tie2-Cre* (3 replicate samples, pooling 3 embryos). Finally, it was isolated at E16.5, from heart ventricles, for WT (4 replicate samples, from one embryo) and *Efnb2$^{flox}$;Nfatc1-Cre* (4 replicate samples, from one embryo). RNASeq data for *Jag1$^{flox}$;Nfatc1-Cre*, *Dll4$^{flox}$;Nfatc1-Cre*, *Dll4$^{flox}$;Cdh5(PAC)-Cre$^{ERT2}$*, *Dll4$^{GOF}$;Tie2-Cre* and *Efnb2flox;Nfatc1-Cre* experiments was generated by CNIC's Genomics Unit and have been deposited in NCBI's GEO database (Edgar *et al*. 2002) under accession number

GSE110614 (https://www.ncbi.nlm.nih.gov/geo/query/acc.cgi?acc=GSE110614).RNASeq data for the *MFng*$^{GOF/GOF}$*;Tie2-Cre* experiment was recovered from GEO (GSE67889)( D'Amato *et al*. 2016a) and reanalized. RNASeq sequencing reads were pre-processed by means of a pipeline that used FastQC (Andrews *et al*.,), to asses read quality, and Cutadapt v1.6 (Martin *et al*., 2011) to trim sequencing reads, eliminating Illumina adaptor remains, and to discard reads that were shorter than 30 bp. Resulting reads were mapped against the mouse transcriptome (GRCm38 assembly, Ensembl release 76) and quantified using RSEM v1.2.20 (Li and Dewey 2011). Around 80-90% of the reads participated in at least one reported alignment. Expected expression counts calculated with RSEM were then processed with an analysis pipeline that used Bioconductor package Limma (Ritchie *et al*., 2015) for normalization and differential expression testing in six pairwise contrasts involving mutant versus WT comparisons. Changes in gene expression were considered significant if associated to Benjamini-Hochberg adjusted p-value < 0.05. The number of genes detected as differentially expressed was 211, 274, 163, 0, 5, and 1928, in comparisons of *Jag1*$^{flox}$*;Nfatc1 Cre*, *Dll4*$^{flox}$*;Nfatc1-Cre*, *Dll4*$^{flox}$*;Cdh5(PAC)-Cre*$^{ERT2}$, *Dll4*$^{GOF}$*;Tie2-Cre* and *Efnb2flox;Nfatc1-Cre* and *MFng*$^{GOF/GOF}$*;Tie2-Cre* against their WT counterparts, respectively.

Enrichment analyses were performed with IPA [Ingenuity Pathway Analysis, Quiagen, http://www.ingenuity.com] and GSEA (Subramanian *et al*., 2005). IPA was used to identify collections of genes associated to canonical pathways, common upstream regulators or functional terms significantly overrepresented on the sets of differentially expressed genes; statistical significance was defined by Benjamini-Hochberg adjusted p-value < 0.05. Circular plots were generated with R visualization package called GOplot (Walter *et al*., 2015) and were summarizing the association between genes and enriched pathways, upstream regulators and functional terms with a chord plot (Krzywinski *et al*., 2009). GSEA was used to identify gene sets from the Hallmark and KEGG MsigDB databases showing statistically significant, concordant differences between mutant and WT genotypes; statistical significance was defined by FDR q-value < 0.25. Comparative heatmaps summarizing GSEA results were generated with Perl and R.

**Ultrasound**

Left ventricle (LV) function and wall thickness were analyzed by transthoracic echocardiography in E19.5 mouse embryos. Mice were adjusted to obtain a target

heart rate of 450±50 beats per minute and examined with a 30 MHz transthoracic echocardiography probe. Images were obtained with Vevo 2100 (VisualSonics, Toronto, Canada) from *Efnb2flox;Nfatc1-Cre* and WT littermates. LV long axis M-Mode views were obtained as described (Cruz-Adalia *et al*., 2010). From these images, interventricular septum end-diastolic thicknesses was measured, and LV systolic function was assessed by estimating LV shortening fraction (SF) and LV ejection fraction (EF) (Cruz-Adalia *et al*., 2010).

**Resection Model**

Immunohistochemical staining of embryonic hearts was performed essentially as described previously (Mukouyama *et al*. 2012). Embryonic hearts between E11.5 and E16.5 were dissected and fixed in 4% paraformaldehyde/PBS 1-2 hours at RT.

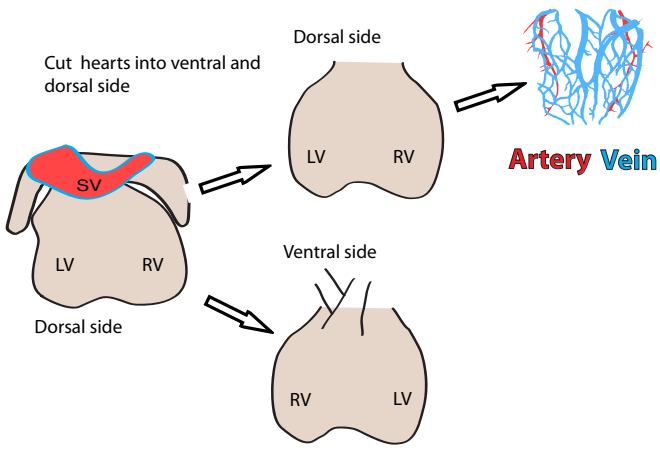



**Figure 3.** Cartoon illustrating experimental procedure for coronary whole-mount staining.

**Staining of Whole-Mount Tissues**

The heart was cut to divide dorsal and ventral potions. The ventral side of heart is facing the upward and dorsal side facing the downward. Permeabilization of the dorsal side of the heart with 0.3% TX100 was done for 30minutes to 1 hour. The tissue was blocked in 10% FBS/PBS for 4 h with gentle mixing on the Mixer at room temperature. Tissues was incubated with gentle mixing on the mixer at 4°C overnight.

**Mounting Heart on Slide**

The hearts were placed on a slide and placed with the outer surface lying upward on the slide (i.e., towards coverslip) to image coronary vasculature. The antibodies used were: anti-Endomucin (Santa Cruz Biotechnology ,1:250) to detect subepicardial veins and anti-Isolectin IB4-Alexa Fluor 647 (Molecular Probes,1:500) to detect intramyocardial arterty ; Confocal microscopy analysis was carried out on a Nikon A1plus confocal.

**Immunohistochemistry, EdU incorporation and detection**

Paraffin sections (7µm) were incubated overnight with primary antibodies, followed by 1h incubation with a fluorescent-dye-conjugated secondary antibody. N1ICD, Dll4, Jag1 and p27 staining was performed using Tyramide signal amplification (TSA).. For EdU pregnant females mice were injected intraperitoneally with 100 µl EdU nucleotides (2 mg $ml^{-1}$ in PBS) at E12.5, 1 h before euthanization and Click-iT EdU Imaging Kit (Thermo Fisher Scientific, C10340) was used to detect EdU incorporation.

**Quantification of immunochemistry**

For p27 and N1ICD quantification, positive nuclei were divided by the total number of nuclei found in the CM, cardiomyocyte for the first and endothelium of the coronary for the second one and counted on sections (≥3). The number of mural cells surrounding intramyocardial vessels expressing both SMA+ and Notch3+ (double positives) was counted and divided by the total number of intramyocardial vessels defined by Iso B4 staining in equivalent sections. The number of subepicardial double positive SMA+, Notch3+ cells was counted and divided by the total number of subepicardial vessels defined by IsoB4. Images were processed with ImageJ software.

**Quantification of compact myocardium thickness**

The method used was a modification of that described by (Yang *et al*. 2012). Briefly, 7µm paraffin sections from E12.5, E15.5 and E16.5 WT and mutant hearts were stained with anti-CD31 or Endomucin to facilitate visualization of ventricular structures. Confocal images were obtained with a NIKON A1R confocal microscope. ImageJ software was used for the measurements. In E15.5 and E16.5 heart sections, left and right ventricles

were analyzed separately. For each measurement, settings were kept constant for all images using the scale bar recorded in each image as the reference distance. The thickness of the compact myocardium was measured by dividing the ventricle in two parts, the left and the right. Several measurements were taken in each region and the mean was expressed in µm.

**Mouse ventricular explant culture**

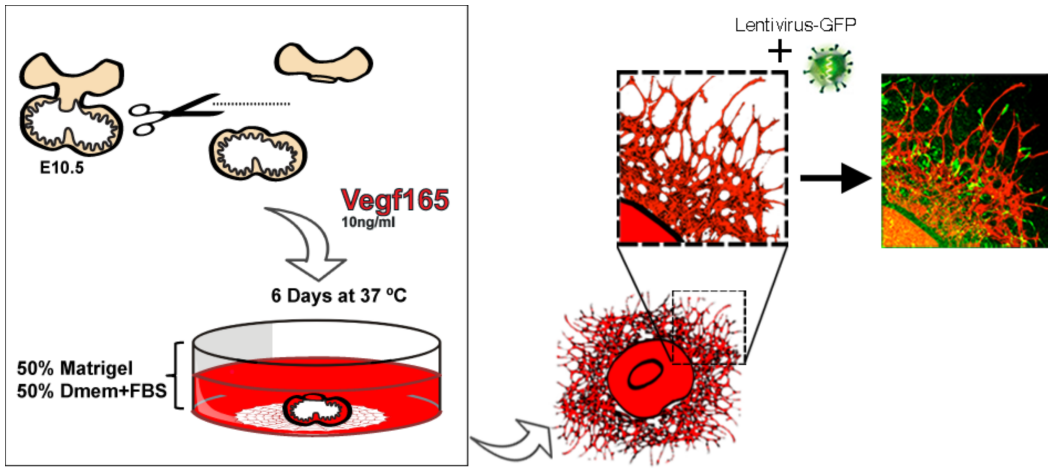



**Figure 4.** Cartoon illustrating experimental procedure for the ventricular explant

Ventricles were dissected out from E10.5 or E11.5 embryos (outflow tract,atria and sinus venosus were removed) rinsed with PBS to remove circulating cells and were placed in a Nunc 4-well plates. Matrigel (Corning® Matrigel® Basement Membrane Matrix, *LDEV-Free, 10mL growth factor reduced, BD Biosciences 354234) was diluited 1:1 with DMEM plus 10% FBS and Vegf (Human-$Vegf_{165}$ Peprotech) 10 ng/ml. Each well had total volume of 400µl and 3-4 hearts max were cultured for 6 days and after that were fixed in PFA4% 10 minutes and washed twice with PBS1X for 15minutes.

**IF on explants**

Explants were permeabilized with Triton x-100 0.5% Block with Histoblock solution (FBS Histoblock) 2-3 hours at RT and incubate with anti-CD31 1:100 (Purified Rat Anti-Mouse CD31 BD Biosciences Pharmingen) overnight at 4ºC. Anti-rat Biotinylated was used as secondary antibody and diluited in BSA 1:150 and amplified with ABC kit and with 3 minute of TSA (tyramides) 1:100 in PBS.

**Lentiviral production**

Full-length murine *Efnb2* was subcloned into the lentiviral vector pRLL-IRES-eGFP (Addgene). Concentrated lentiviruses expressing pRLL-IRES-eGFP or pRLL-*Efnb2*-IRES-eGFP were obtained as described previously (Esteban *et al*. 2011). Viruses were titrated in Jurkat cells, and infection efficiency (GFP-expressing cells) and cell death (propidium iodide staining) were monitored by flow cytometry. Ventricle explants were treated with Lentivirus by adding 40µl of $1x10^8$ particles in the first day of the assay directly to the 400µl DMEM. Infection was tested the sixth day by GFP detection before performing the immunofluorescence.

**Statistics**

Statistical analyses were performed using Student's t test in Graph Pad (Prism 7.0). Data are presented as means ± s.d., unless otherwise indicated. Statistical analysis was carried out using Prism 5 (GraphPad). All statistical tests were performed using two-sided, unpaired Student's t-tests , except for Figure 5 and 8 where we performed one-way ANOVA with Tukey's multiple comparison tests and Figure 10 where we performed one-way ANOVA with Dunnett's multiple tests to assess statistical significance with a 95% confidence interval; results are marked with one asterisk (*) if $P$ <0.05, two (**) if $P$ <0.01 and three (***) if $P$ <0.001. Sample size was chosen empirically according to previous experience in the calculation of experimental variability. No statistical method was used to predetermine sample size. The numbers of animals used are described in the corresponding figure legends. Animals were genotyped before the experiment and were caged together and treated in the same way. Variance was comparable between groups throughout the manuscript. We chose the appropriate tests according to the data distributions. The experiments were not randomized. The investigators were not blinded to allocation during experiments and outcome assessment.

# Results

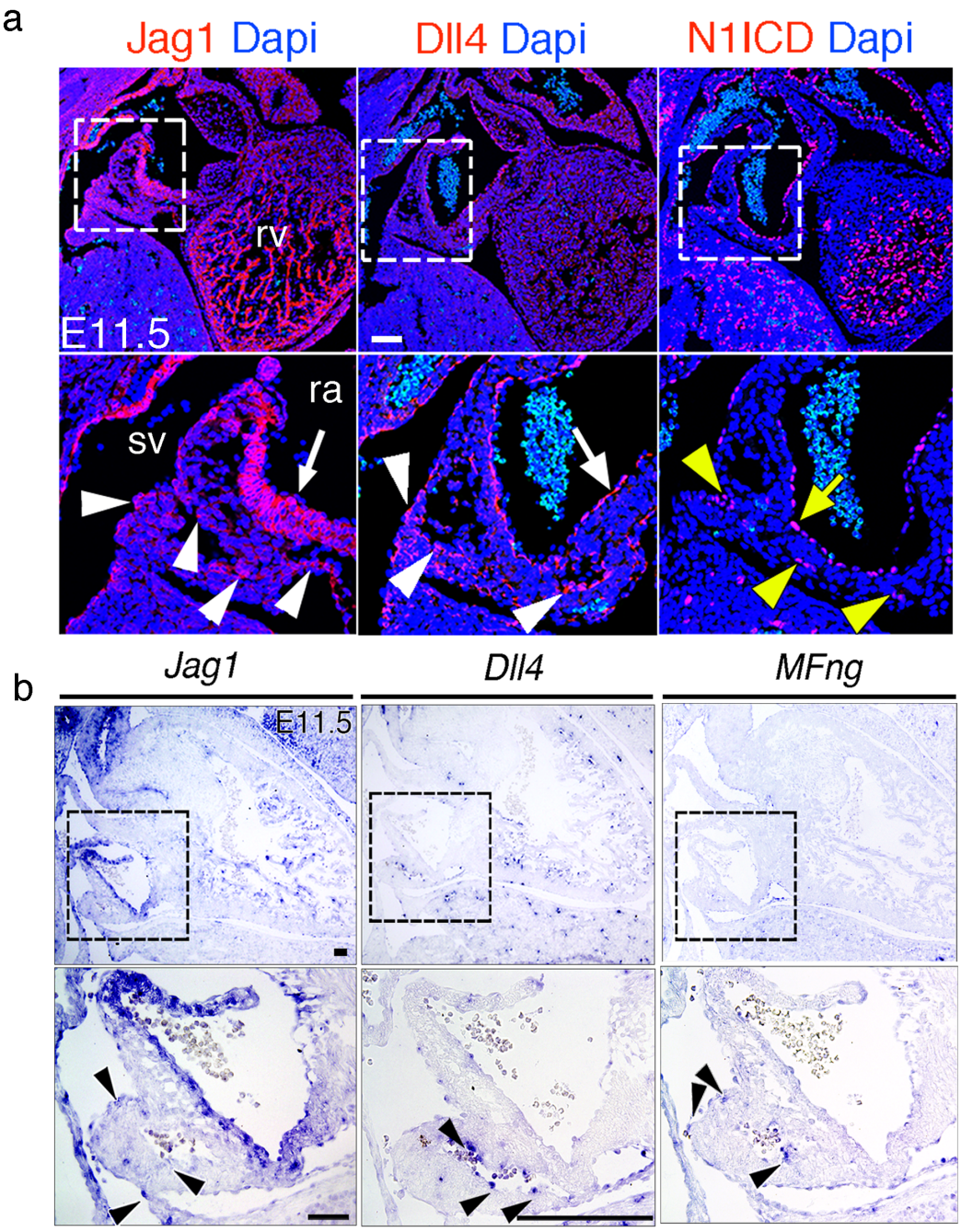



**Fig.5. Jag1, Dll4 and Manic Fringe expression in the SV of control hearts at E11.5** (**a**) Immunostaining for Jag1, Dll4 and N1ICD (red) in SV (arrowheads) and right ventricle (arrow). Magnified views of boxed areas; *Jag1*, *Dll4* and *MFng* are expressed in scattered endothelial cells lining the SV (arrowheads), while *Jag1* is also expressed in atrial myocardium (arrow). (**b**) ISH of control heart for *Jag1*, *Dll4* and *MFng* in SV endothelium. Magnified views of boxed areas; *Jag1*, *Dll4*, and *MFng* are expressed in scattered endothelial cells lining the SV (arrowheads). sv, sinus venosus; ra, right atrium; rv, right ventricle;. Scale bars, 100 μm.

**Jag1, Dll4, and MFng are co-expressed in SV and sub-epicardial vessels**

We examined the SV and coronary vessels for the spatio-temporal expression of Jag1, Dll4, and MFng. At embryonic day (E) 11.5 Jag1 was expressed in some SV EC, in the surrounding myocardium and in ECs extending into the right atrium (**Fig. 5a,b**). Dll4 and N1ICD were expressed in ECs emanating from the SV and in the endocardium lining the right atrium **(Fig. 5a,b**). *MFng* was also found expressed in some SV ECs (**Fig.5b**). Thus the spatial distribution of the Notch ligands is highly heterogeneous in SV endothelium. Moreover either Jag1 or Dll4 could potentially activate Notch1 in the SV.

At E13.5, Jag1, *Dll4* and *MFng* were all expressed in EC of the developing coronary arteries, which are located intra-myocardially, whereas *Dll4* and *MFng* were also detected in prospective veins, located sub-epicardially (**Fig.6a**). At E15.5, Jag1, *Dll4* and *MFng* were all expressed in arterial ECs, whereas *MFng* was still found in some veins (**Fig.6b**). *Jag1* expression persisted in coronary artery endothelium at E17.5, was co-expressed the Notch reporter *CBF1:H2B-Venus* and N1ICD (**Fig.6c**).

Thus, the expression of Notch ligands, *MFng*, and N1ICD is widespread in early SV endothelium and persists in remodelling coronary arteries at later developmental stages.

**Most ventricular free-wall coronary vessels derive from Nfatc1$^{+}$ progenitors**

To inactivate the Notch ligands in the SV endothelium we used the *Nfatc1-Cre* driver line reported to be active in chamber endocardium and a subset of SV ECs (Wu *et al*., 2012). To confirm the endocardial specificity of this line, we crossed it with the *Rosa26-LacZ* reporter line (Soriano *et al.,* 1999). X-gal-stained heart sections of E11.5 embryos identified patchy LacZ expression in SV endothelium (**Fig.7a**). β-gal staining was consistent with Nfatc1 protein nuclear localisation in a subset of ECs lining the SV (**Fig.7a**). At E12.5, co-labelling with an anti-Pecam1 antibody revealed in 60% β-gal $^{+}$ staining of Pecam1$^{+}$ sub-epicardial vessels in the right ventricle, and about 50% in the left ventricle (**Fig.7b**). Moreover, the proximity of β-gal-tagged intra-myocardial vessels to the ventricular endocardium lining at the base of the ventricular wall (**Fig. 7b**), is consistent with a chamber endocardial origin of coronary arteries in this region. Taken together, the data show that SV-derived Nfatc1+ progenitors give rise to 50-80% of sub-epicardial vessels in the ventricular wall.

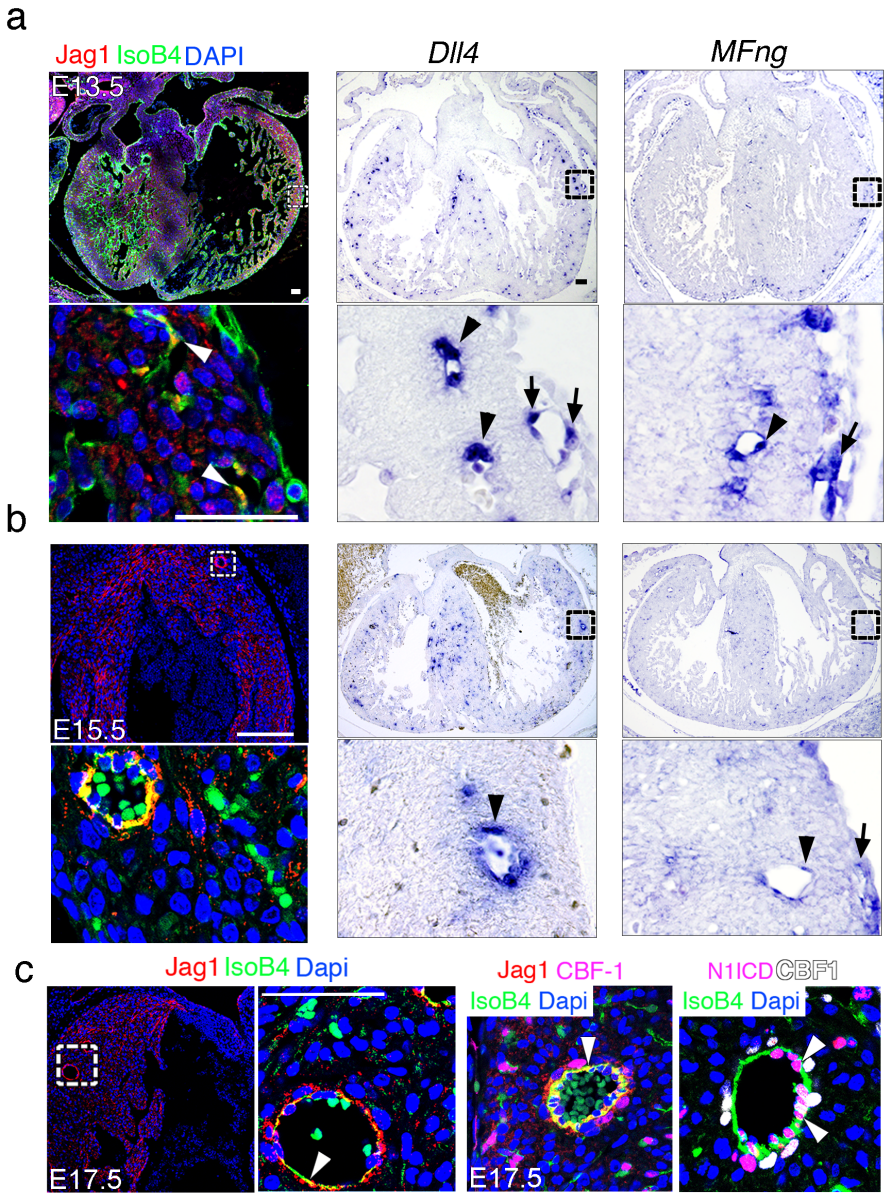



**Fig.6 Jag1, Dll4 and Manic Fringe expression between E13.5-E17.5** (**a**) E13.5 control heart. Immunohistochemistry for Jag1 (red) and IsoB4 (green). Inset, co-staining of Jag1 and IsoB4 in coronary arteries (white arrowheads). ISH for *Dll4* and *MFng* expression. Insets, expression in coronary arteries (black arrowheads) and sub-epciardial vein (arrows). (**b**) E15.5 control heart. Immunohistochemistry for Jag1 (red; top) and co-staining with IsoB4 (green; bottom). Inset, co-staining of Jag1 and IsoB4 in coronary artery. ISH for *Dll4* and *MFng* expression. Insets, expression in coronary artery (black arrowhead) and sub-epicardial vein (arrow). Scale bars, 50 µm. (**c**) E17.5 control heart. Immunohistochemistry for Jag1 (red) and IsoB4 (green). Inset, co-staining of Jag1 and IsoB4 in coronary artery (yellow arrowheads). E17.5 *CBF1:H2B-Venus* heart. Immunohistochemistry for Jag1 (red), GFP/Venus (magenta) and IsoB4 (green). CBF1:H2B-Venus-positive cell contact Jag1-expressing cell in coronary endothelium (arrowhead). Immunohistochemistry for N1ICD (magenta), GFP/Venus white) and IsoB4 (green). *CBF1:H2B-Venus*-positive cell in contact with N1ICD-expressing cell in coronary endothelium (arrowheads). Dapi counterstain (blue). Scale bars, 50 µm.

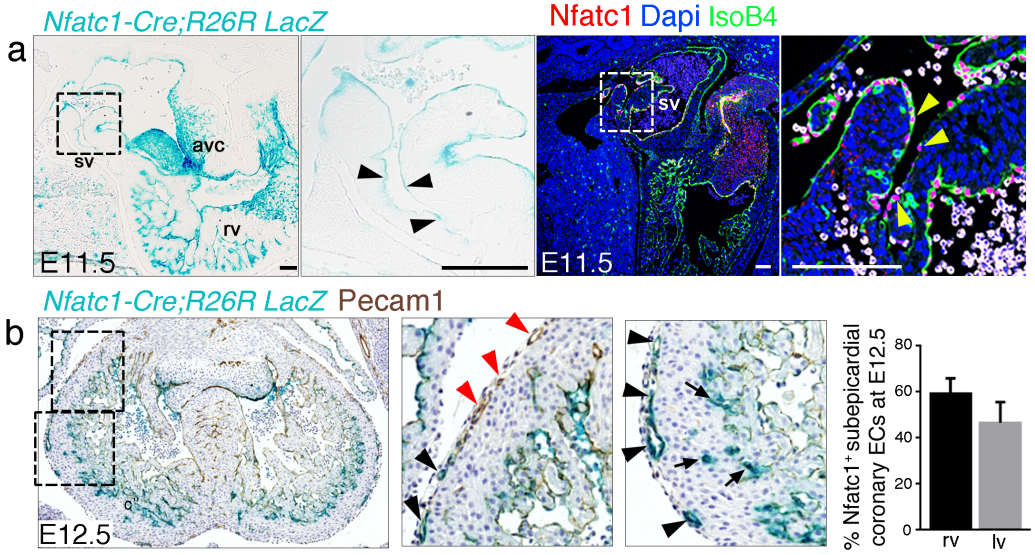



**Fig.7 Nfatc1$^+$ progenitors give rise to the majority of coronary vessels. (a)** Sagittal section of a E11.5 *Nfatc1-Cre;R26R-LacZ* heart showing LacZ expression in sinus venosus (sv; arrowheads in inset), right ventricle (rv) and atrioventricular canal (avc). Sagittal section of a E11.5 control heart co-immunostained for Nfatc1 (red) and IsoB4 (green). The yellow arrowheads indicate nuclear Nfatc1 staining in SV endothelial cells. Dapi counterstain (blue). Scale bars 100 µm. (**b**) E12.5 *Nfatc1-Cre;R26R-LacZ* heart co-stained for LacZ and Pecam-1. (Top) LacZ staining is weak in vessels proximal to the AVC (red arrowheads) and strong in distal vessels (Top, Bottom, black arrowheads). (Bottom) LacZ staining in vessels close to chamber endocardium is consistent with endocardial origin of° coronary arteries (arrows). Quantification of *Nfatc1-Cre*-driven LacZ staining measured as percentage (%) of Nfatc1-positive vessels of the total sub-epicardial vessels (Pecam-1-stained). Data are mean +/- s.d. (n=3 sections from 4 embryos). Data are mean +/- s.d. (n= 2 control). Scale bars, 100 µm.

To trace the fate of Nfatc1+ cells relative to Notch activity, we crossed *Nfatc1-Cre;Rosa26-RFP* mice with the Notch reporter line *CBF:H2B-Venus*. The *CBF:H2B-Venus* line has been shown to label the endocardium as early as E8.5 (D'Amato *et al*., 2016). Whole-mount staining of E11.5 *CBF:H2B-Venus;Nfatc1-RFP* hearts showed CBF:H2B-Venus labelling in some Nfatc1$^+$ cells of the SV confirming that the Notch pathway is active in SV endothelium (**Fig.8a**). At E12.5, 80% of the nuclei positive for endothelial-specific nuclear protein Erg in the sub-epicardial capillaries were also positive for *Nfatc1-Cre*-driven red fluorescent protein (RFP) .(**Fig. 8b)**

To further characterize Notch activity at this early stage of coronary development we analyzed *Nfatc1-Cre; Rosa26-RFP;CBF1:H2B-Venus* mice at E12.5. Some RFP-labelled capillaries on the dorsal side of the heart were co-labelled with *CBF1:H2B-Venus* while others were labelled with *CBF1:H2B-Venus* only (**Fig.8a**), indicating Notch activity is present in Nfatc1$^+$ and Nfatc1$^-$ populations of SV-derived EC. At E12.5, N1ICD was

detected in endomucin (Emcn)-positive ECs in subepicardial capillaries emerging from the SV suggesting that Notch signaling is active in SV endothelium and could be regulating coronary sprouting angiogenesis (**Fig.8c**).

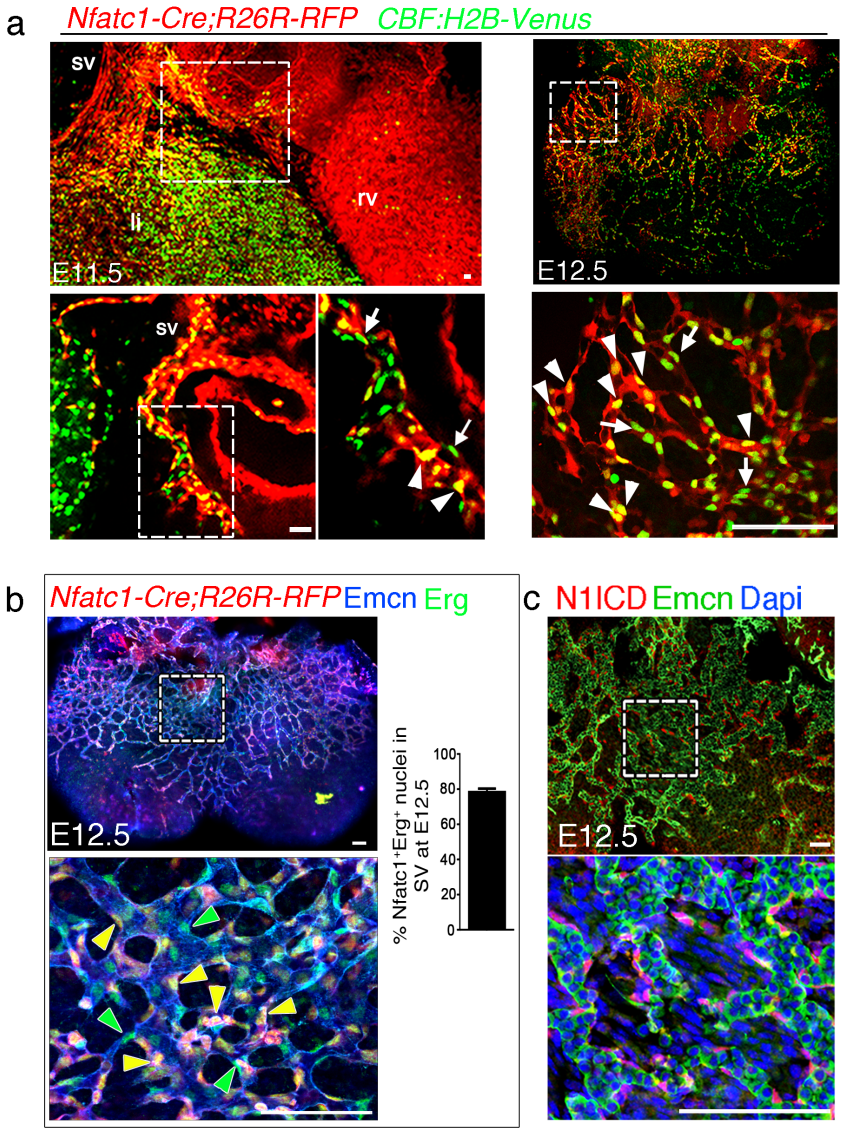



**Fig.8 Nfatc1 include early arterial progenitors. (a)** *Nfatc1-Cre;Rosa26-RFP:CBF1:H2B-Venus* heart. Dorsal view of whole-mount immunofluorescence for RFP (red) and immunohistochemistry for GFP (green). Z-stack of SV endothelium showing *Nfatc1-Cre;Rosa26-RFP-CBF1:H2B-Venus* double-positive nuclei (arrowheads) and *CBF1:H2B-Venus* single-positive nuclei (arrows). (**b**) E12.5 *Nfatc1-Cre;Rosa26-RFP* heart. Dorsal view of whole-mount RFP immunofluorescence (red), and immunhistochemistry for Emcn (blue) and Erg (green). Sub-epicardial vessel endothelium contains *Nfatc1-Cre;Rosa26-RFP*-positive (yellow arrowheads) and *Nfatc1-Cre;Rosa26-RFP*-negative nuclei (green arrowheads). Dapi counterstain (blue). Quantification of Nfatc1-Erg dual-positive nuclei as percentage of total nuclei in subepicardial vessels. (**c**) Dorsal view of whole-mount immunofluorescence for N1ICD (red) and Emcn (green). Dapi counterstain (blue).Data are mean +/- s.d. (n= 2 control). sv, sinus venosus; rv, right ventricle; li, liver. Scale bars, 100 µm.

**Endocardial *Jag1* inactivation arrests SV sprouting, whereas *Dll4* deletion causes excessive SV sprouting**

To test Notch ligand function in SV and chamber endocardium we crossed floxed Jag1 and Dll4 alleles with the *Nfatc1-Cre* driver line. *Jag1* inactivation with the *Nfatc1-Cre* driver line resulted in lethality at E13.5 (**Suppl. Table 1**). Whole-mount Endomucin (Emcn) staining at E12.5 revealed a well-formed vascular network in control hearts (**Fig.9a**), while *Jag1$^{flox}$;Nfatc1-Cre* mutants showed a poorly developed vascular network, characterised by vascular malformations, decreased endothelial branching (**Fig.9a**) and 60% reduction in EC proliferation (**Fig.10a**). Ventricular wall thickness in endocardial Jag1 mutants was reduced 50-60% relative to controls **(Fig.9c**) and the epicardium in these embryos was partially detached. At E12.5 N1ICD$^{+}$ nuclei were associated with sub-epicardial vessels in control embryos but were absent from *Jag1$^{flox}$;Nfatc1-Cre* mutants, contrasting with unaltered N1ICD$^{+}$ expression in the ventricular endocardium (**Fig.9b**). These data suggest that endocardial Jag1 deletion in SV arrests primitive coronary plexus formation and myocardial growth.

*Dll4* inactivation with the *Nfatc1-Cre* driver line resulted in the death of most mutants at E10.5 (**Suppl. Table 1**). However about a third of the mutant embryos survived until E13.5, possibly due to *Cre* mosaicism (**Suppl. Table 1**). Whole-mount Emcn immunostaining of E12.5 *Dll4$^{flox}$;Nfatc1-Cre* hearts revealed a comparatively denser capillary network (**Fig.9a**), characterized by numerous capillary malformations (**Fig.9a**) with increased endothelial branching, and 60% above-normal EC proliferation (**Fig.10a**). These defects were associated with a 50-60% reduction in ventricular wall thickness (**Fig.9b**) and a partially detached epicardium (**Fig.9c**). The proportion of N1ICD$^{+}$ nuclei in sub-epicardial vessels was 80% reduced (**Fig.9c**) and N1ICD$^{+}$ expression in ventricular endocardium was diminished due to the dependence of Notch1 signaling on Dll4 (D'Amato *et al.,* 2016b). Endocardial inactivation of Dll4 in SV thus causes excessive expansion of the primitive coronary plexus and impairs myocardial growth.

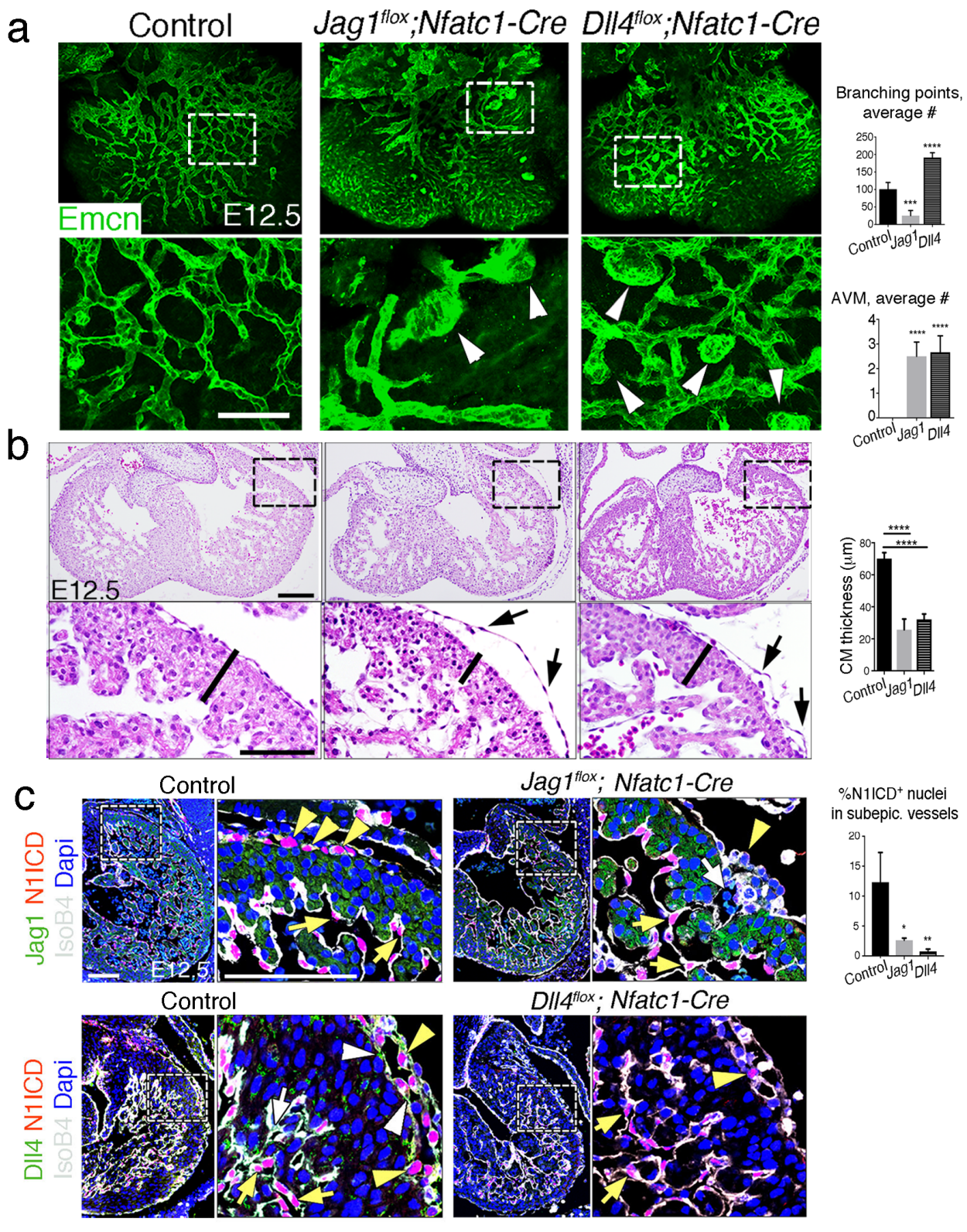

a
Control
Jag1flox;Nfatc1-Cre
Dll4flox;Nfatc1-Cre
Emcn
E12.5
Branching points, average #
AVM, average #
Control
Jag1
Dll4
b
E12.5
CM thickness (μm)
c
Control
Jag1flox; Nfatc1-Cre
Jag1 N1ICD IsoB4 Dapi
E12.5
Control
Dll4flox; Nfatc1-Cre
Dll4 N1ICD IsoB4 Dapi
%N1ICD+ nuclei in subepic. vessels

**Fig.9. Endocardial *Jag1* or *Dll4* inactivation disrupts coronary plexus formation.** (**a**) Whole mount dorsal view of immunohistochemistry for Emcn (green) in E12.5 Control WT, *Jag1$^{flox}$;Nfatc1-Cre* and *Dll4$^{flox}$;Nfatc1-Cre* mutant hearts showing AVMs (Arrowheads). (**b**) Hematoxylin–eosin (H&E) staining on control E12.5 WT, *Jag1$^{flox}$;Nfatc1-Cre* and *Dll4$^{flox}$;Nfatc1-Cre* heart sections. Arrows, detached epicardium. Black bars, compact myocardium (CM) thickness. (**c**) Immunohistochemistry for Jag1 and Dll4 (green) isolectinB4 (IB4, white), N1ICD (red) on E12.5 control WT (right), *Jag1$^{flox}$;Nfatc1-Cre* and *Dll4$^{flox}$;Nfatc1-Cre* heart sections (left). Dapi counterstain (blue). Arrowheads, sub-epicardial vessels. Arrows, endocardium. Quantification of *Jag1$^{flox}$;Nfatc1-Cre* and *Dll4$^{flox}$;Nfatc1-Cre* data at E12.5; average number of AVM and branching points in sub-epicardial vessel plexus, CM thickness, N1ICD-positive nuclei as a percentage of total nuclei in sub-epicardial vessels Data are mean +/- s.d. (n=3 sections from 4-7 control WT and n=3 from 3-5 mutant embryos). *$P < 0.05$, **$P < 0.01$, ***$P < 0.005$ ****$P < 0.0001$ by one-way ANOVA with Tukey's multiple comparison tests. Scale bars, 100 μm.

**Jag1 and Dll4 are regulating proliferation of the endothelium from the SV while myocardial patterning is maintained**

Although in both *Jag1$^{flox}$;Nfatc1-Cre* and *Dll4$^{flox}$;Nfatc1-Cre* mutant embryos reduced myocardial proliferation was detected, the subepicardial endothelium appeared to be 60% reduced in *Jag1$^{flox}$;Nfatc1-Cre* and 60% above normal in *Dll4$^{flox}$;Nfatc1-Cre* measured by EdU incorporation over all ERG$^{+}$ nuclei in Endomucin marking vessels (**Fig.10a**). In situ hybridization for *Gja5*/*Cx40* marking trabecular myocardium or *Hey2* marking compact myocardium, were showing normal expression suggesting that myocardial patterning was not affected by defective coronary development (**Fig.10b).** To determine whether metabolic compartmentalization between trabecular and compact myocardium was conserved we examined the expression of *Pdk1* and *Ldha,* two glycolytic enzymes involved in glucose metabolism. *Pdk1* and *Ldha* were both expressed normally in compact myocardium, suggesting that the activation of the glucose-based metabolism gene program was normal in both genotypes, and that patterning of the compact myocardium was conserved (**Fig.10b**).

**Arrested myocardial growth in endocardial Jag1 or Dll4 mutants is due to a global hypoxic and metabolic stress response**

To evaluate the global gene transcriptional changes resulting from by defective SV sprouting we performed RNA sequencing (RNA-seq) on E12.5 *Jag1$^{flox}$;Nfatc1-Cre* and *Dll4$^{flox}$;Nfatc1-Cre* hearts.

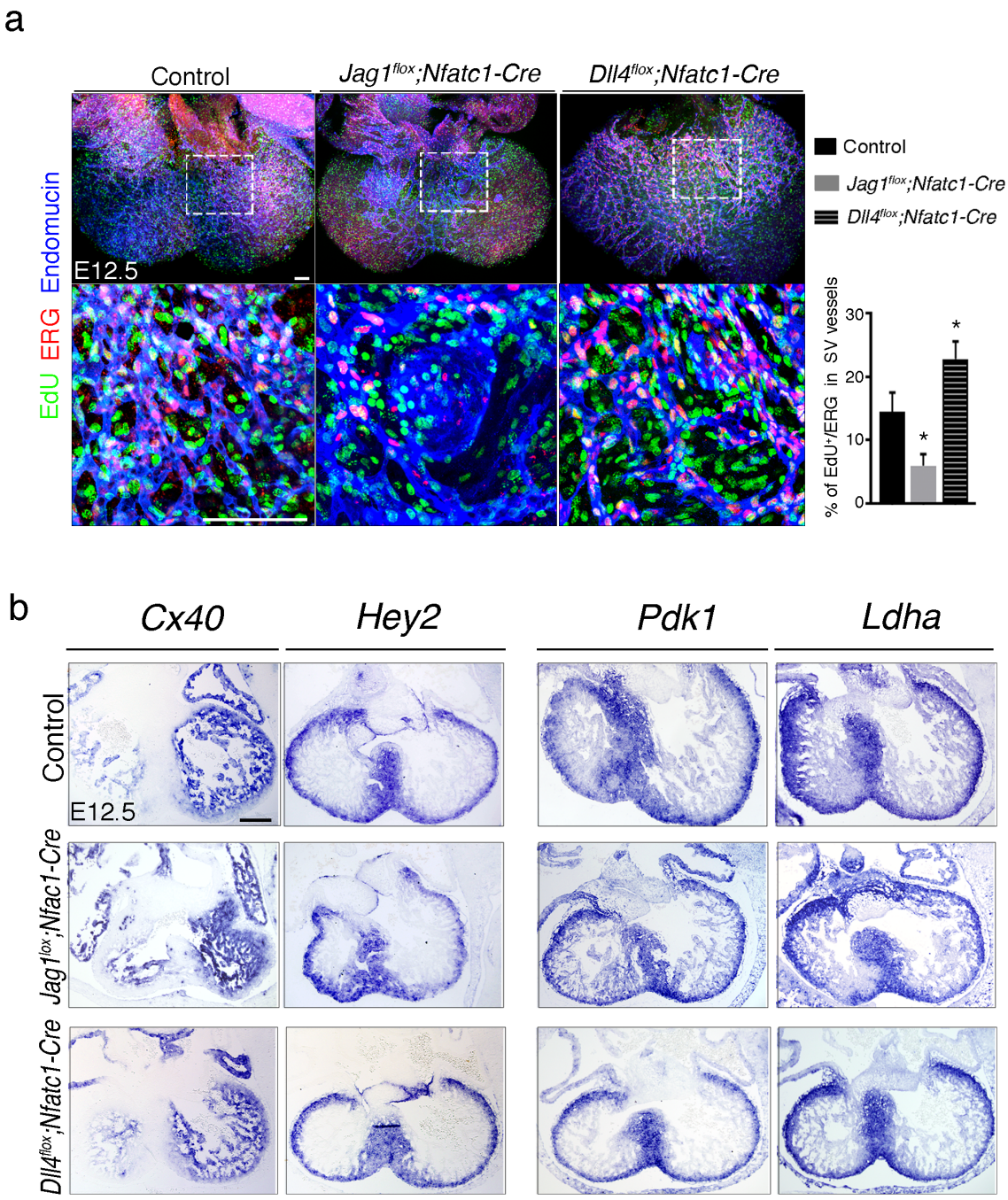



**Fig. 10**. **Endocardial *Jag1* or *Dll4* deletion disrupts endothelial proliferation without affecting myocardial patterning. (a)** Dorsal view of whole-mount stained hearts for EdU (green), ERG (red), and Emcn (blue), in E12.5 control, *Jag1$^{flox}$;Nfat-Cre* and *Dll4$^{flox}$;Nfatc1-Cre* mutants. Quantification of EdU-Erg dual positive nuclei as percentage (%) of total nuclei in sub-epicardial vessels.. Data are mean ± s.d. (n=3 control hearts and n=3 mutant hearts). *$P$ < 0.05 by Student's *t*-test. Source data are available in Supplementary Table 5. .(**b**) ISH of trabecular myocardium marker *Cx40,* compact myocardium marker *Hey2,* and glycolytic markers *Pdk1* and *Ldha* on E12.5 control, *Jag1$^{flox}$;Nfat-Cre and Dll4$^{flox}$;Nfatc1-Cre* heart sections. Scale bars, 100 µm.

RNA-seq analysis yielded 205 differentially expressed genes (DEG) in the *Jag1$^{flox}$;Nfatc1-Cre* transcriptome (128 upregulated, 77 downregulated) and 257 DEGs in the *Dll4$^{flox}$;Nfatc1-Cre* transcriptome (164 upregulated, 93 downregulated**; Fig.11**; **Suppl. Table3**)

Comparative transcriptome profiling identified 31 common DEG (27 upregulated, and 4 downregulated) (**Fig.11a,b**). Ingenuity Pathway Analysis (IPA) identified the enrichment of EC functions (**Fig.11c**). The main GO terms upregulated in both genotypes were angiogenesis and EC development (**Fig.11c**), while capillary vessel density was reduced in both genotypes, possibly reflecting the lack of a normal-sized capillary network (**Fig11c; Suppl. Table 3**). EC proliferation and heart contraction were upregulated in *Jag1flox;Nfatc1-Cre* embryos, and EC migration was upregulated in *Dll4flox;Nfatc1-Cre* mice (**Fig.11c; Suppl. Table 3**). Analysis of upstream regulators revealed activation of hypoxia (Hif1α), acute inflammatory response (Nf-κb1a), intracellular stress pathways (Atf4), and response to metabolic stress pathways (Foxo), while cell cycle and DNA repair pathways (Myc, Tp53) were negatively regulated (**Fig.11d**).

The comparative transcriptome profiling of RNA-seq from *Jag1$^{flox}$;Nfatc1-Cre and Dll4$^{flox}$;Nfatc1-Cre* identified 31 common DEG (27 upregulated, and 4 downregulated) (**Fig.11a**). Among them *Mt2* and *Mt1,* indicators of oxidative stress, were upregulated. Moreover *Vegfa* and *Slc2a3* upregulation was confirming the high hypoxic response in both mutant hearts, while Dll1, another notch1 ligand important in arterial identity, was downregulated, indicating the lack in coronary artery development **(Fig.11b)**.

Ingenuity Pathway Analysis (IPA) identified a strong relationship with EC functions and Gene Onthology terms as "Angiogenesis, Development of vasculature or vasculogenesis" were common to both genotype (**Fig.11c**). EC proliferation and heart contraction were upregulated in *Jag1$^{flox}$;Nfatc1-Cre* embryos, and migration of EC was upregulated in *Dll4$^{flox}$;Nfatc1-Cre* mice (**Fig.11c**). Analysis of upstream regulators revealed that hypoxia (Hif1α), acute inflammatory response (Nf-κb1a), intracellular stress pathways (Creb1), and response to metabolic stress pathways (Foxo) were all activated, while cell cycle and DNA repair pathways (Myc, Tp53) were negatively regulated (**Fig.11c**). Genes prominently downregulated in both genotypes were Notch pathway elements (*Jag1, Dll4, Dll1, Notch1, HeyL*; **Fig.11c,d**), and ISH showed reduced expression of *HeyL* and the Notch target *Efnb2* in subepicardial vessels (**Fig.12c**).

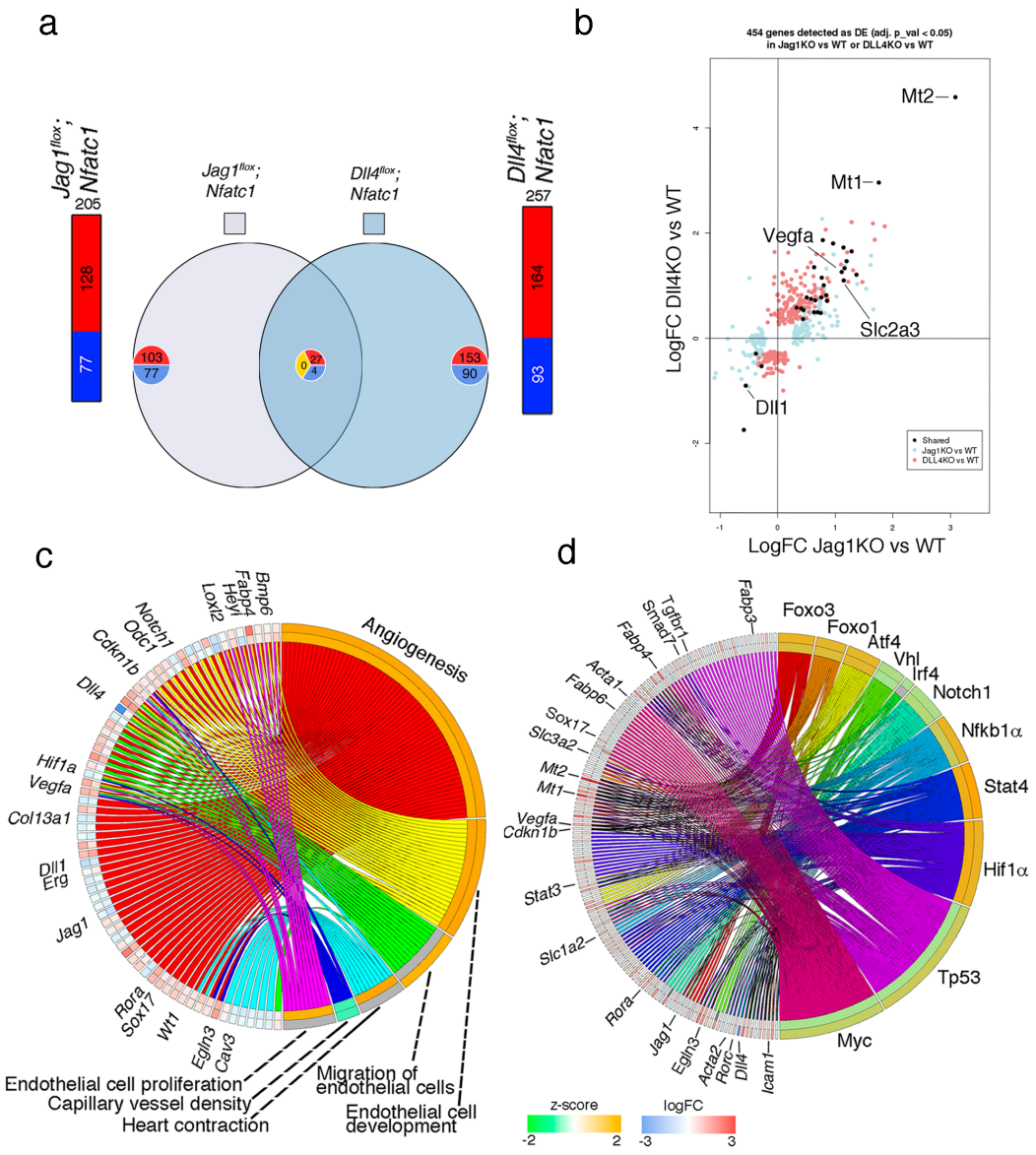



**Fig.11**, **Comparative gene expression profiling** (**a**) Chart showing the total number of DEGs identified by RNA-seq ($P < 0.05$) in the indicated genotypes. Numbers in red and blue sections indicate upregulated and downregulated genes, respectively. Venn diagram representation of the comparative analysis of differentially expressed genes (DEG) (**b**) Scatter plot of the DEGs in *Jag1$^{flox}$;Nfatc1-Cre* (blue dots) and *Dll4$^{flox}$;Nfatc1-Cre* (red dots). Shared DEGs (black dots). (**c**). Circular plot of representative DEG, simultaneously presenting a detailed view of the relationships between expression changes (left semicircle perimeter) and processes (right semicircle perimeter). In the left semicircle perimeter, the inner ring represents *Jag1$^{flox}$;Nfatc1-Cre* data and the outer ring *Dll4$^{flox}$;Nfatc1-Cre* data. Activation z-score scale: green repression; orange, activation; white, unchanged. LogFC scale: red, upregulated; blue, downregulated; white, unchanged. (**d**) Right, circular plot showing representative DEG belonging to selected upstream regulators.

Fabp4, a member of the fatty acid binding protein family, was upregulated (**Fig.11c**), and found in the atrio-ventricular groove in *Jag1flox;Nfatc1-Cre* hearts (**Fig. 12c**), while extending sub-epicardially into the base of the heart in *Dll4flox;Nfatc1-cre* hearts (**Fig.12c**). Vegfa was upregulated in all the cardiac tissues (**Fig.12c**), suggesting a cardiac hypoxic response in mutant embryos. Cell cycle-associated genes such as Cdkn1b/p27, a negative regulator of cell proliferation, were also upregulated in both genotypes (**Fig.12a**), and p27 nuclear staining was increased 2-fold throughout the heart (**Fig.12b**), indicating decreased cell proliferation.

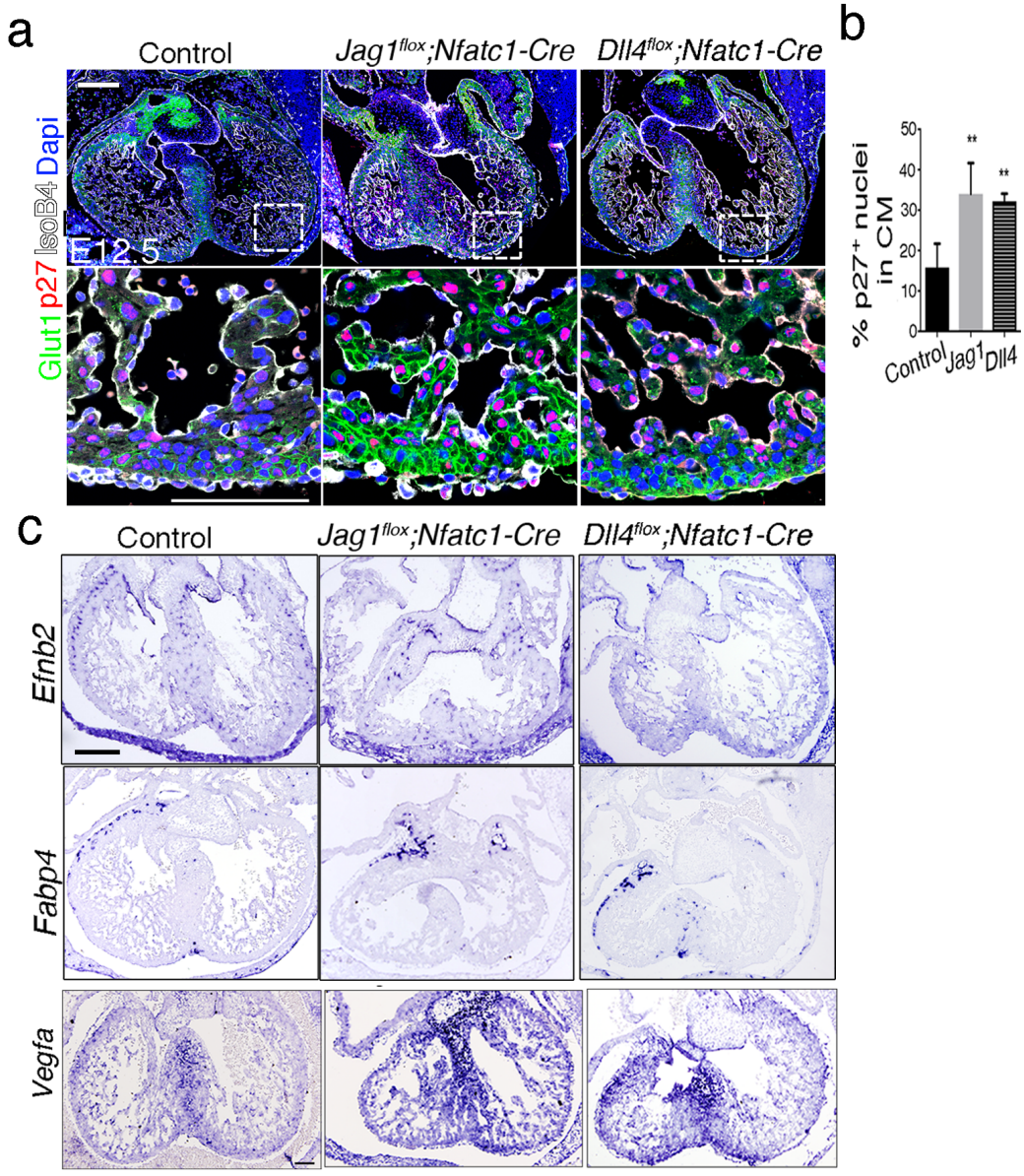


**Fig.12 Gene profiling analysis of E12.5 hearts.** (**a**) Immunohistochemistry of p27 (red), Glut1 (green), and IsoB4 (white) on E12.5 control, *Jag1flox;Nfatc1-Cre*, and *Dll4flox;Nfatc1-Cre* mutant heart sections. Dapi counterstain (blue). (**b**) Quantification of % of p27 in CM. p27-positive nuclei as a % of total CM nuclei. Data are mean +/- s.d. (n= 3 sections from 4-7 control embryos and n= 3 from 3-5 mutant embryos). *P < 0.05 by Student's t-test.. (**c**) ISH of *Efnb2, Fabp4* arterial markers and *Vegfa* on E12.5 control, $Jag1^{flox}$*;Nfatc1-Cre* and $Dll4^{flox}$*;Nfatc1-Cre* heart sections.. Scale bars, 100 μm.

**Defective coronary remodelling and maturation in endothelial *Jag1* and *Dll4* mutants**

To examine whether endothelial Jag1 is required for coronary vessel remodelling, we crossed $Jag1^{flox}$ mice with the tamoxifen-inducible endothelial driver line $Cdh5\text{-}Cre^{ERT2}$. Tamoxifen administration at E9.5 produced E15.5 $Jag1^{flox}$*;*$Cdh5\text{-}Cre^{ERT2}$ embryos with thinner ventricular walls (**Fig.14a**). The coronary tree displayed markedly reduced artery formation, and increased vein density (**Fig.13a,c**), suggesting defective coronary plexus remodelling. *Efnb2* and *Dll4* endothelial expression was confined to smaller calibre vessels in the ventricles (**Fig.14b**), whereas *Fapb4* appeared to be upregulated (**Fig.14b**).

Endothelial N1ICD staining in the ventricles was increased by 30% (**Fig.13b,c**), presumably due to the persistence of numerous smaller vessels. To determine the extent of smooth muscle cell differentiation and pericyte coverage, we stained for α-smooth muscle actin (αSMA) and Notch3, respectively. The proportion of αSMA- and Notch3-positive cells was reduced in E16.5 coronary arteries (**Fig.13b,c**), suggesting that mural cells were recruited but failed to differentiate.

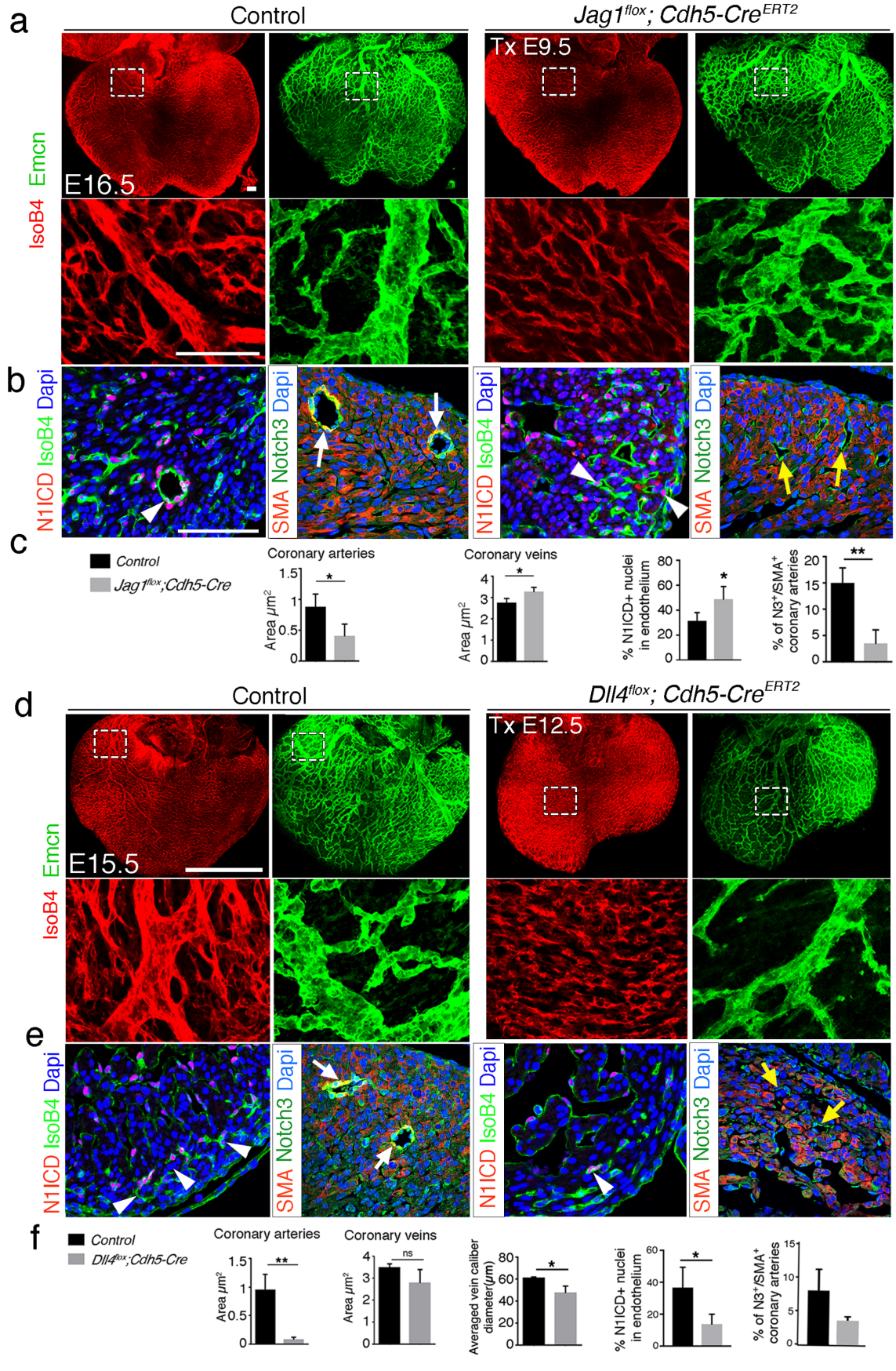

a
Control
Jag1flox; Cdh5-CreERT2
Tx E9.5
E16.5
Emcn
IsoB4
b
N1ICD IsoB4 Dapi
SMA Notch3 Dapi
c
Control
Jag1flox;Cdh5-Cre
Coronary arteries
Coronary veins
Area µm2
% N1ICD+ nuclei in endothelium
% of N3+/SMA+ coronary arteries
d
Control
Dll4flox; Cdh5-CreERT2
Tx E12.5
E15.5
e
f
Control
Dll4flox;Cdh5-Cre
Coronary arteries
Coronary veins
ns
Averaged vein caliber diameter(µm)
% N1ICD+ nuclei in endothelium
% of N3+/SMA+ coronary arteries

**Fig. 13. Late endothelial *Jag1* or *Dll4* inactivation disrupts coronary plexus remodelling. (a)** Dorsal view of whole-mount immunochemistry for Emcn (green) and IsoB4 (red) in E16.5 control and *Jag1$^{flox}$;Cdh5-Cre$^{ERT2}$* mutant hearts, tamoxifen (Tx)-induced at E9.5. Scale bars, 100 µm. **(b)** Control and *Jag1$^{flox}$;Cdh5-Cre$^{ERT2}$* mutant heart sections at E16.5. Left, immunostaining for N1ICD (red), and IsoB4 (green). Right, α-smooth-muscle actin (SMA, red) and Notch3 (green). Dapi counterstain (blue). Arrowheads indicate N1ICD-positive nuclei. Arrows point to SMA-Notch3 co-immunostaining. Yellow arrows point to small calibre intramyocardial vessels in Jag1 mutant. **(c)** Quantified data from E15.5 control and *Jag1flox;Cdh5-Cre$^{ERT2}$* hearts: area of coverage by coronary arteries and veins; N1ICD-positive nuclei as a percentage of total endothelial nuclei; and SMA-Notch3 co-immunostaining in coronary arteries. (**d**) Whole-mount dorsal view of immunohistochemistry for Emcn (green) and IsoB4 (red) in E15.5 control and *Dll4$^{flox}$;Cdh5-Cre$^{ERT2}$* mutant hearts tamoxifen (Tx)-induced at E12.5. **(e)** Control and *Dll4$^{flox}$;Cdh5-Cre$^{ERT2}$* mutant heart sections at E15.5. Immunohistochemistry on left for N1ICD (red) and IsoB4 (green), and on right SMA (red) and Notch3 (green.. Dapi counterstain (blue). Arrowheads indicate N1ICD-positive nuclei. Arrows point to SMA-Notch3 co-immunostaining. Yellow arrows point to small calibre intramyocardial vessels in *Dll4* mutant. Scale bars as in (a). (**f**) Quantified data from E16.5 control and *Dll4flox;Cdh5-Cre$^{ERT2}$* hearts: area covered by coronary arteries; area covered by veins; mean vein calibre; percentage of N1ICD-positive nuclei in endothelium as a percentage (%) of total nuclei; and SMA-Notch3 co-immunostaining in coronary arteries. Data are mean +/- s.d. (n= 3 sections from 3 control embryos and from 3-4 mutant embryos). *****P < 0.05, ******P < 0.01, by Student's t-test; n.s. not significant.

To determine the role of Dll4 in coronary vessel remodelling we crossed *Dll4$^{flox}$* mice with the *Cdh5-Cre$^{ERT2}$* driver line to obtain *Dll4$^{flox}$;Cdh5-Cre$^{ERT2}$* mice. Tamoxifen-induced *Dll4* inactivation from E12.5 onwards produced E15.5 embryos with thinner ventricular walls (**Fig. 14a**). The coronary tree displayed a complete absence of arteries (**Fig.13d,f**); although patterning of the veins appeared unaffected, their calibre was reduced (**Fig.13d,f**). N1ICD staining in the endothelium was decreased by 60% compared with controls (**Fig.13e,f**), likely due to reduced EC contribution to the arteries. Furthermore, *Dll4$^{flox}$;Cdh5-Cre$^{ERT2}$* mutants had deficient smooth muscle cell differentiation (**Fig.13e,f**).

RNA-seq of E15.5 *Dll4$^{flox}$;Cdh5-Cre$^{ERT2}$* mutant ventricles yielded 156 DEGs (136 upregulated; 20 downregulated; **Suppl. Table 2**). As expected, *Dll4* was downregulated and *Vegfa* was upregulated, suggesting cardiac hypoxia,. *Cdkn1a/p21* was also upregulated, indicating impaired cell proliferation (**Suppl. Table 2**). *Efnb2* and *Dll4* showed reduced endothelial expression in smaller calibre vessels (**Suppl. Table 2**) and ISH for *Efnb2* transcript in both *Jag1$^{flox}$;Cdh5-Cre$^{ERT2}$*and *Dll4$^{flox}$;Cdh5-Cre$^{ERT2}$* mutants was confined to very small calibre vessels (**Fig.14b**), whereas *Fapb4*, was upregulated (**Suppl. Table 2**) and found in the endothelium of both mutants, a strong indication of a (**Fig.14b**). IPA

identified strong upregulation of endothelial cell functions (**Suppl. Table 3**) and analysis of upstream regulators identified enrichment for transcriptional activators associated with innate inflammatory responses (Irfs and Stats), suggesting defective vascular integrity, while other upstream regulators were associated with cardiovascular disease, including hypertrophy (Nfatc2) and oxidative stress responses (Nfe212; **Suppl. Table 3**).

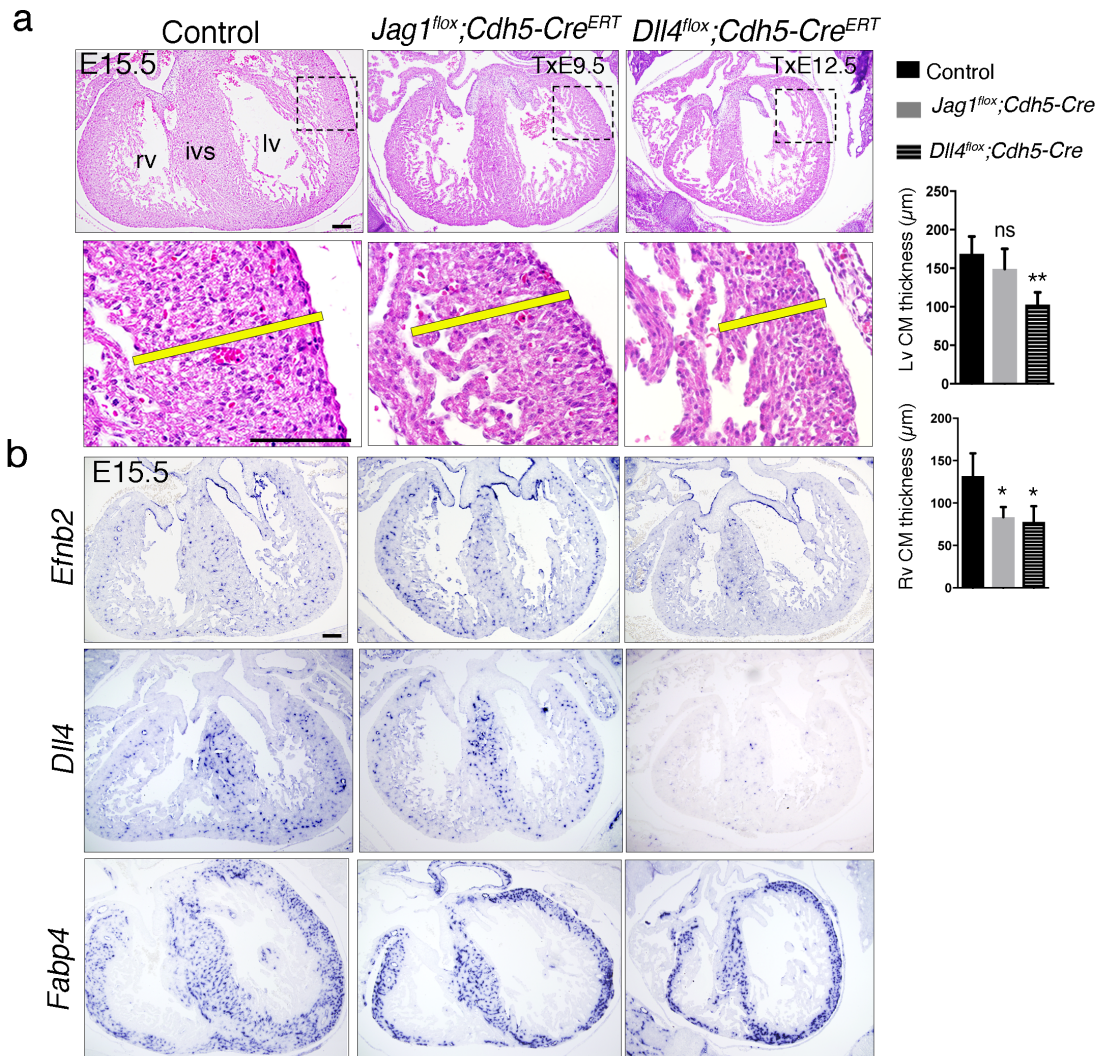



**Fig.14**. **Induced endothelial *Jag1* or *Dll4* deletion disrupts myocardial growth and arterial differentiation (a)** H&E staining of transverse heart sections of E15.5 control, and *Jag1$^{flox}$;Cdh5-Cre$^{ERT2}$* tamoxifen (Tx)-induced mice at E9.5, and E16.5 control and *Dll4$^{flox}$; Cdh5-Cre$^{ERT2}$* mice Tx-induced at E12.5. Quantification of compact myocardium thickness in left ventricle (lv) and right ventricle (rv). ivs, interventricular septum. Data are mean +/- s.d. (n= 3 sections from 3 control embryos and from 3-4 mutant embryos). *P < 0.05, **P < 0.01, by Student's t-test; n.s. not significant **(b)** ISH of heart sections of arterial markers *Efnb2, Dll4*, and *Fabp4* on E15.5 control, *Jag1$^{flox}$;Cdh5-Cre$^{ERT2}$* mice Tx-induced at E9.5 and *Dll4$^{flox}$; Cdh5-Cre$^{ERT2}$* mice Tx-induced at E12.5. Scale bars, 100 µm.

ISH for *Efnb2* transcript in both E15.5 *Jag1$^{flox}$;Cdh5-Cre$^{ERT2}$*and *Dll4$^{flox}$*;*Cdh5-Cre$^{ERT2}$* mutants was confined to very small calibre vessels (**Fig.14b**). Interestingly up-regulation of *Fabp4*, a molecule needed for fatty acid transport across the vessel wall, was found in the endothelium of both mutants, a strong indication of a defective cardiac metabolic remodelling (**Fig.14b**).

Histological analysis revealed reduction in the thickness of the ventricular wall in both left and right ventricles for *Dll4$^{flox}$*;*Cdh5-Cre$^{ERT2}$* mutants and of right ventricles for *Jag1$^{flox}$;Cdh5-Cre$^{ERT2}$* mutants (**Fig.14a**).

**Forced endothelial *Dll4* expression disrupts coronary vascular remodelling**

To examine coronary development in mice with endothelial *Dll4* gain-of-function, we generated a transgenic line (*Dll4$^{GOF}$*) bearing a *Rosa26-CAG-floxNeoSTOPflox-Dll4-6xMycTag* expression cassette (**Fig.15d**). *Tie2-Cre*-mediated removal of the *floxed NeoSTOP* sequences resulted in a mild 1.2-fold endothelial *Dll4* overexpression that permitted survival of transgenic embryos bearing a single copy of the *Dll4$^{GOF}$* allele (**not shown**). At E12.5, endothelial *Dll4* overexpression did not affect sprouting from SV but the coronary vasculature of *Dll4$^{GOF}$;Tie2-Cre* embryos displayed malformations similar to those in *Jag1*- and *Dll4*;*Cdh5-Cre$^{ERT2}$* mutants (**Fig.15e**). At E14.5, forced *Dll4* expression lead to increased although not significant sub-epicardial vein coverage and vascular malformations (**not shown**). However, by E16.5 the arterial coverage was substantially decreased (**Fig.16a**). Accordingly, *Efnb2* expression was restricted to smaller calibre vessels in *Dll4$^{GOF}$* transgenics (**Fig.17c**). In contrast, sub-epicardial veins were more numerous and dense (**Fig.16a**). N1ICD expression was increased and extended to the prospective veins (**Fig.17a**), consistent with a Notch gain-of-function phenotype. Arterial smooth muscle cell coverage was also substantially reduced (**Fig.17a**), suggesting defective pericyte and/or smooth muscle differentiation.

Therefore, endothelial *Dll4* overexpression blocks coronary artery formation, vessel remodelling and maturation, and impairs cardiac growth. These results were somewhat surprising, as our loss-of-function data support a pro-arteriogenic role for Dll4.

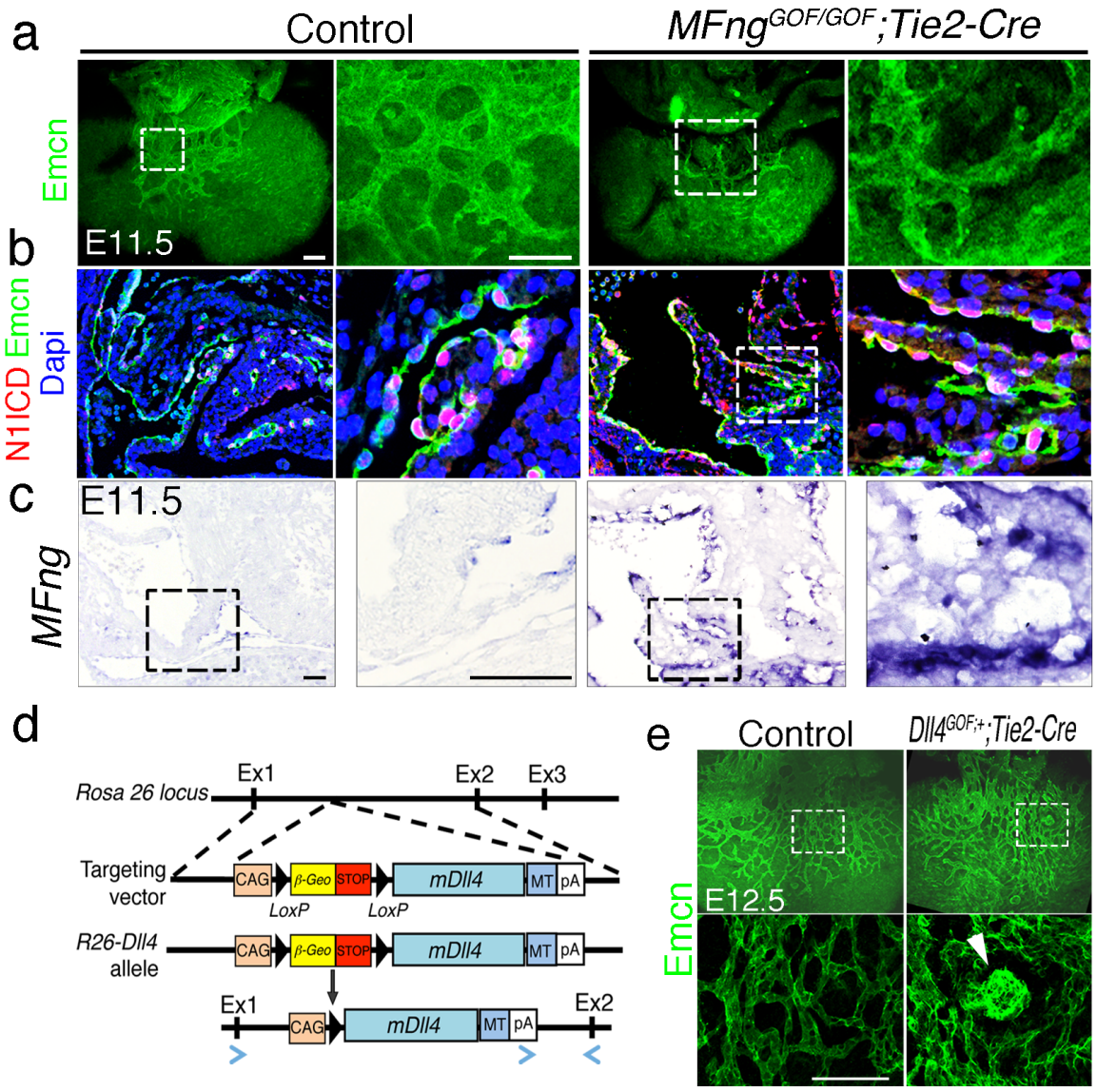



**Fig.15. Forced *Dll4* or *MFng* expression leads to early SV sprouting defects (a)** Dorsal view of whole-mount immunochemistry for Emcn (green) in E11.5 control and *MFng*$^{GOF}$*;Tie2-Cre* hearts. **(b)** Immunohistochemistry for N1ICD (red) and Emcn (green) on E11.5 control and *MFng*$^{GOF}$*;Tie2-Cre* heart sections. Dapi counterstain (blue). arrowheads indicate N1ICD-stained nuclei. sv, sinus venosus. Scale bars, 100 µm. **(c)** ISH in E11.5 control and *MFng*$^{GOF}$*;Tie2-Cre* heart sections showing *MFng* overexpression in sinus venosus (sv) of *MFng*$^{GOF}$*;Tie2-Cre* mutant heart. **(d)** Gene targeting strategy used to generate the conditional *Dll4*$^{GOF}$*;Tie2-Cre* mutant. **(e)** Dorsal view of whole-mount immunochemistry for Emcn (green). Arrow points to an arterio-venous malformation. Scale bar, 100 µm.

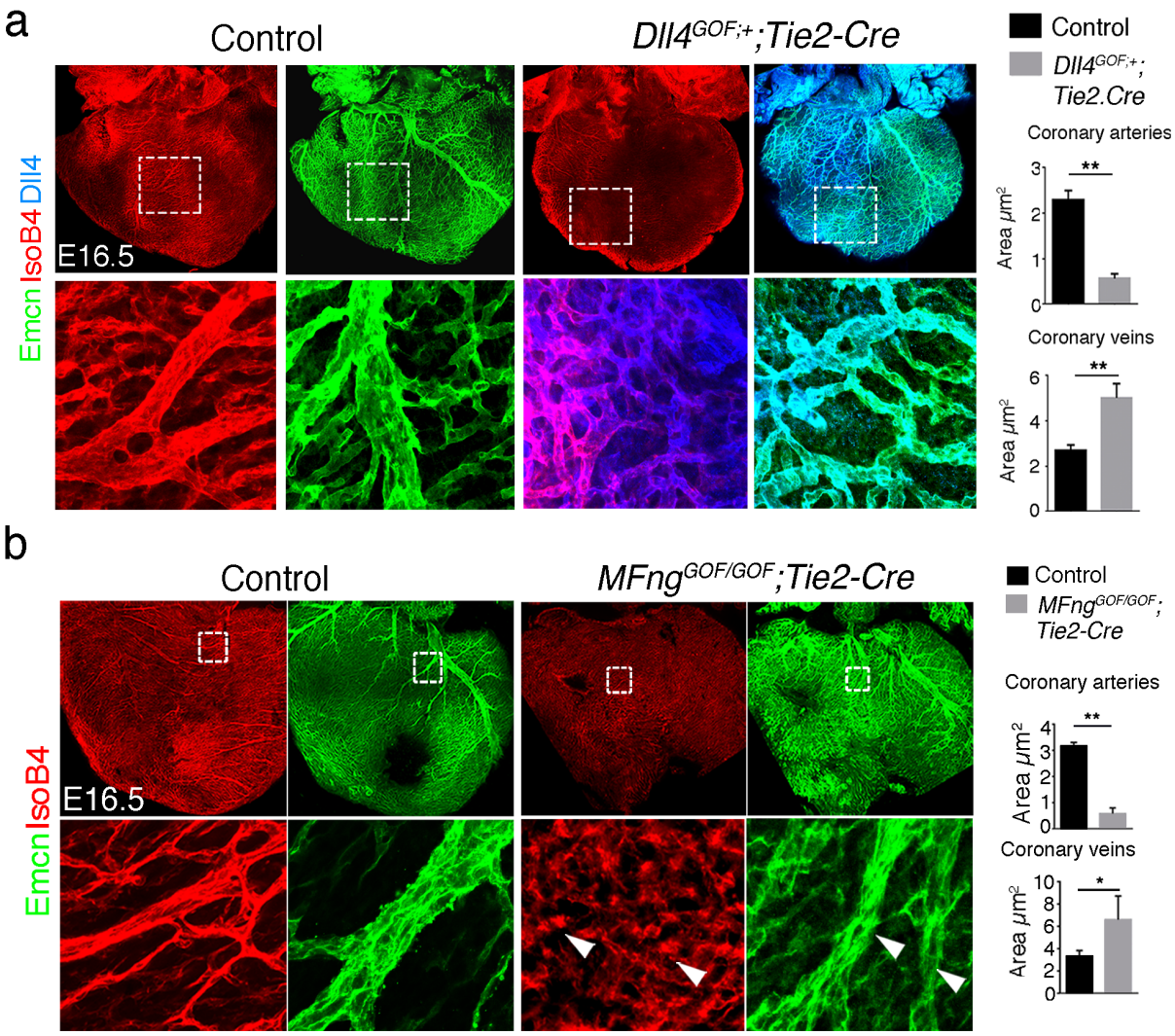



**Fig.16. Forced *MFng* and *Dll4* expression impair left coronary development.** (**a**) Dorsal view of whole-mount immunhistochemistry for IsoB4 (red) and Emcn (green) in E16.5 control and *Dll4*$^{GOF}$*;Tie2-Cre* hearts. Scale bar, 100 µm (**b**) Dorsal view of whole-mount immunohstochemistry for IsoB4 (red) and Emcn (green) in E16.5 control and *MFng*$^{GOF}$*;Tie2-Cre* hearts. Scale bars as in **(a).** Quantification data from E16.5 control and *Dll4*$^{GOF}$*;Tie2-Cre,* and control and *MFng*$^{GOF}$*;Tie2-Cre* mutant hearts: area covered by coronary arteries (IsoB4); area covered by veins (Emcn). Data are mean ± s.d $^{**}P < 0.01$; $^{*}P < 0.05$. n.s not significant.

**Forced endothelial *MFng* expression phenocopies *Dll4* gain-of-function in coronaries**

To support the *Dll4*$^{GOF}$ result, we used a transgenic line conditionally expressing MFng (*MFng*$^{GOF}$) to test whether increased MFng activity favoured Dll4-mediated signaling and thus impaired arteriogenesis (D´Amato *et al.*, 2016). At E11.5,

*MFng*$^{GOF}$*;Tie2-Cre* embryos displayed reduced SV sprouting, increased Notch1 signaling and myocardial wall thinning (**Fig.15a**). However, by E16.5 *MFng*$^{GOF}$*;Tie2-Cre* embryos displayed an extensive vascular network, although the arteries appeared atrophied (**Fig.16b**) and prospective veins appeared more numerous and intricately branched (**Fig.16b**). *MFng*$^{GOF}$*;Tie2-Cre* embryos displayed numerous capillary malformations (**Fig.16b**), suggesting defective arterial-venous differentiation. The decreased arterial coverage, and increased vein coverage in *MFng*$^{GOF}$*;Tie2-Cre* embryos, was associated with increased Notch1 activity (**Fig.17b**) consistent with a Notch gain-of-function phenotype. The expression of the Notch target *Efnb2* was restricted to smaller calibre vessels (**Fig.17c**), and *Vegfa* was upregulated throughout the heart (**not shown**), suggesting hypoxia. Pericyte coverage and smooth muscle differentiation were significantly decreased at E16.5, as shown by co-staining of αSMA and Notch3 (**Fig.17b**), suggesting a coronary artery maturation defect.

RNA-seq analysis of E15.5 *MFng*$^{GOF}$*;Tie2-Cre* ventricles identified > 1900 DEGs ($P < 0.05$) and 500 DEG with abs (logFC) > 0.5 (372 upregulated, 128 downregulated; **Suppl. Table 2**). Among prominent up-regulated genes was the p21-encoding gene *Cdkn1a*, suggesting that cell proliferation was decreased in transgenic hearts. IPA identified several enriched terms highly relevant to EC function, including vessel morphogenesis and guidance during angiogenesis (**Suppl. Table 3**). These functions were exemplified by semaphorins, which regulate tip-cell fate decisions and branching morphogenesis upstream of DLL4–NOTCH (Kim *et al.*, 2011) Analysis of upstream regulators (**Suppl. Table 3**) identified activation of innate and adaptive immune pathways (Irf3, Irf7, Creb1), consistent with type I and type II interferon responses. Also upregulated were hypoxia (Hif1α), intracellular stress pathways (Atf4,) and pro-fibrotic pathways such as Tgfβ (Smad3). In contrast, transcriptional activators involved in hedgehog signaling (Glis2) and regulation of hemodynamics (Klf2) were downregulated.

In sum, endothelial *MFng* overexpression compromises endothelial structural integrity, disrupts vessel remodelling, and impairs cardiac growth and maturation, phenocopying the endothelial *Dll4* gain-of-function phenotype.

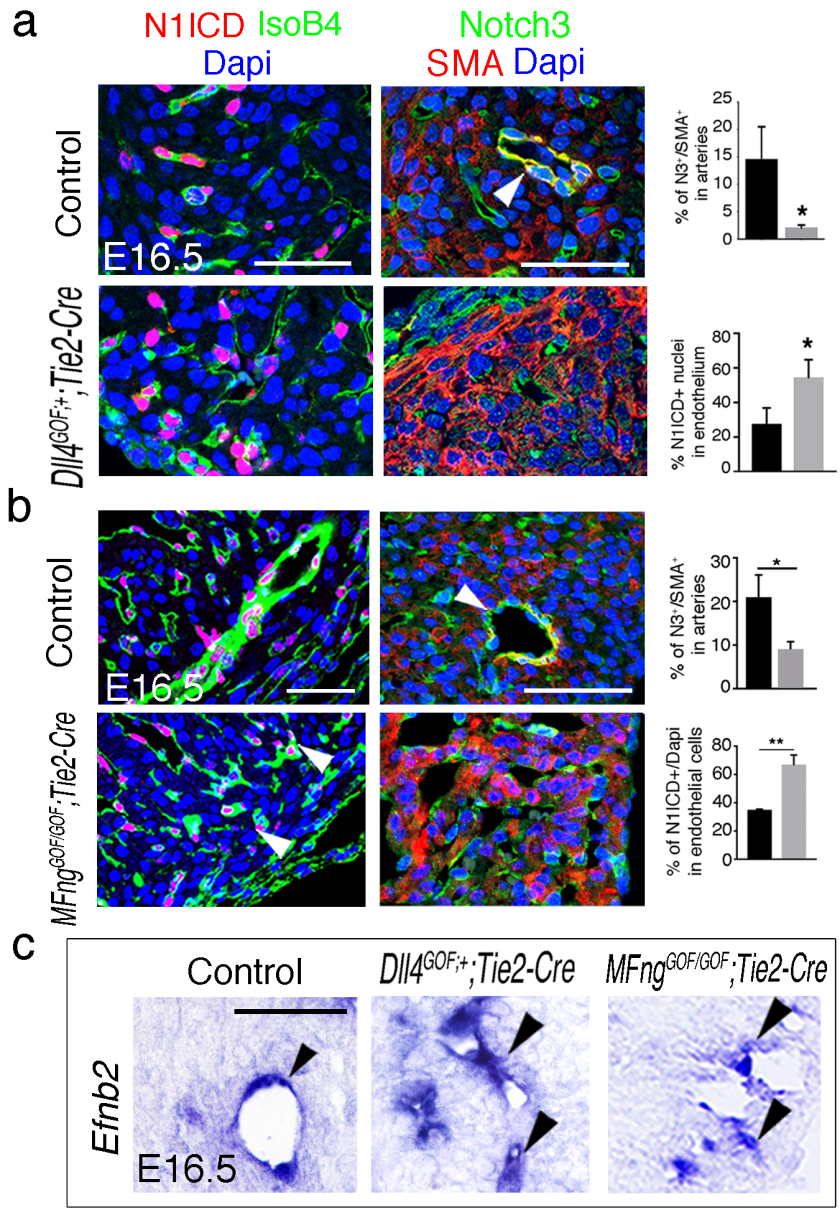



**Fig.17. Forced endothelial *Dll4* or *MFng* expression disrupts coronary arteriovenous differentiation and remodelling**. **(a)** E16.5 control and *Dll4*$^{GOF}$*;Tie2-Cre* mutant hearts. Left; Immunohistochemistry for N1ICD (red) and IsoB4 (green). Right; Immunohistochemistry for SMA (red) and Notch3 (green). Quantified data for control and *Dll4*$^{GOF}$*;Tie2-Cre* hearts, SMA-Notch3 co-immunostaining in coronary arteries and percentage of N1ICD-positive nuclei in endothelium as percentage (%) of total nuclei. **(b)** E16.5 control and *MFng*$^{GOF}$*;Tie2-Cre* mutant hearts. Left; Immunohistochemistry for N1ICD (red) and IsoB4 (green). Right; Immunohistochemistry for SMA (red) and Notch3 (green). Dapi counterstain (blue). Quantified data for control and *MFng*$^{GOF}$*;Tie2-Cre* hearts, SMA-Notch3 co-immunostaining in coronary arteries and percentage of N1ICD-positive nuclei in endothelium as percentage (%) of total nuclei. Data are mean ± s.d. (n= 3 sections from 3 control and n= 3 sections from 4 mutant embryos). *$P < 0.05$, **$P < 0.01$, by Student's *t*-test. **(c)** ISH of *Efnb2* on E16.5 control *Dll4*$^{GOF}$*;Tie2-Cre* and *MFng*$^{GOF}$*;Tie2-Cre* heart sections. Arrowheads indicate coronary arteries. Scale bars, 100 μm.

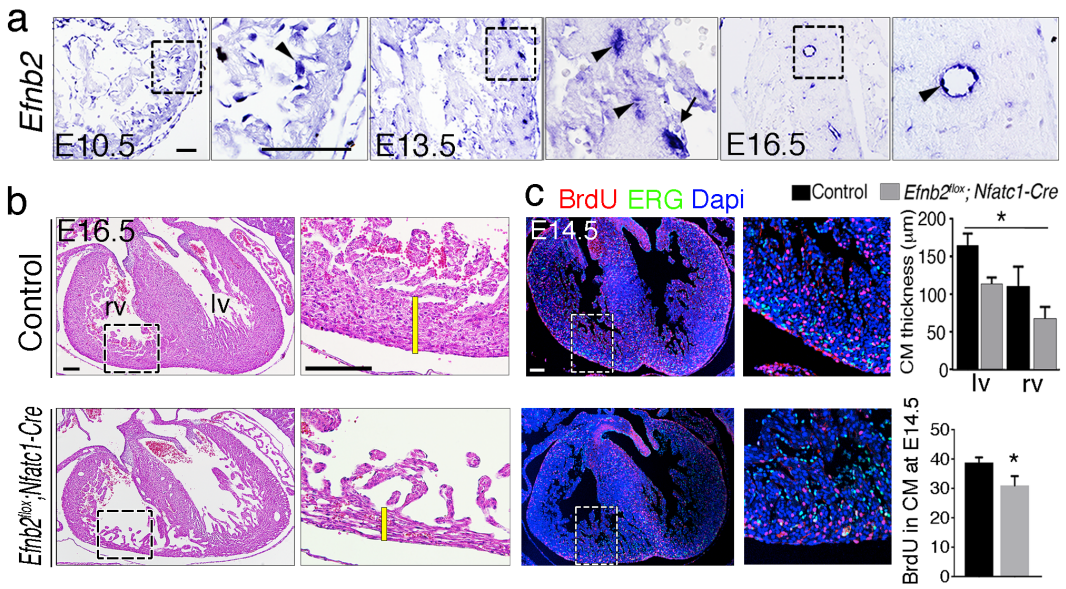



**Fig.18**. **Endocardial *Efnb2* deletion causes thin myocardium and decreased compact myocardium (CM) proliferation. (a) Efnb2 expression in developing coronaries.** ISH in control embryos showing *Efnb2* expression in chamber endocardium at E10.5 (arrowheads), coronary arteries (arrowheads) and a coronary vein (arrow) at E13.5, and in a coronary artery at E16.5 (arrowhead). Scale bars, 50 µm. **(b)** H&E staining of transverse heart sections of E16.5 control and *Efnb2$^{flox}$;Nfatc1-Cre* mutant hearts. The yellow bars indicate CM thickness **(c)** Immunohistochemistry for BrdU (red) and ERG (green) of E14.5 control and *Efnb2$^{flox}$;Nfatc1-Cre* hearts. Charts showing quantified data for control and *Efnb2$^{flox}$;Nfatc1-Cre* hearts compact myocardium thickness in left ventricle (lv) and right ventricle at E16.5. BrdU-stained nuclei in CM as a percentage (%) of all Dapi-stained nuclei at E14.5. Data are mean +/- s.d. (n= 3 sections from 3 control embryos and n=3 sections from 3 mutant embryos). *$P < 0.05$ by Student's *t*-test. Scale bars, 100 µm.

## *Efnb2* is required for coronary arteriogenesis and vessel branching

*Efnb2* is required for arterial-venous differentiation and vascular maturation (Kania and Klein 2016) and is a Notch target during ventricular chamber development (Grego-Bessa *et al.*, 2007). Moreover *Efnb2$^{flox/flox}$;Tie2-Cre* mice are lethal at E10.5 and show severe cardiac phenotype including a thin compact myocardium (Gerety *et al.*, 2002). We reasoned that *Efnb2* might mediate Notch function in coronary morphogenesis. *Efnb2* is expressed in ventricular endocardium at E10.5 (**Fig.18a**) but not in SV endothelium (**not shown**). At E13.5, *Efnb2* was found in emerging arteries and prospective veins, and at E16.5 was confined to arteries (**Fig.18a**). *Efnb2* is thus expressed dynamically in a pattern similar to *Dll4* and *MFng*.

To examine EphrinB2 function in coronary angiogenesis, we crossed mice bearing a conditional *Efnb2*$^{flox}$ allele with the *Nfatc1-Cre* line. About 60% of the resulting *Efnb2*$^{flox}$*;Nfatc1-Cre* mutants survived until birth, but none survived beyond postnatal day 21 (P21, **Suppl. Table 1**). Histological examination showed that the compact myocardium in the left and right ventricles was 30% thinner at E16.5 (**Fig.18b**), which could be attributed to the reduced proliferation observed at E14.5 (**Fig.18c**). Whole-mount IsoB4 immunostaining revealed reduced arterial coverage in E15.5 *Efnb2*$^{flox}$*;Nfatc1-Cre* hearts (**Fig.19a**), while vein coverage was unchanged (**Fig.19a**). The presence of smaller calibre arteries coincided with higher Notch1 activity (**Fig.19b**), suggesting negative feedback between Efnb2 and Notch1 signaling.

Although the patterning of prospective vein**s** was unchanged we found occasional venous malformations (**Fig.22g**) and trans-mural communications or shunts between the endocardium and epicardium, which we interpret as arteriovenous fistulae (**Fig.20a**). Accordingly, the venous marker *EphB4* was expressed ectopically in a subset of intra-myocardial vessels at E16.5 (**Fig.19c**), suggesting coronary vessel acquisition of venous identity. *Vegfa* was upregulated throughout the heart (**Fig.20a**), suggesting hypoxia. Smooth muscle cell coverage of the arteries was reduced substantially (**Fig.19d**), suggesting a vessel maturation defect. Ink perfusion in *Efnb2*$^{flox}$*;Nfatc1-Cre hearts* at E16.5 and E18.5 detected likely haemorrhaging in the most distal section of the coronary arterial tree (**Fig.20b,c**), consistent with vessel leakiness, while aortic connections were normal (**Fig.20b,c**). Thus, endocardial Ephrinb2 is required for coronary arterial remodelling and EC structural integrity. Myocardial growth and maturation are impaired in absence of endocardial *Efnb2*.

A subset of *Efnb2flox;Nfatc1-Cre* mutants survived post-natally until P21, allowing for the analysis of post-natal heart function in mutants. At P0 *Efnb2*$^{flox}$*;Nfatc1-Cre* mutant hearts had a thinner compact myocardium and displayed a muscular VSD compared to control (**Fig.21a**). ECG revealed the presence of cardiac arrhythmias (**Fig.21b**). Ultrasound echocardiography on mutant mice at P0 revealed increased LV mass and volume but EF and FS were unchanged (**Fig.21c**). Although post-natal *Efnb2flox;Nfatc1-Cre* mutant hearts display abnormal morphology, they are functionally normal, possibly because of compensatory hypertrophy of the myocardium.

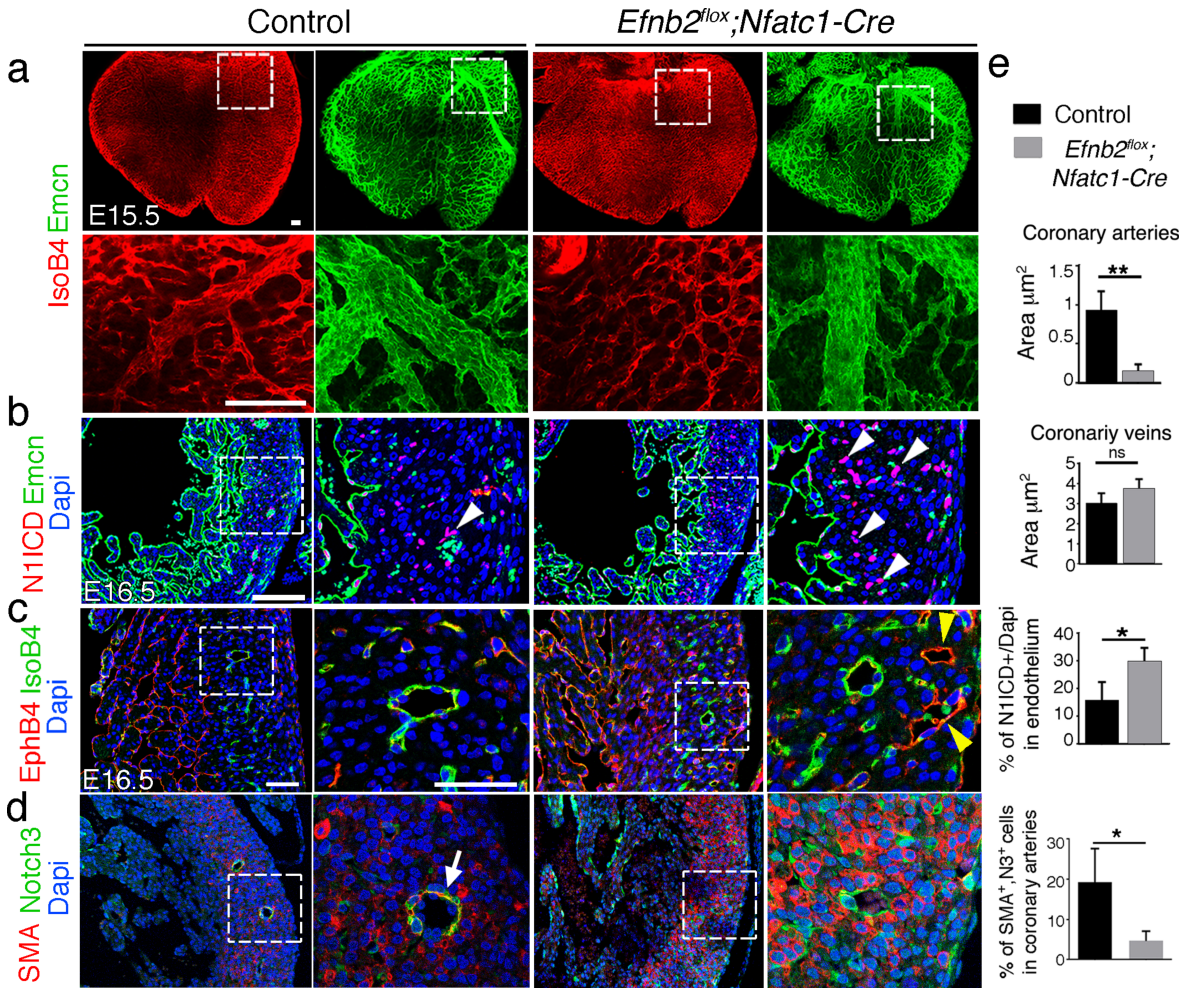



**Fig.19. Endocardial *Efnb2* inactivation disrupts coronary artery differentiation and remodelling. (a)** Dorsal view of whole-mount immunochemistry for IsoB4 (red) and Emcn (green) in E15.5 control and *Efnb2$^{flox}$;Nfatc1-Cre* hearts. .Scale bars,100 µm. **(b)** Immunohistochemistry of N1ICD (red) and Emcn (green) on E16.5 control and *Efnb2$^{flox}$;Nfatc1-Cre* heart sections. Dapi-counterstained (blue). Arrowheads indicate N1ICD-stained nuclei. Scale bars, 100 µm. **(c)** Immunohistochemistry for EphB4 (red) and IsoB4 (green) on E16.5 control and *Efnb2$^{flox}$;Nfatc1-Cre* heart sections. Dapi-counterstained (blue). Yellow arrowheads indicate EphB4-stained vessels. Scale bar, 50 µm. **(d)** Immunohistochemistry for SMA (red) and Notch3 (green) on E16.5 control and *Efnb2$^{flox}$;Nfatc1-Cre* heart sections. Dapi-counterstain (blue). Arrow points to a coronary artery stained by SMA and Notch3**. (e)** Quantified data for control and WT and *Efnb2flox;Nfatc1-Cre* hearts: at E15.5, area covered by coronary arteries and area covered by veins. At E16.5 percentage of N1ICD- stained nuclei in endothelium as percentage (%) of total nuclei, and SMA-Notch3 co-immunostaining in coronary arteries. Data are mean ± s.d. (n= 3 sections from 3 control and n= 3 sections from 4 mutant embryos). $^{*}P < 0.05$, $^{**}P < 0.01$, by Student's *t*-test; n.s., not significant.

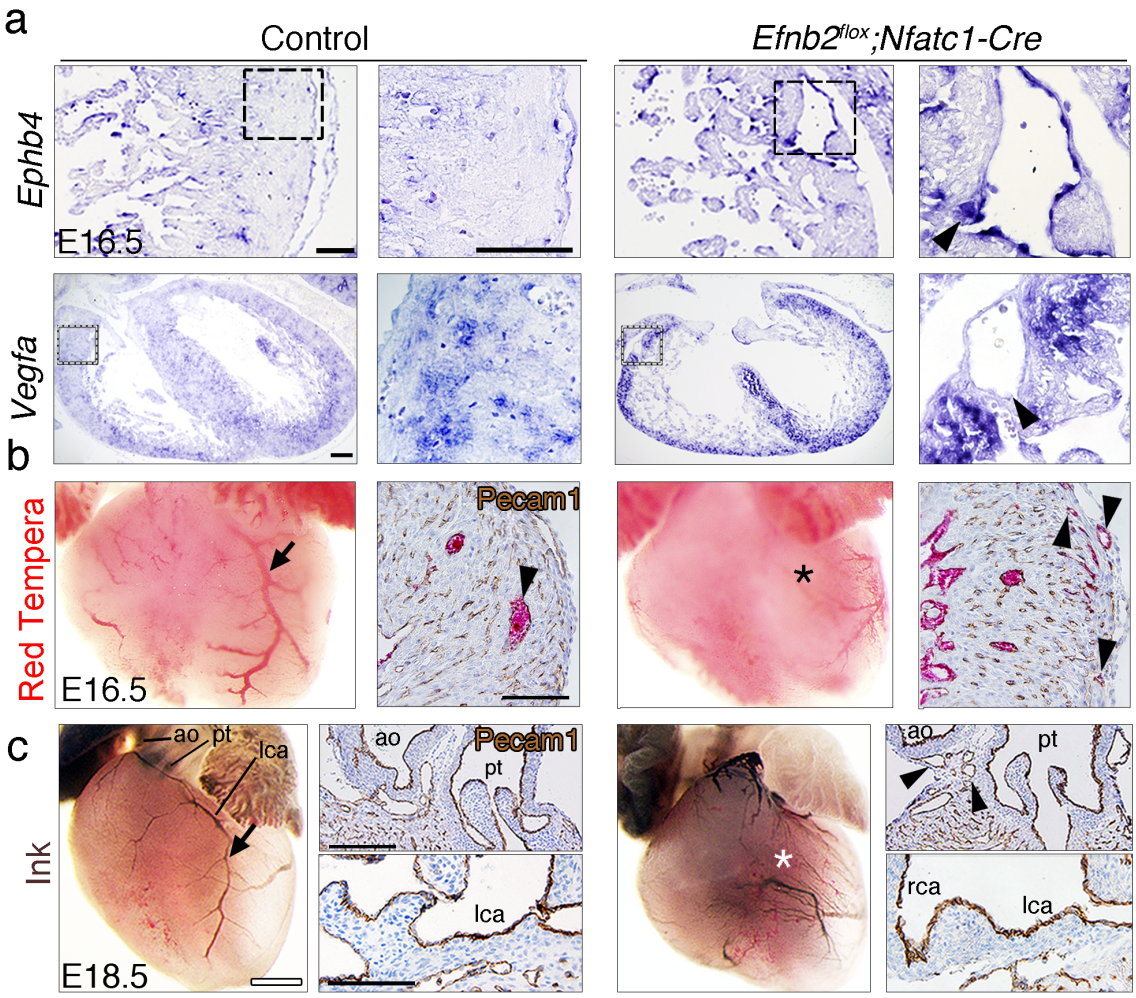



**Fig.20**. **Endocardial deletion of *Efnb2* causes arteriovenous fistulae and disrupts arterial endothelial integrity. (a)** ISH of venous marker *Ephb4* on control and *Efnb2$^{flox}$;Nfatc1-Cre* mutant showing increased *Ephb4* expression and a severe arteriovenous malformation or fistula (arrowhead). ISH of *Vegfa* on control and *Efnb2$^{flox}$;Nfatc1-Cre* mutant showing increased *Vegfa* expression in myocardium and an arteriovenous fistula (arrowhead). Scale bars, 50 µm. **(b)** Visualization of the coronary arterial vasculature at E16.5. Whole mount heart aortic Red Tempera perfusion of the left coronary artery in control (arrow) and absence of perfusion in *Efnb2$^{flox}$;Nfatc1-Cre* mutant (asterisk). Pecam-1 staining of histological sections showing larger perfused coronaries in control (arrowhead) and smaller perfused coronaries in the mutant (arrows). **(c)** Visualization of the coronary arterial vasculature at E18.5. Whole-mount heart aortic ink perfusion of the left coronary artery (lca) in control (arrow) and absence in *Efnb2$^{flox}$;Nfatc1-Cre* mutant (asterisk). Pecam-1 staining of histological sections showing numerous peritruncal vessels surrounding the pulmonary trunk (pt; arrowheads) in the mutant, while lca rooting to the aorta is maintained Scale bars, 100 µm.

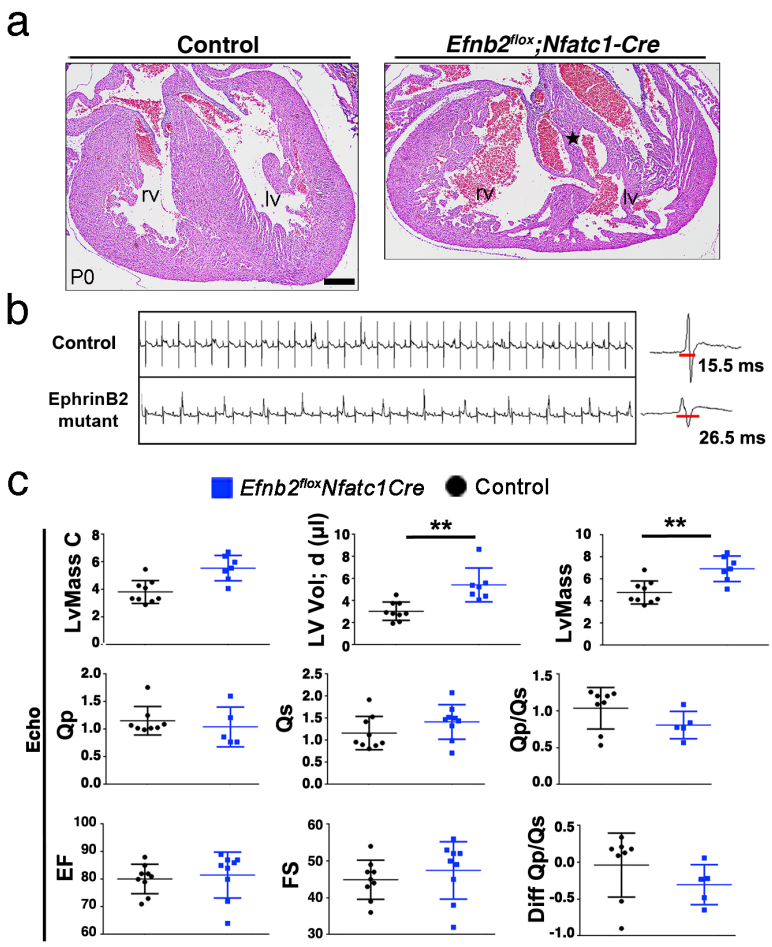



**Fig.21**. **Endocardial *Efnb2* deletion leads to VSD and arrhythmias but heart function is unaffected. (a)** H&E staining of transverse heart sections of P0 control and *Efnb2*$^{flox}$*;Nfatc1-Cre* mutant hearts. **(b)** ECG showing arrhythmias in Efnb2 mutant pups (**c**) Echocardiography analysis in P0 mice of ventricular ejection fraction (EF) and fractional shortening (FS), Left ventricle Mass (LvMass), Blood flow in the systemic circulation(Qs) , Blood flow in the pulmonary circulation (Qp) in WT and mutant mice. Data are mean ± s.d.. $^{**}P < 0.01$, by Student's *t*-test; Source data are available in Supplementary Table 5.

## Notch mutants display arterio-venous malformations

We found that both loss and gain of function mutations of multiple Notch pathway components, result in the formation of AVMs in mutant embryo hearts as described in other contexts (Benedito *et al*., 2008; Kim *et al*., 2008; Trindade et al., 2008; Krebs *et al*., 2010), In addition we found that Efnb2 mutants exhibit AVMs in the coronaries that phenocopy the Notch1 gain of function mutants as described previously (Krebs *et al*., 2010).

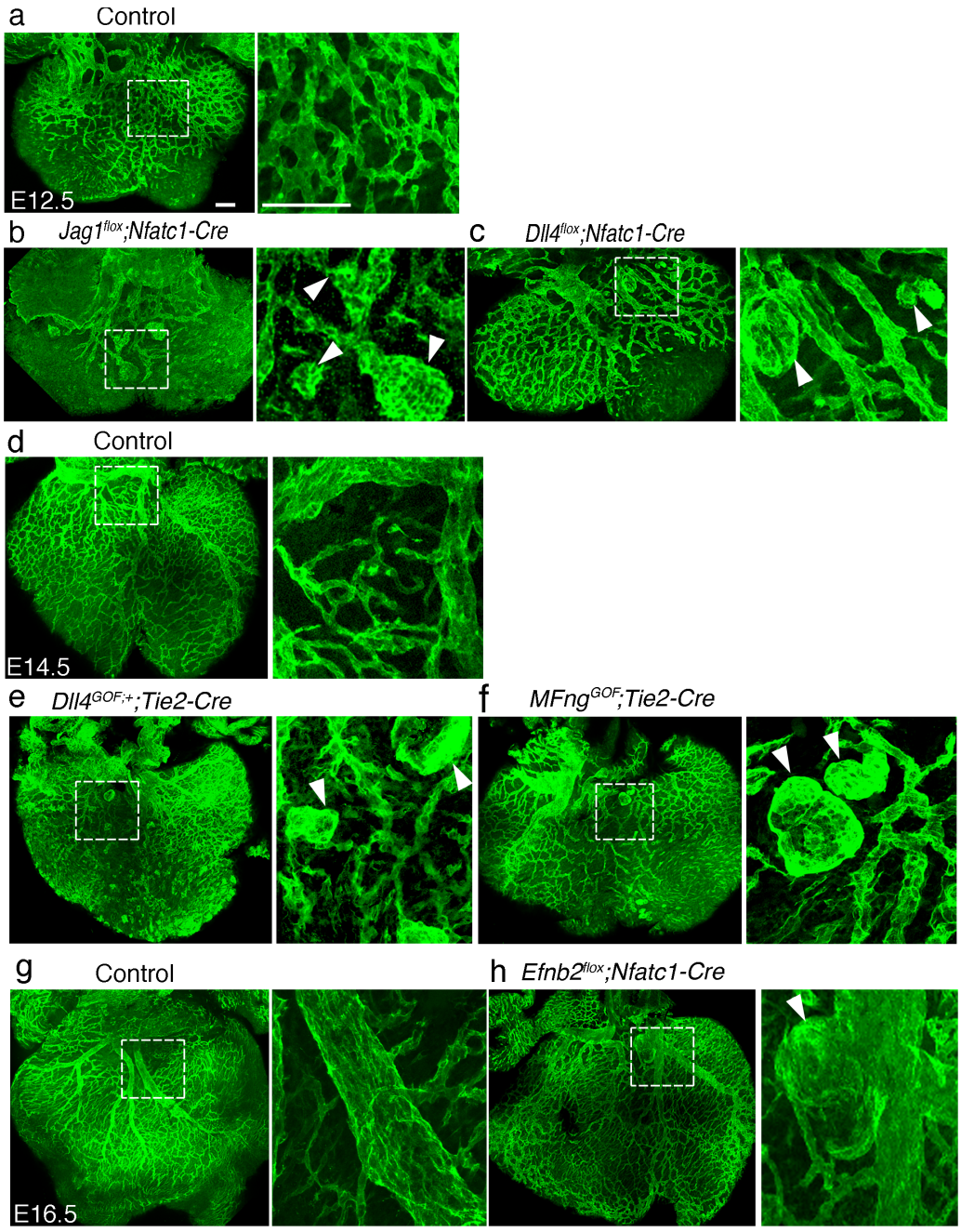



**Fig.22. Coronary vessels of Notch pathway and Notch effector mutants display vascular malformations**. Dorsal views of whole-mount immunostaining for Emcn (green). (a) E12.5 control heart, (b) E12.5 *Jag1flox;Nfatc1-Cre* heart, (c) E12.5 *Dll4flox;Nfatc1-Cre* heart, (d) E14.5 control heart, (e) E14.5 *MFngGOF;Tie2-Cre* heart, (f) E14.5 *Dll4GOF;Tie2-Cre* heart, (g) E16.5 control heart, (h) E16.5 *Efnb2flox;Nfatc1-Cre* heart. Scale bars, 100 μm.

The appearance of AVMs at E12.5 in *Jag1$^{flox}$;Nfatc1-Cre* and *Dll4$^{flox}$;Nfatc1-Cre* points to the crucial roles of the ligands in directing the sprouting angiogenesis from the SV, suggesting that progenitor cells from the SV are showing an arterial identity in early stages (**Fig. 22b,c**). These data further indicate that chamber endocardium and SV

endocardium are molecularly and functionally linked and severe alteration in the formation of the coronary plexus in mouse embryos may result in early communications between the epicardium and endocardium and thus in the formation of zone of discontinuity in the ventricular myocardium.

The formation of AVMs is a consequence of the inability of the vascular beds to maintain distinct arterial and venous identities. Whole mount staining of hearts from *MFng$^{GOF}$;Tie2-Cre*, *Dll4$^{GOF}$;Tie2-Cre* and *Efnb2$^{flox}$;Nfatc1-Cre* lines between E14.5 and E16.5 suggest that the right level of Notch signaling is required to maintain vascular bed identity (**Fig. 22e,f,h**).

**Comparative transcriptome profiling reveals a common hypoxia-dependent gene signature in endocardial/endothelial Notch mutants**

To identify gene expression changes across stages and genotypes we performed Gene Set Enrichment Analysis (GSEA; (Subramanian *et al*., 2005). with the six genotypes under study (**Fig.23** and **Suppl. Table4**). Clustering analysis uncovered similar enrichment patterns in gene sets from the Hallmark (Liberzon *et al*., 2015) and KEGG (http://www.genome.jp/kegg/) collections. *MFng$^{GOF}$;Tie2-Cre* mice had the highest number of enriched gene sets, followed by *Dll4$^{flox}$;Cdh5-Cre$^{ERT2}$*, *Dll4$^{flox}$;Nfatc1-Cre* and *Jag1$^{flox}$;Nfatc1-Cre*, with *Dll4$^{GOF}$;Tie2-Cre* and *Efnb2$^{flox}$;Nfatc1-Cre* having the least number of enriched gene signatures, reflecting the spectrum of phenotype severity in the coronary endothelium (**Fig.23 and Suppl. Table 4**).

Hallmark gene sets enriched in the *Dll4$^{flox}$;Nfatc1-Cre* and *Jag1$^{flox}$;Nfatc1-Cre* transcriptomes were implicated in cell cycle regulation (Myc targets, DNA repair E2F targets) and metabolism (oxidative phosphorylation) and were downregulated in endocardial *Jag1$^{flox}$;Nfatc1-Cre* mutants; in contrast, cell stress pathways (unfolded protein response, reactive oxygen species pathway) and innate-immunity (interferon alpha response) were more prominent in *Dll4$^{flox}$;Nfatc1-Cre* mutants (**Fig.23a,b**).

These differences possibly relate to the presence of a capillary plexus network in *Dll4$^{flox}$;Nfatc1-Cre* and its absence in *Jag1$^{flox}$;Nfatc1-Cre* mutants. In general, gene sets in common across the different genotypes represented key physiological processes such as hypoxia, glycolysis, oxidative stress, innate immunity, and apoptosis, which were upregulated, while proliferation was downregulated (**Fig. 23** and **Suppl. Table 4**).

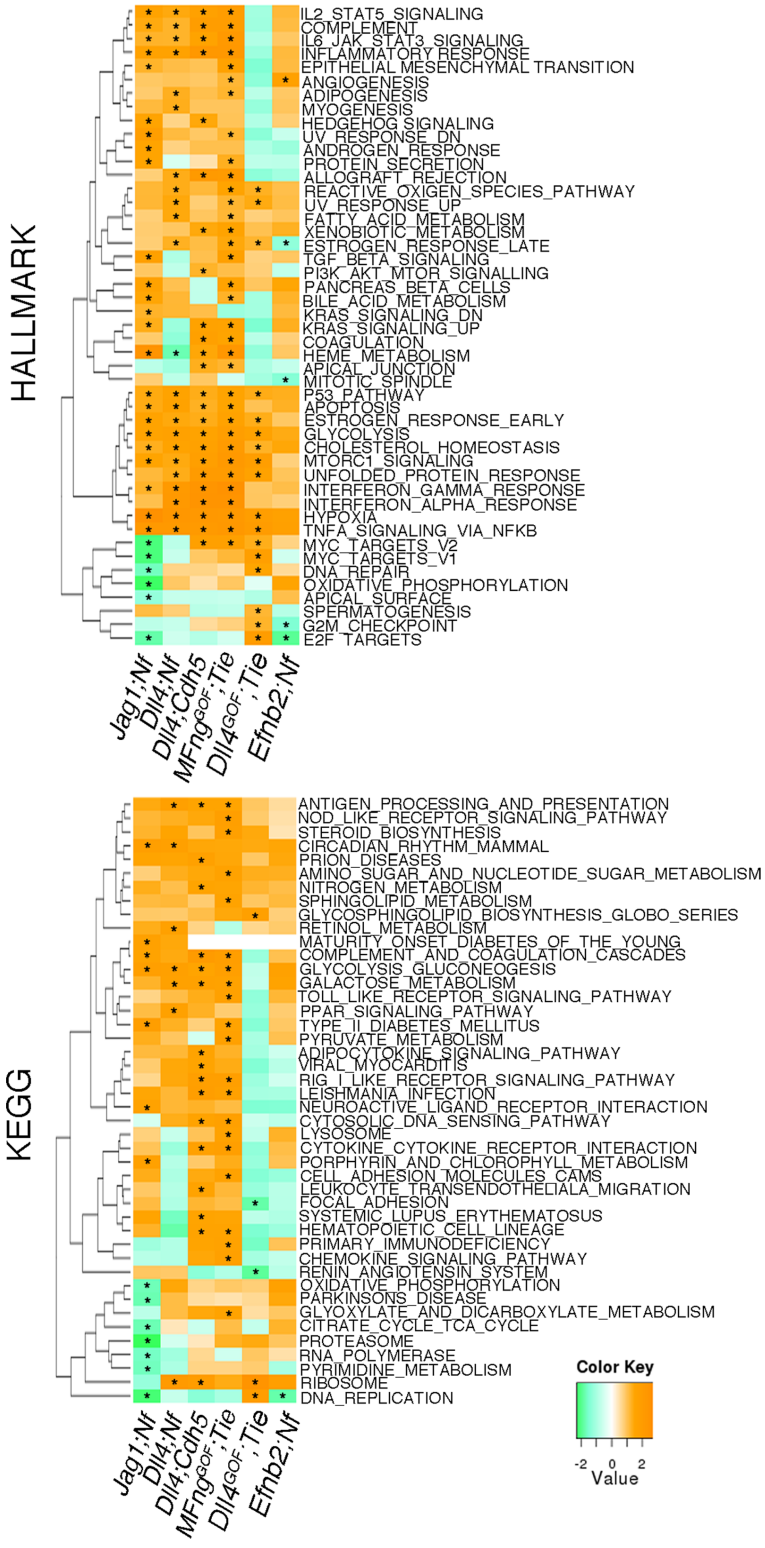



**Fig.23 Comparative analysis of HALLMARK and KEGG gene sets (g)** Gene set enrichment analysis (GSEA) results for expression profile comparisons of *Jag1$^{flox}$;Nfatc1-Cre, Dll4$^{flox}$;Nfatc1-Cre, Dll4$^{flox}$;Cdh5-Cre, MFng$^{GOF}$;Tie2-Cre, Dll4$^{GOF}$;Tie2-Cre and Efnb2$^{flox}$;Nfatc1-Cre* against control counterparts. Gene sets enriched with false discovery rate (FDR) < 0.25 are indicated with asterisks. Positive and negative normalized enrichment scores are colour coded. Orange colour indicates overexpression in the mutant.

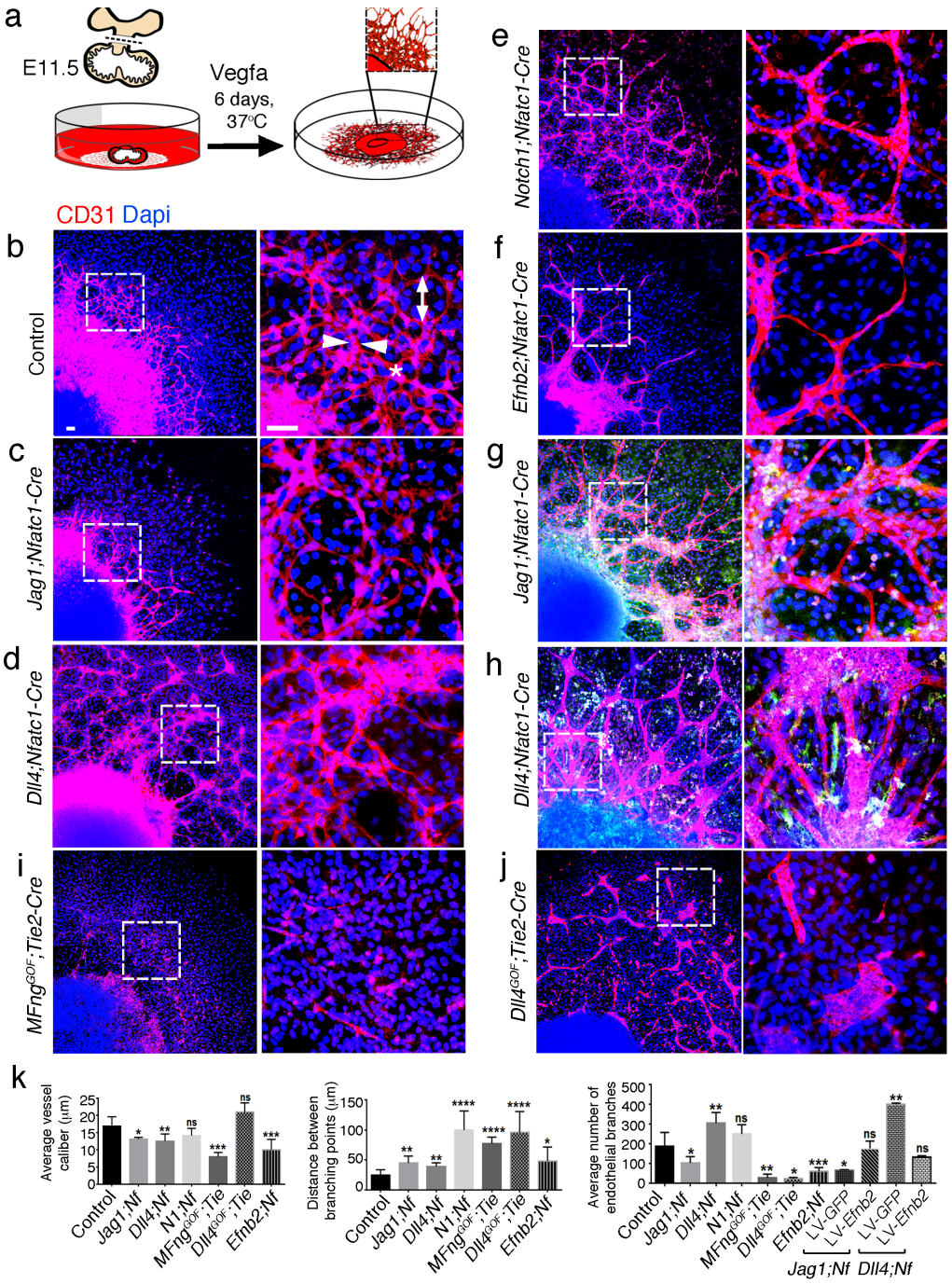



**Fig. 24. *Efnb2* rescues disrupted arterial branching in endocardial *Jag1* and *Dll4* mutant explants. (a)** Scheme depicting the ventricular explant assay. Representative images of E11.5 cultured ventricular explants from the following embryos: (**b**) control (n= 8-10), (**c**) *Jag1*$^{flox}$*;Nfatc1-Cre* (n=4), **(d)** *Dll4*$^{flox}$*;Nfatc1-Cre* (n=5)**, (e)** *Notch1*$^{flox}$*;Nfatc1-Cre* (n=4)**, (f)** *Efnb2*$^{flox}$*;Nfatc1-Cre* (n=5-7)**, (g)** *Jag1*$^{flox}$*;Nfatc1-Cre* infected with *Efnb2*-overexpressing lentivirus (n=4)**,** (**h**) *Dll4*$^{flox}$*;Nfatc1-Cre* infected with *Efnb2*-overexpressing lentivirus (n=5-7), **(i)** *MFng*$^{GOF}$*;Tie2-Cre* (n=3) and, **(j)** *Dll4*$^{GOF}$*;Tie2-Cre* (n=3). **(k)** Quantification of vessel calibre (arrowheads), distance between branching points (double ended arrow), and average number of endothelial branches (asterisk). Data are means ± s.d.. ****$P < 0.0001$; ***$P < 0.001$; **$P < 0.01$; *$P < 0.05$. by Student's *t*-test. n.s not significant .Source data are available in Supplementary Table 5. Scale bars, 100 µm.

### *Efnb2* is required for coronary arterial vessel branching

To model coronary development *ex vivo*, we developed a ventricular tissue explant assay for angiogenic growth (**Fig.24**). Compared with controls, *Jag1$^{flox}$;Nfatc1-Cre* explants had a lower angiogenic potential, manifested as smaller calibre vessels, a lower number of trans-mural endothelial branches, and longer distances between branching points (**Fig.24c,k**). Conversely, *Dll4$^{flox}$;Nfatc1-Cre* or *Notch1$^{flox}$;Nfatc1-Cre* explants yielded more densely interconnected vascular networks of larger vessel calibre, longer distances between vessel branching points, and more trans-mural endothelial branches (**Fig.24d,k**). *Notch1$^{flox}$;Nfatc1-Cre* explants displayed a phenotype similar to *Dll4$^{flox}$;Nfatc1-Cre* explants, although the differences in vessel calibre and endothelial branch number did not reach significance (**Fig.24d,e,k**).

*Efnb2$^{flox}$;Nfatc1-Cre* explants formed sparsely interconnected networks with a low vessel calibre, a reduced number of trans-mural endothelial branches, and increased distances between branching points, similar to those seen in *Jag1$^{flox}$;Nfatc1-Cre* explants (**Fig.24f,k**). *MFng$^{GOF}$;Tie2-Cre* and *Dll4$^{GOF}$;Tie2-Cre* explants showed a broadly similar phenotype, with substantial lengthening of branching point distance and a below-normal mean number of endothelial branches (**Fig.24i,j,k**). In contrast, *MFng$^{GOF}$;Tie2-Cre* explants had smaller calibre vessels than *Dll4$^{GOF}$;Tie2-Cre* explants (**Fig.24i,j,k**).

We next tested the link between *Efnb2* and the Notch ligands in relation to endothelial branching and morphogenesis. Delivery of a lentiviral *Efnb2* transgene to *Jag1$^{flox}$;Nfatc1-Cre* ventricular explants reverted the below-normal endothelial branch number to the number seen in control explants (**Fig.24g,k**). Likewise, the lentiviral *Efnb2* transgene also reverted the elevated number of endothelial branches in *Dll4$^{flox}$;Nfatc1-Cre* explants to control levels (**Fig.24h,k**), indicating defect rescue in both mutants.

Taken together, these observations indicate that Jag1 and Efnb2 promote coronary vessel sprouting and branching, whereas Dll4, MFng, and Notch1 inhibit these processes. *Efnb2* mediates signaling from both Jag1 and Dll4 to ensure balanced endothelial connections during coronary angiogenesis.

### Myocardial *Mib1* inactivation results in aberrant coronary arterial patterning

Myocardial inactivation of Jag1 and Jag2, or Mib1 leads to thinner ventricular walls, accompanied by reduced cardiomyocyte proliferation, disrupted ventricular chamber

patterning, and cardiomyopathy (D'Amato *et al*., 2016a; Luxán *et al*., 2015), suggesting that defective myocardial compaction can lead to defective coronary patterning. To further determine examine the effect of inactivating Notch in the myocardium on coronary vessels growth and patterning we examined coronary formation in *Mib1$^{flox}$;cTnt-Cre* mice. Whole mount IsoB4 and Emcn staining revealed that coronary arteries developed poorly and failed to reach the heart apex (**Fig.25a-h,i**) whereas coronary veins appeared unaffected (**Fig.25a'-h´,j**). Moreover arterio-venous malformations were present (**Fig.25 c,c',d,d'**). Thus, loss of *Mib1* in myocardium phenocopies endocardial/endothelial loss- and gain-of-function of Notch in coronary arterial remodelling. These data suggest that compaction and coronary formation are two interlinked processes regulated by Notch wherein Notch-dependent coronary development is required for ventricular chamber growth and cardiomyocyte proliferation, while proper compaction of the myocardium, also regulated by Notch, is necessary for proper patterning coronaries formation.

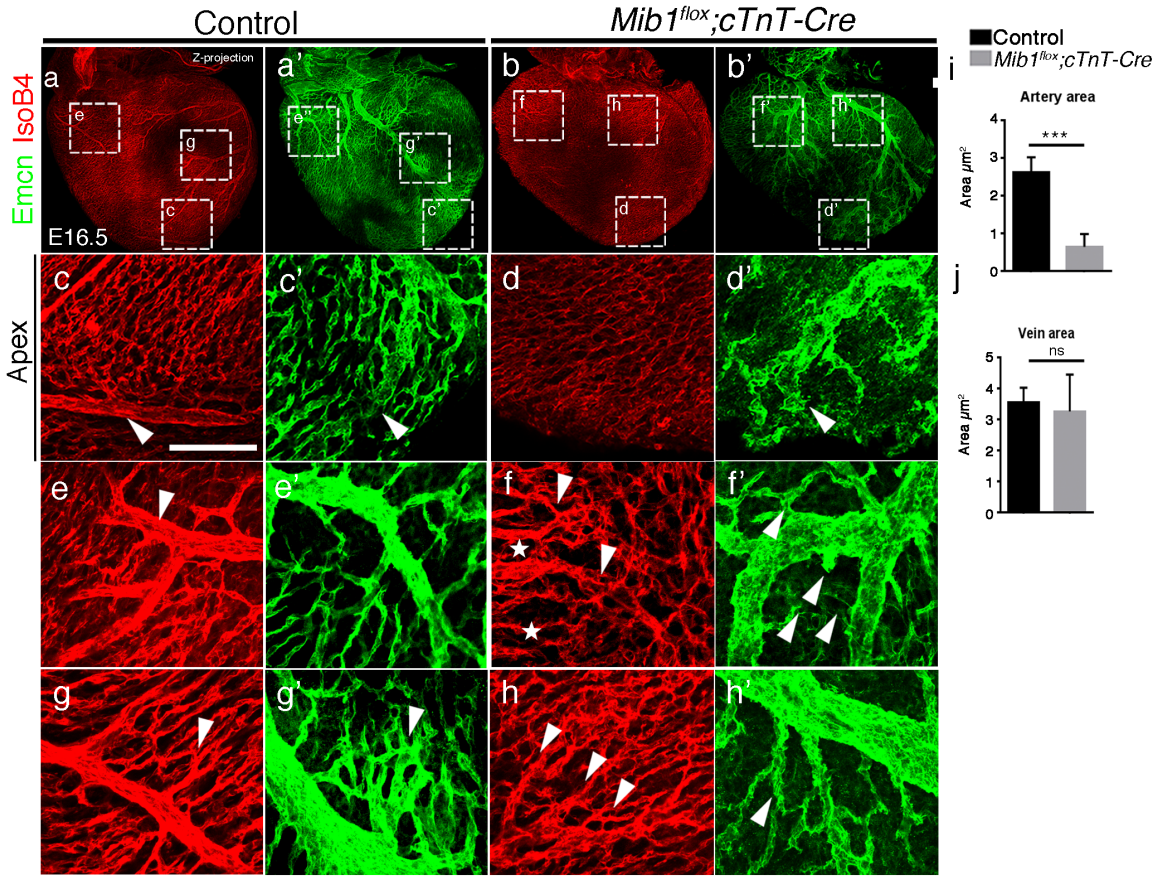


**Fig. 25. Myocardial inactivation of *Mib1* distrupta coronary artery differentiation and remodelling.** Dorsal view of whole-mount immunochemistry for IsoB4 (red) and Emcn (green) in E16.5 control **(a,a')** and *Mib1*$^{flox/flox}$*;TnT-Cre/+* (*Mib1*$^{flox}$*;Tnt-Cre*) **(b,b')** hearts. Scale bars,100 μm. **(c,c')** Apex showing connection between coronary artery and vein in wt but not in Mib1 mutant (d,d'). Coronary artery trees are normal in control (**e,g**) but not formed and properly assembled in mutant (**f,h**). (**i,j**) Quantification data from E16.5 control and *Mib1*$^{flox}$*;Tnt-Cre* mutant hearts : area covered by coronary arteries (IsoB4); area covered by veins (Emcn). Data are means ± s.d..; ***$P < 0.001$ by Student's *t*-test;. n.s not significant

# Discussion

In the early embryo, blood circulating through the heart provides oxygen and nutrients to the developing myocardium via diffusion mechanisms. As the heart grows in pace with the rest of the embryo, the increased demand placed on the heart pumping function requires that muscular force increases proportionally by thickening of the myocardial wall. Thereafter, a well-formed coronary vasculature is required to supply with oxygen and nutrients the cells within the myocardium, which can no longer be nutritionally sustained by diffusion alone. The development of the coronaries is therefore a crucial step in cardiac development and has been the object of intense investigation. Deciphering the signalling mechanisms behind the development of the coronaries is essential to understand congenital abnormalities in coronary development and to diagnose and treat associated pathologies, such as myocardial ischaemia, malignant arrhythmias and sudden death (Angelini 2007; Perez-Pomares 2015).

The coronary vasculature develops in a unique manner to the other vascular beds in the developing embryo. Early studies suggested that coronary arteries originate from the sinuses of Valsalva (Hutchins *et al*., 1988) while veins originate from the sinus venosus. Later, it was shown that coronary vasculature is established well before being connected to the systemic circulation (Bogers *et al*.,1989). Several recent studies have identified multiple sources of endothelial progenitors that give rise to the coronary arteries and veins. These are the pro-epicardium, the endocardium and the sinus venosus (Tian *et al*., 2015). The cells originating from these sources form a primary vascular plexus covering the heart. In the final stages of coronary development, the peritruncal ring of coronary arterial vasculature around the aortic trunk connects at the base of the aorta, whereas the venous capillaries form connections with the coronary sinus. These processes permit the coronary system to be integrated with the systemic blood circulation.

**SV endothelial progenitors have a mixed arterial-venous identity**

Lineage tracing analysis using an endothelial inducible Cre driver line (*Cdh5-Cre$^{ERT2}$*) led Red-Horse et al. to suggest that coronary arteries derived from veins by developmental reprogramming (Red-Horse *et al*., 2010). In this model, endothelium sprouts from the SV and invades the sub-epicardial space where it gives rise to veins (**Fig. 26**). Subsequently the sub-epicardial veins de-differentiate and re-differentiate into arteries located deeper within the myocardium. In this study, we show that the Notch ligands Jag1, Dll4, the Notch modifier MFng and the active Notch1receptor (N1ICD) are all expressed

in SV endothelium and sub-epicardial capillaries, with Dll4 and MFng expression still maintained at later stages in prospective veins. The Notch pathway elements were co-expressed with the venous marker endomucin, which is also expressed in SV and chamber endocardium. We suggest that nascent sub-epicardial vessels have a mixed arterial/venous identity, which is progressively defined by reiterated Notch signaling and rule out an arterial re-programming mechanism leading to coronary artery formation. Notch signaling during embryonic angiogenesis is necessary for arterial-venous specification, namely the reversible commitment of EC to the arterial or venous fate, preceding the onset of blood flow (Swift & Weinstein 2009). SV endothelium heterogeneity in relation to arterial-venous identity is consistent with the notion that early vascular beds are highly plastic during embryonic development.

**Nfatc1+ progenitors give rise to the majority of coronary vessels**

A second major source of endothelium is the ventricular endocardium. Endocardial cells separate and join the coronary plexus near the interventricular septum (Red-horse *et al.*, 2010). However, estimates of the contribution of the endocardium to coronary artery formation vary between a large majority (Wu *et al*., 2012), to very little (Zhang *et al*., 2016) depending on the study. Our lineage tracing study shows that the endocardial-specific *Nfatc1-Cre* driver is active in ventricular endocardium and in SV endothelium, and labels the majority of sub-epicardial vessels as well. Therefore we conclude that coronary arteries in the ventricular free wall derive mainly from sub-epicardial vessels, which is in agreement with previous lineage-tracing studies (Chen *et al*., 2014; Tian *et al*., 2015; Zhang *et al*., 2016). Moreover, we find Nfatc1 protein expression in a subset of SV EC**s**, suggesting anatomical continuity and potential intermixing of endothelial and endocardial cells lining the SV and primitive common atrium. The possibility of shared developmental origin of SV endothelium and endocardium may underpin recently reported compensatory, fail-safe mechanisms that ensure adequate growth of the coronary capillary plexus (Sharma *et al*., 2015).

### Jag1 and Dll4 have antagonistic roles in SV endothelial sprouting angiogenesis

Since Jag1 and Dll4 ligands are co-expressed in the SV endothelium, they could potentially trigger Notch activity during coronary development, in a cooperative way or act competitively, as has been shown in retinal angiogenesis (Benedito *et al*., 2009). The existence of two Notch ligands with opposing roles allows the integration of different angiogenic processes such as the selection of endothelial tip cells versus stalk cells (Benedito *et al*., 2009). In the retina, Dll4 is expressed preferentially in tip cells whereas Jag1 is expressed preferentially in stalk cells. In the SV we could not determine Dll4 and Jag1 ligand expression patterns simultaneously and we must assume that they are respectively expressed in tip and stalk cells at the coronary angiogenic front.

*Jag1* or *Dll4* inactivation in the SV early in coronary development resulted in arrested or excessive angiogenesis respectively, consequently impairing cardiomyocyte proliferation and ventricular wall growth. Capillary entanglements suggestive of vascular malformations were present in the early plexus of *Jag1$^{flox}$;Nfatc1-Cre* and *Dll4$^{flox}$;Nfatc1-Cre* mutants. Functional capillary connections between arteries and veins are required for coronary perfusion, as arterio-venous shunting compromises flow. The vascular malformations seen in Notch mutants have been attributed to unresolved intermingling of arteries and veins during differentiation and/or a failure to maintain distinct arterial or venous identities in the vascular bed (Krebs *et al.*, 2004; Gale *et al.*, 2004). Their presence in the early vascular networks of *Jag1$^{flox}$;Nfatc1-Cre* and *Dll4$^{flox}$;Nfatc1-Cre* mutants, could therefore be indicative that endothelial progenitors begin to differentiate into arteries and veins very soon after exiting the SV.

The process of SV sprouting, migration, and covering of the dorsal part of the heart, and concomitant communication with the chamber endocardium would ensure proper perfusion of the compact myocardium at later stages. The presence of early zones of discontinuity in the compact myocardium of the *Jag1$^{flox}$;Nfatc1-Cre* mutants, suggestive of arterio-venous fistulae reinforces the idea that SV endothelium and endocardium are functionally connected to allow tight developmental control of the coronary plexus. There is some evidence suggesting that Notch could be regulating through the semaphorin-plexin axis or via other signals, the migration of the SV endothelium for the correct perfusion of the heart, and its future connections with the greater arterial vessels (Epstein *et al*., 2015).

**Dll4 and Jag1 function to direct coronary artery remodelling at later stages**

Loss of endothelial Notch function during coronary development resulted in smaller diameter arteries and increased number of veins, consistent with Notch promoting commitment to the arterial fate (Krebs *et al*., 2004; Duarte *et al*., 2004; Fischer *et al*., 2004; **Fig. 26**). Moreover, the hierarchical organization of the coronary vascular tree was profoundly altered in Notch mutants, implying a requirement of Notch for higher order complexity of the coronary vessels (**Fig. 26**). This phenotype was much stronger in *Dll4$^{flox}$;Cdh5-Cre$^{ERT2}$* mutants, which displayed a complete absence of coronary arterial tree, than in *Jag1$^{flox}$;Cdh5-Cre$^{ERT2}$* mutants, suggesting that Dll4 is the ligand driving arterial differentiation and remodelling. *Jag1$^{flox}$;Cdh5-Cre$^{ERT2}$* mutants showed increased veins and markedly reduced arterial tree formation, accompanied by an increase of N1ICD$^{+}$ nuclei, as expected for an inhibitory Notch ligand. However, there was persistence of numerous smaller vessels that expressed both *Efnb2* and *Dll4*, suggesting that *Jag1* deletion was not complete. These observations suggested defective coronary plexus remodelling in Notch mutants. Moreover the lack of expression of the Notch downstream targets examined in *Dll4$^{flox}$;Cdh5-Cre$^{ERT2}$* mutants indicated that Dll4 could be the ligand primarily driving Notch activation, but at the same time both mutants are required for normal branching of the arterial tree.

Moreover, because of the position of the arterial endothelium intra-myocardially and of the vein endothelium sub-epicardially, any variation in Notch activity during the remodelling of the coronary arterial could impact on the compaction of the myocardium through the disruption of the assembly of the coronary tree**.** Quantification of the compact myocardial thickness in both *Dll4$^{flox}$;Cdh5-Cre$^{ERT}$* and *Jag1$^{flox}$;Cdh5-Cre$^{ERT2}$* mutants suggest that the severity of the coronary phenotypes is reflected in the severity of the reduction in the thickness of the myocardium.

**Defective remodelling and smooth muscle coverage in Notch loss- and gain- of function mutants**

Notch loss- or –gain-of function resulted in vascular remodelling defects with the lack of a normal coronary arterial tree and substantial reduction in arterial smooth muscle cell coverage, suggesting impaired pericyte recruitment/differentiation Notch loss-of-function lead to reduced formation of arteries and arterial branching defects, however this

was associated with a reduction of arterial calibre as seen in other loss of function settings (Benedito *et al.*, 2008). However, gain of Notch function also lead to smaller calibre arteries and increased veins (**Fig. 26**), when the opposite outcome was anticipated (Uyttendaele *et al.*, 2001;Trindade *et al.*, 2008; Krebs 2010).

Therefore, once the primary coronary plexus is established, above or below normal variations of Notch activity leads to arterial differentiation arrest and the adoption of a "default" venous identity. Notch is associated with remodelling of the arteries through vascular "pruning", whereby some vascular connections regress and others reinforce, depending on local tissue demands (Korn & Augustin 2015). However, Notch is also crucial for remodelling of the veins (Ehling *et al.*, 2013) suggesting that increased vein density in the Notch mutants might be the result of a pruning defect. Various Notch pathway mutants show coronary vessel haemorrhaging, indicative of a rupture of endothelial structural integrity, reminiscent of vascular disorders (Park-Windhol & D'Amore 2016) and tumours (Goel *et al.*, 2011). Moreover, the activation of pro-coagulation gene signatures observed in our transcriptome analysis, is consistent with loss of the endothelial barrier and vascular leakage.

Consistent with defective vascular barrier function, prominent transcriptomic signatures across all genotypes and developmental stages targeting Notch activity in endothelium were related with ischaemic cell death (apoptosis), and innate-immune responses mediated by type I and type II interferons. Part of the maladaptive response in myocardial infarction is mediated by type I interferon activation and results in excessive production of inflammatory cytokines/chemokines and inflammatory cell infiltration of the heart (King et al., 2017). Therapies that mitigate this response might improve myocardial function and survival. Thus, pathological hallmarks of adult coronary heart disease are recapitulated during embryonic development when coronaries fail to develop normally. Understanding how vascular remodelling, cardiac growth and maturation are interconnected may provide clues for designing therapeutic strategies for ischemic heart disease.

Epicardium-specific ablation of *Notch1* or *Rbpj* impaired coronary artery formation (Del Monte *et al*., 2011) and smooth muscle cell differentiation of epicardial-derived cells (EPDCs) (Grieskamp *et al*., 2011). The observation of diminished perivascular coverage due to defective smooth muscle differentiation, is further evidence of vascular instability in the coronaries of Notch mutants, and supports the view that Jag1 is necessary for

perivascular smooth muscle differentiation and maturation downstream of Vegf-Dll4-Notch1 (High *et al.*, 2008; Pedrosa *et al.*, 2015). However, we also observed in *MFng*$^{GOF}$*;Tie2-Cre* embryos vascular instability and defective smooth muscle differentiation. This observation indicates that both Dll4 and Jag1 ligands are crucial for the regulation of vessel maturation, likely by regulating the levels of N1ICD.

**EphrinB2 mediates arterial remodelling downstream of Notch1**

Coronary maturation defects observed in *Jag1* and *Dll4* mutants might be attributed to the loss of EphrinB2 function. Dll4-Notch signaling was shown to activate *Efnb2* expression in EC (Iso *et al.*, 2006) and during ventricular development (Grego-Bessa *et al.*, 2007). *Efnb2* inactivation leads to coronary artery remodelling defects, similar to those resulting from late *Jag1* and *Dll4* inactivation, suggesting that ephrinB2 acts as a key effector acting downstream of the Notch ligands to promote arterial remodelling. This notion is supported by angiogenic explant assays, in which the opposing effect of *Jag1* and *Dll4* deficiency on vessel branching is rescued by transduction of an *Efnb2*-expressing lentivirus, identifying ephrinB2 as a common effector of both ligands during coronary artery development. These data reinforce prior observations that *Efnb2* loss-of-function phenotypes are virtually identical to the vascular phenotype caused by Notch1 activation in the endothelium (Krebs *et al*., 2010) suggesting a possible feedback loop between them.

**Cardiac growth and patterning requires communication between endocardium, coronary endothelium and myocardium**

One common feature among the various endothelial Notch loss- and gain-of-function models analyzed here is the thinner ventricular wall associated with defective compact myocardium proliferation. Notch ablation in the endothelial progenitors results in thin ventricular wall without affecting myocardial patterning. In this situation the myocardium requires the trophic support from coronaries to promote cardiomyocyte proliferation and growth of the ventricular wall. Alternatively, myocardial inactivation of *Jag1*, or combined inactivation of *Jag1* and *Jag2*, or *Mib1*, leads to thinner ventricular walls, accompanied by reduced cardiomyocyte proliferation, disrupted ventricular chamber patterning, and cardiomyopathy (Luxán et al., 2013; (D'Amato *et al*., 2016a).

Moreover, we used a conditional deletion of myocardial *Mib1* that is reported to induce LVNC as a consequence of reduced endocardial Notch1 activity during chamber compaction, patterning and maturation (Luxan *et al*., 2013). We found that the decreased Notch1 activity was also found to be affecting the coronary artery development without impairing the SV early sprouting. We observed in *Mib1;cTnT-Cre* mutants defective migration of both LCA and RCA which cannot migrate to the apex of the cardiomyopathic heart failing to assemble in a proper coronary tree. Coronary arteries were smaller and associated to an increased number of endothelial cells invading the compact myocardium suggesting that the cardiomyocyte could be hypoxic.

In contrast, chamber patterning is maintained in SV endothelium *Jag1*, *Dll4* and *Efnb2* mutants, and in late endothelial *Dll4* and *Jag1* mutants, indicating that reduced ventricular wall thickness in these mutants arises as a consequence of the lack of a well-developed coronary system. These observations suggest that coronary arteries provide metabolic substrates for compact myocardium growth, rather than myocardial patterning signals. In addition, our data imply that ventricular compaction relies on two interlinked Notch-dependent processes: patterning and maturation of the ventricles, and timely development of a functional coronary vessel network, as previously suggested (D'Amato *et al.*, 2016a).

These data imply that myocardial patterning and coronary artery development are Notch-dependent processes that can be experimentally segregated by using tissue-specific Cre lines. Both processes have an impact on the growth of the compact myocardium, leading to the development of a cardiomyopathy, left ventricular non-compaction (LVNC). In the future, analysis of the coronary status by angiography or MRI may help to diagnose more carefully congenital heart defects. This may have clinical relevance for the study, stratification and treatment of cardiomyopathies.

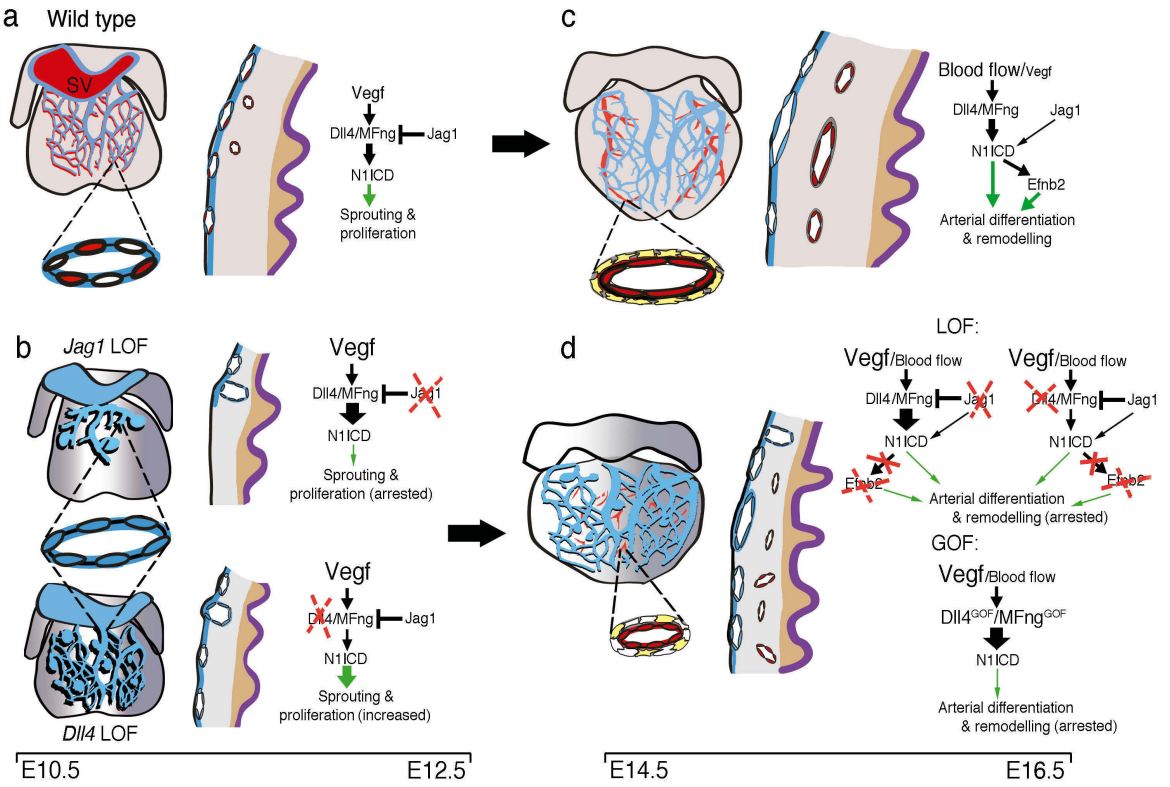



**Fig.26** Sequential antagonistic and complementary roles of Jag1 and Dll4 in coronary vessel development. **(a,b)** Embryonic stages E10.5-E12.5. **(a)** *Left*, Sinus venous (SV)-derived vessels covering the dorsal surface of a wild-type heart. The zoomed view shows detail of a subepicardial vessel with a subset of ECs expressing N1ICD (red). *Centre*, Cross-section through the ventricular wall. SV-derived ECs invade the space between the epicardium and myocardium and cover the heart dorsally. Some ECs invade the myocardium as they exit the SV and differentiate into arteries. *Right*, For EC sprouting and proliferation, the balance between Dll4/MFng and Jag1 modulates Notch signaling output downstream of Vegf. **(b)** *Left*, *Jag1$^{flox}$;Nfatc1-Cre* mutants (top) show arrested coronary angiogenesis, whereas *Dll4$^{flox}$;Nfatc1-Cre* mutants (bottom) show excessive angiogenesis; both mutants display vascular malformations. The zoomed view shows detail of a sub-epicardial vessel with ECs lacking N1ICD expression (blue). *Centre,* Mutant hearts have a thin myocardial wall, but maintain myocardial patterning (grey-brown boundary). *Right*, Mutants are characterized by high Vegf signaling. Endocardial *Jag1* deletion disrupts the balance with Dll4/MFng, leading to increased Notch1 signaling and arrested sprouting and proliferation. In contrast, endocardial *Dll4* deletion results in decreased Notch1 signaling and increased sprouting and proliferation. **(c,d)** Embryonic stages E14.5-E16.5. **(c)** *Left*, Coronary vasculature covering the dorsal surface of the wild-type heart. The zoomed view shows detail of a coronary artery with an inner layer of ECs expressing N1ICD (red) and an outer layer of smooth muscle cells (yellow). *Centre*, Patterning of the capillaries gives rise to larger veins on the outer heart surface and larger arteries intramyocardially. *Right*, Blood flow, rather than Vegf, drives arterial differentiation and remodelling; the balance between Dll4/MFng and Jag1 modulates Notch signaling output downstream of blood flow and upstream of Efnb2. **(d)** *Left*, the coronary vasculature covering the dorsal surface of the heart in Notch mutants is mis-patterned and contains numerous vascular malformations. The zoomed view shows detail of a coronary artery with an inner layer consisting of a “leaky” endothelium and an outer layer of poorly differentiated perivascular cells. *Centre*, Arteries consist of smaller calibre vessels, whereas veins are more numerous and unremodelled. Mutant hearts have a thin myocardial wall but maintain myocardial patterning (grey-brown boundary). *Right*, In the mutants, abnormally high Vegf signaling supersedes the influence of blood flow. The late endothelial deletion of *Jag1* or *Dll4*, leads to increased (*Jag1*) or decreased (*Dll4*) Notch1 signaling, and disrupts arterial differentiation and remodelling. Inactivation of *Efnb2,* that functions downstream of Notch leads to a similar phenotype (LOF, loss of function). Notch gain-of-function (GOF), resulting from *MFng* or *Dll4* overexpression, also results in disrupted arterial differentiation and remodelling.

# Conclusions

## Conclusions

**1.** The endothelium of the SV and of the sub-epicardial vessels expresses the "arterial markers" Jag1, Dll4 and MFng at E11.5, indicative of the highly heterogeneous and plastic potential of these progenitors cells.

**2**. SV endothelium *Jag1* inactivation arrests sprouting, whereas *Dll4* deletion causes excessive SV sprouting. Thus, the ligands Jag1 and Dll4 have antagonistic roles in the SV endothelium.

**3.** Arrested myocardial growth in SV endothelium *Jag1* or *Dll4* mutants is due to a global hypoxic and metabolic stress response.

**4**. Jag1 and Dll4/MFng signaling to Notch1 is crucial during coronary vessel development. Notch signaling activity in the coronary endothelium also indirectly affects compaction by regulating remodelling

**5.** Forced endothelial *Dll4* expression disrupts coronary vascular remodelling and forced endothelial *Mfng* over-expression phenocopies *Dll4* gain-of-function in coronaries.

**6.** Ephrinb2 is required for coronary arteriogenesis and vessel branching and attenuates the antagonistic Jag1 and Dll4 signaling in arterial branching morphogenesis.

**7.** Loss- or gain-of-function models of Notch activity cause arterio-venous malformations (AVM) and endothelial leakiness in the heart.

8. Ventricular compaction relies on two interlinked Notch-dependent processes: patterning and maturation of the ventricles, and timely development of a functional coronary vessel network

## Conclusiones

1. El endotelio del SV y de los vasos sub-epicárdicos expresa los "marcadores arteriales" Jag1, Dll4 y MFng a E11.5. Esto indica el comportamiento altamente heterogéneo y plástico de estas células progenitoras.

2. La inactivación de *Jag1* en el endotelio del SV bloquea la expansión del SV mientras que la eliminación de *Dll4* causa una expansión excesiva del SV. Los ligandos Jag1 y Dll4 tienen funciones antagónicas en el SV.

3. El crecimiento del miocardio está bloqueado en los mutantes de *Jag1* o *Dll4* en el endotelio del SV y se debe a una respuesta hipóxica global y a estrés metabólico.

4. La señalización de Jag1 y de Dll4 hacia Notch1, modificada por MFng, es crucial para el desarrollo de los vasos coronarios. La actividad de señalización de Notch en el endotelio coronario también afecta indirectamente a la compactación, regulando el remodelado y la maduración

5. La expresión forzada de MFng en el endotelio altera la remodelación vascular coronaria y fenocopia la ganancia de función de Dll4 en el endotelio de las coronarias.

6. Ephrinb2 se requiere para la arteriogénesis y la ramificación de las coronaria, y atenúa la señalización antagonista de Jag1 y Dll4 en la morfogénesis de las arterias coronarias.

7. Los modelos de pérdida o ganancia de función de la vía de Notch muestran malformaciones artero-venosas (AVM) y permeabilidad endotelial en el corazón.

8. La compactación de los ventrículos se produce debido a dos procesos interconectados que dependen de la vía de señalización de Notch: el establecimiento del patrón y la maduración ventricular,así como la formación de una red coronaria functional.

# Bibliography

# Bibliography


Adams, R. H., Diella, F., Hennig, S., Helmbacher, F., Deutsch, U. and Klein, R. (2001) 'The Cytoplasmic Domain of the Ligand EphrinB2 Is Required for Vascular Morphogenesis but Not Cranial Neural Crest Migration', *Cell,* 104(1), 57-69.

Adams, R. H., Wilkinson, G. A., Weiss, C., Diella, F., Gale, N. W., Deutsch, U., Risau, W. and Klein, R. (1999) 'Roles of ephrinB ligands and EphB receptors in cardiovascular development: demarcation of arterial/venous domains, vascular morphogenesis, and sprouting angiogenesis', *Genes & Development,* 13(3), 295-306.

Amyere, M., Revencu, N., Helaers, R., Pairet, E., Baselga, E., Cordisco, M., Chung, W., Dubois, J., Lacour, J.-P., Martorell, L., Mazereeuw-Hautier, J., Pyeritz, R. E., Amor, D. J., Bisdorff, A., Blei, F., Bombei, H., Dompmartin, A., Brooks, D., Dupont, J., González-Enseñat, M. A., Frieden, I., Gérard, M., Kvarnung, M., Hanson-Kahn, A. K., Hudgins, L., Léauté-Labrèze, C., McCuaig, C., Metry, D., Parent, P., Paul, C., Petit, F., Phan, A., Quere, I., Salhi, A., Turner, A., Vabres, P., Vicente, A., Wargon, O., Watanabe, S., Weibel, L., Wilson, A., Willing, M., Mulliken, J. B., Boon, L. M. and Vikkula, M. (2017) 'Germline Loss-of-Function Mutations in EPHB4 Cause a Second Form of Capillary Malformation-Arteriovenous Malformation (CM-AVM2) Deregulating RAS-MAPK Signaling', *Circulation,* 136(11), 1037-1048.

Andrews S. 'FastQC A Quality Control tool for High Throughput Sequence Data', [online],available:http://www.bioinformatics.babraham.ac.uk/projects/fastqc

Angelini P. Normal and anomalous coronary arteries in humans. In: Angelini P (ed). Coronary Artery Anomalies . Philadelphia: Lippincott, Williams and Wilkins, 1999. pp. 27–150.

Angelini, P. (2007) 'Coronary Artery Anomalies', *An Entity in Search of an Identity,* 115(10), 1296-1305.

Angelini, P., Velasco, J. A. and Flamm, S. (2002) 'Coronary Anomalies', *Incidence, Pathophysiology, and Clinical Relevance,* 105(20), 2449-2454.

Benedito, R., Roca, C., Sorensen, I., Adams, S., Gossler, A., Fruttiger, M. and Adams, R. H. (2009) 'The notch ligands Dll4 and Jagged1 have opposing effects on angiogenesis', *Cell,* 137(6), 1124-35.

Benedito, R., Rocha, S. F., Woeste, M., Zamykal, M., Radtke, F., Casanovas, O., Duarte, A., Pytowski, B. and Adams, R. H. (2012) 'Notch-dependent VEGFR3 upregulation allows angiogenesis without VEGF-VEGFR2 signalling', *Nature,* 484(7392), 110-114.

Benedito, R., Trindade, A., Hirashima, M., Henrique, D., da Costa, L. L., Rossant, J., Gill, P. S. and Duarte, A. (2008) 'Loss of Notch signalling induced by Dll4 causes arterial calibre reduction by increasing endothelial cell response to angiogenic stimuli', *BMC Dev Biol,* 8, 117.

Bogers B , Gittenberger-de Groot A , Poelmann R , Péault B , Huysmans H . Development of the origin of the coronary arteries, a matter of ingrowth or outgrowth? *Anat Embryol* (Berl) 1989 ;180 :437 –441 .

Bray, S. J. (2016) 'Notch signalling in context', *Nat Rev Mol Cell Biol*.

Brückner, K., Perez, L., Clausen, H. and Cohen, S. (2000) 'Glycosyltransferase activity of Fringe modulates Notch–Delta interactions', *Nature,* 406, 411.

Cai, C.-L., Martin, J. C., Sun, Y., Cui, L., Wang, L., Ouyang, K., Yang, L., Bu, L., Liang, X., Zhang, X., Stallcup, W. B., Denton, C. P., McCulloch, A., Chen, J. and Evans, S. M. (2008) 'A myocardial lineage derives from Tbx18 epicardial cells', *Nature,* 454(7200), 104-108.

Cano, E., Carmona, R., Ruiz-Villalba, A., Rojas, A., Chau, Y.-Y., Wagner, K. D., Wagner, N., Hastie, N. D., Muñoz-Chápuli, R. and Pérez-Pomares, J. M. (2016) 'Extracardiac septum transversum/proepicardial endothelial cells pattern embryonic coronary arterio–venous connections', *Proc Natl Acad Sci U S A,* 113(3), 656-661.

Cavallero, S., Shen, H., Yi, C., Lien, C.-L., Kumar, S. R. and Sucov, H. M. (2015) 'CXCL12 signaling is essential for maturation of the ventricular coronary endothelial plexus and establishment of functional coronary circulation', *Dev Cell,* 33(4), 469-477.

Chabriat, H., Joutel, A., Dichgans, M., Tournier-Lasserve, E. and Bousser, M.-G. (2009) 'CADASIL', *The Lancet Neurology,* 8(7), 643-653.

Chen, H., Shi, S., Acosta, L., Li, W., Lu, J., Bao, S., Chen, Z., Yang, Z., Schneider, M. D., Chien, K. R., Conway, S. J., Yoder, M. C., Haneline, L. S., Franco, D. and Shou, W. (2004) 'BMP-10 is essential for maintaining cardiac growth during murine cardiogenesis', *Development (Cambridge, England),* 131(9), 2219-2231.

Chen, H. I., Poduri, A., Numi, H., Kivela, R., Saharinen, P., McKay, A. S., Raftrey, B., Churko, J., Tian, X., Zhou, B., Wu, J. C., Alitalo, K. and Red-Horse, K. (2014) 'VEGF-C and aortic cardiomyocytes guide coronary artery stem development', *The Journal of Clinical Investigation,* 124(11), 4899-4914.

Combs, M. D., Braitsch, C. M., Lange, A. W., James, J. F. and Yutzey, K. E. (2011) 'NFATC1 promotes epicardium-derived cell invasion into myocardium', *Development,* 138(9), 1747-1757.

'Coronary artery surgery study (CASS): a randomized trial of coronary artery bypass surgery. Survival data', (1983) *Circulation,* 68(5), 939-950.

Costa, G., Harrington, K. I., Lovegrove, H. E., Page, D. J., Chakravartula, S., Bentley, K. and Herbert, S. P. (2016) 'Asymmetric division coordinates collective cell migration in angiogenesis', *Nat Cell Biol,* 18(12), 1292-1301.

# Bibliography


Cruz-Adalia, A., Jiménez-Borreguero, L. J., Ramírez-Huesca, M., Chico-Calero, I., Barreiro, O., López-Conesa, E., Fresno, M., Sánchez-Madrid, F. and Martín, P. (2010) CD69 Limits the Severity of Cardiomyopathy After Autoimmune Myocarditis, *Circulation,* 122(14), 1396-1404.

D'Amato, G., Luxan, G., del Monte-Nieto, G., Martinez-Poveda, B., Torroja, C., Walter, W., Bochter, M. S., Benedito, R., Cole, S., Martinez, F., Hadjantonakis, A.-K., Uemura, A., Jimenez-Borreguero, L. J. and de la Pompa, J. L. (2016a) 'Sequential Notch activation regulates ventricular chamber development', *Nat Cell Biol,* 18(1), 7-20.

D'Amato, G., Luxán, G. and de la Pompa, J. L. (2016b) 'Notch signalling in ventricular chamber development and cardiomyopathy', *The FEBS Journal,* 283(23), 4223-4237.

de la Pompa, J. L., Wakeham, A., Correia, K. M., Samper, E., Brown, S., Aguilera, R. J., Nakano, T., Honjo, T., Mak, T. W., Rossant, J. and Conlon, R. A. (1997) 'Conservation of the Notch signalling pathway in mammalian neurogenesis', *Development,* 124(6), 1139-48.

de la Pompa, J. L., Timmerman, L. A., Takimoto, H., Yoshida, H., Elia, A. J., Samper, E., Potter, J., Wakeham, A., Marengere, L., Langille, B. L., Crabtree, G. R. and Mak, T. W. (1998) 'Role of the NF-ATc transcription factor in morphogenesis of cardiac valves and septum', *Nature,* 392(6672), 182-186.

de la Pompa, J. L. and Epstein, J. A. (2012) 'Coordinating tissue interactions: Notch signaling in cardiac development and disease', *Dev Cell,* 22(2), 244-54.

del Monte, G., Casanova, J. C., Guadix, J. A., MacGrogan, D., Burch, J. B., Perez-Pomares, J. M. and de la Pompa, J. L. (2011) 'Differential Notch signaling in the epicardium is required for cardiac inflow development and coronary vessel morphogenesis', *Circ Res,* 108(7), 824-36.

Del Monte, G., Grego-Bessa, J., González-Rajal, A., Bolós, V. and De La Pompa, J. L. (2007) 'Monitoring Notch1 activity in development: Evidence for a feedback regulatory loop', *Developmental Dynamics,* 236(9), 2594-2614.

Dodge-Khatami, A., Mavroudis, C. and Backer, C. L. (2000) 'Congenital Heart Surgery Nomenclature and Database Project: anomalies of the coronary arteries', *The Annals of Thoracic Surgery,* 69(3, Supplement 1), 270-297.

Duarte, A., Hirashima, M., Benedito, R., Trindade, A., Diniz, P., Bekman, E., Costa, L., Henrique, D. and Rossant, J. (2004) 'Dosage-sensitive requirement for mouse Dll4 in artery development', *Genes & Development,* 18(20), 2474-2478.

Edgar, R., Domrachev, M. and Lash, A. E. (2002) 'Gene Expression Omnibus: NCBI gene expression and hybridization array data repository', *Nucleic Acids Research,* 30(1), 207-210.

Ehling, M., Adams, S., Benedito, R. and Adams, R. H. (2013) 'Notch controls retinal blood vessel maturation and quiescence', *Development,* 140(14), 3051-3061.

Epstein, Jonathan A., Aghajanian, H. and Singh, Manvendra K. (2015) 'Semaphorin Signaling in Cardiovascular Development', *Cell Metabolism,* 21(2), 163-173.

Esteban, V., Méndez-Barbero, N., Jesús Jiménez-Borreguero, L., Roqué, M., Novensá, L., Belén García-Redondo, A., Salaices, M., Vila, L., Arbonés, M. L., Campanero, M. R. and Redondo, J. M. (2011) 'Regulator of calcineurin 1 mediates pathological vascular wall remodelling', *The Journal of Experimental Medicine,* 208(10), 2125-2139.

Fatima, A., Culver, A., Culver, F., Liu, T., Dietz, W. H., Thomson, B. R., Hadjantonakis, A.-K., Quaggin, S. E. and Kume, T. (2014) 'Murine Notch1 is required for lymphatic vascular morphogenesis during development', *Developmental dynamics : an official publication of the American Association of Anatomists,* 243(7), 957-964.

Fischer, A., Schumacher, N., Maier, M., Sendtner, M. and Gessler, M. (2004) 'The Notch target genes Hey1 and Hey2 are required for embryonic vascular development', *Genes & Development,* 18(8), 901-911.

Fischer, A., Steidl, C., Wagner, T. U., Lang, E., Jakob, P. M., Friedl, P., Knobeloch, K.-P. and Gessler, M. (2007) 'Combined Loss of Hey1 and HeyL Causes Congenital Heart Defects Because of Impaired Epithelial to Mesenchymal Transition', *Circ Res,* 100(6), 856-863.

Gale, N.W. *et al.* Haploinsufficiency of delta-like 4 ligand results in embryonic lethality due to major defects in arterial and vascular development. *Proc Natl Acad Sci U S A* 101, 15949-15954 (2004).

Garg, V. (2006) 'Molecular genetics of aortic valve disease', *Current Opinion in Cardiology,* 21(3), 180-184.

Garg, V., Muth, A. N., Ransom, J. F., Schluterman, M. K., Barnes, R., King, I. N., Grossfeld, P. D. and Srivastava, D. (2005) 'Mutations in NOTCH1 cause aortic valve disease', *Nature,* 437(7056), 270-274.

Gerety, S. S. and Anderson, D. J. (2002) 'Cardiovascular ephrinB2 function is essential for embryonic angiogenesis', *Development,* 129(6), 1397-1410.

Gerety, S. S., Wang, H. U., Chen, Z.-F. and Anderson, D. J. (1999) 'Symmetrical Mutant Phenotypes of the Receptor EphB4 and Its Specific Transmembrane Ligand ephrin-B2 in Cardiovascular Development', *Molecular Cell,* 4(3), 403-414.

Gerhardt, H., Golding, M., Fruttiger, M., Ruhrberg, C., Lundkvist, A., Abramsson, A., Jeltsch, M., Mitchell, C., Alitalo, K., Shima, D. and Betsholtz, C. (2003) 'VEGF guides angiogenic sprouting utilizing endothelial tip cell filopodia', *The Journal of Cell Biology,* 161(6), 1163-1177.

Goel, S. *et al.* Normalization of the vasculature for treatment of cancer and other diseases. *Physiological reviews* 91, 1071-1121 (2011).

Grego-Bessa, J., Luna-Zurita, L., del Monte, G., Bolos, V., Melgar, P., Arandilla, A., Garratt, A. N., Zang, H., Mukouyama, Y. S., Chen, H., Shou, W., Ballestar, E., Esteller, M., Rojas, A., Perez-Pomares, J. M. and de la Pompa, J. L. (2007) 'Notch signaling is essential for ventricular chamber development', *Dev Cell,* 12(3), 415-29.

Grieskamp, T., Rudat, C., Lüdtke, T. H.-W., Norden, J. and Kispert, A. (2011) 'Notch Signaling Regulates Smooth Muscle Differentiation of Epicardium-Derived CellsNovelty and Significance', *Circ Res,* 108(7), 813-823.

Grunwald, I. C., Korte, M., Adelmann, G., Plueck, A., Kullander, K., Adams, R. H., Frotscher, M., Bonhoeffer, T. and Klein, R. (2004) 'Hippocampal plasticity requires postsynaptic ephrinBs', *Nature Neuroscience,* 7, 33.

Guadix, J. A., Carmona, R., Muñoz-Chápuli, R. and Pérez-Pomares, J. M. (2006) 'In vivo and in vitro analysis of the vasculogenic potential of avian proepicardial and epicardial cells†', *Developmental Dynamics,* 235(4), 1014-1026.

Hasan, S. S., Tsaryk, R., Lange, M., Wisniewski, L., Moore, J. C., Lawson, N. D., Wojciechowska, K., Schnittler, H. and Siekmann, A. F. (2017) 'Endothelial Notch signalling limits angiogenesis via control of artery formation', *Nat Cell Biol,* 19(8), 928-940.

He, L., Tian, X., Zhang, H., Wythe, J. D. and Zhou, B. (2014) 'Fabp4-CreER lineage tracing revealstwo distinctive coronary vascular populations', *J Cell Mol Med,* 18(11), 2152-2156.

Herbert, S. P., Huisken, J., Kim, T. N., Feldman, M. E., Houseman, B. T., Wang, R. A., Shokat, K. M. and Stainier, D. Y. R. (2009) 'Arterial-Venous Segregation by Selective Cell Sprouting: An Alternative Mode of Blood Vessel Formation', *Science,* 326(5950), 294-298.

High, F. A. and Epstein, J. A. (2008) 'The multifaceted role of Notch in cardiac development and disease', 9, 49.

High, F. A., Lu, M. M., Pear, W. S., Loomes, K. M., Kaestner, K. H. and Epstein, J. A. (2008) 'Endothelial expression of the Notch ligand Jagged1 is required for vascular smooth muscle development', *Proc Natl Acad Sci U S A,* 105(6), 1955-9.

Huang, D. W., Sherman, B. T. and Lempicki, R. A. (2009) 'Systematic and integrative analysis of large gene lists using DAVID bioinformatics resources', *Nature Protocols,* 4, 44.

Hutchins GM1, Kessler-Hanna A, Moore GW. Development of the coronary arteries in the embryonic human heart. *Circulation*. 1988 Jun;77(6):1250-7.

Hwa, J. J., Beckouche, N., Huang, L., Kram, Y., Lindskog, H. and Wang, R. A. (2017) 'Abnormal arterial-venous fusions and fate specification in mouse embryos lacking blood flow', *Scientific Reports,* 7, 11965.

Ishii, Y., Langberg, J., Rosborough, K. and Mikawa, T. (2009) 'Endothelial cell lineages of the heart', *Cell and tissue research,* 335(1), 67-73.

Iso, T., Maeno, T., Oike, Y., Yamazaki, M., Doi, H., Arai, M. and Kurabayashi, M. (2006) 'Dll4-selective Notch signaling induces ephrinB2 gene expression in endothelial cells', *Biochemical and Biophysical Research Communications,* 341(3), 708-714.

Itoh, M., Kim, C.-H., Palardy, G., Oda, T., Jiang, Y.-J., Maust, D., Yeo, S.-Y., Lorick, K., Wright, G. J., Ariza-McNaughton, L., Weissman, A. M., Lewis, J., Chandrasekharappa, S. C. and Chitnis, A. B. (2003) 'Mind Bomb Is a Ubiquitin Ligase that Is Essential for Efficient Activation of Notch Signaling by Delta', *Dev Cell,* 4(1), 67-82.

Ivins, S., Chappell, J., Vernay, B., Suntharalingham, J., Martineau, A., Mohun, Timothy J. and Scambler, Peter J. (2015) 'The CXCL12/CXCR4 Axis Plays a Critical Role in Coronary Artery Development', *Dev Cell,* 33(4), 455-468.

J., O. (1998) 'The origin of coronary arteries', *Circulation,* 38(150).

Jakobsson, L., Franco, C. A., Bentley, K., Collins, R. T., Ponsioen, B., Aspalter, I. M., Rosewell, I., Busse, M., Thurston, G., Medvinsky, A., Schulte-Merker, S. and Gerhardt, H. (2010) 'Endothelial cells dynamically compete for the tip cell position during angiogenic sprouting', *Nat Cell Biol,* 12(10), 943-953.

Jarriault, S., Brou, C., Logeat, F., Schroeter, E. H., Kopan, R. and Israel, A. (1995) 'Signalling downstream of activated mammalian Notch', *Nature,* 377, 355.

Jiao K, Kulessa H, Tompkins K, Zhou Y, Batts L, Baldwin HS, Hogan BL (2003) An essential role of Bmp4 in the atrioventricular septation of the mouse heart. *Genes & development* 17: 2362-7

Jorissen, E., Prox, J., Bernreuther, C., Weber, S., Schwanbeck, R., Serneels, L., Snellinx, A., Craessaerts, K., Thathiah, A., Tesseur, I., Bartsch, U., Weskamp, G., Blobel, C. P., Glatzel, M., De Strooper, B. and Saftig, P. (2010) 'The Disintegrin/Metalloproteinase ADAM10 Is Essential for the Establishment of the Brain Cortex', *The Journal of Neuroscience,* 30(14), 4833-4844.

Joukov, V., Kaipainen, A., Jeltsch, M., Pajusola, K., Olofsson, B., Kumar, V., Eriksson, U. and Alitalo, K. (1997) 'Vascular endothelial growth factors VEGF-B and VEGF-C', *Journal of Cellular Physiology,* 173(2), 211-215.

Joutel, A., Corpechot, C., Ducros, A., Vahedi, K., Chabriat, H., Mouton, P., Alamowitch, S., Domenga, V., Cécillion, M., Maréchal, E., Maciazek, J., Vayssière, C., Cruaud, C., Cabanis, E.-A., Ruchoux, M. M., Weissenbach, J., Bach, J. F., Bousser, M. G.

and Tournier-Lasserve, E. (1996) 'Notch3 mutations in CADASIL, a hereditary adult-onset condition causing stroke and dementia', *Nature,* 383, 707.

Kakuda, S. and Haltiwanger, R. S. (2017) 'Deciphering the Fringe-Mediated Notch Code: Identification of Activating and Inhibiting Sites Allowing Discrimination between Ligands', *Dev Cell,* 40(2), 193-201.

Kania, A. and Klein, R. (2016) 'Mechanisms of ephrin-Eph signalling in development, physiology and disease', *Nat Rev Mol Cell Biol,* 17(4), 240-56.

Kanzler, B., Kuschert, S. J., Liu, Y. H. and Mallo, M. (1998) 'Hoxa-2 restricts the chondrogenic domain and inhibits bone formation during development of the branchial area', *Development,* 125(14), 2587-97.

Katz, T. C., Singh, M. K., Degenhardt, K., Rivera-Feliciano, J., Johnson, R. L., Epstein, J. A. and Tabin, C. J. (2012) 'Distinct Compartments of the Proepicardial Organ Give Rise to Coronary Vascular Endothelial Cells', *Dev Cell,* 22(3), 639-650.

Kim, J., Oh, W.J., Gaiano, N., Yoshida, Y. & Gu, C. Semaphorin 3E-Plexin-D1 signaling regulates VEGF function in developmental angiogenesis via a feedback mechanism. *Genes & development* **25**, 1399-1411 (2011).

King, K.R. ,Aaron D Aguirre, Yu-Xiang Ye, Yuan Sun, Jason D Roh, Richard P Ng Jr, Rainer H Kohler, Sean P Arlauckas, Yoshiko Iwamoto, Andrej Savol, Ruslan I Sadreyev, Mark Kelly, Timothy P Fitzgibbons, Katherine A Fitzgerald, Timothy Mitchison, Peter Libby, Matthias Nahrendorf & Ralph Weissleder. IRF3 and type I interferons fuel a fatal response to myocardial infarction. *Nat Med* 23, 1481-1487 (2017).

Kisanuki YY, Hammer RE, Miyazaki J, Williams SC, Richardson JA, Yanagisawa M (2001) Tie2-Cre transgenic mice: a new model for endothelial cell-lineage analysis in vivo. *Developmental biology* 230: 230-42.

Koch U, Fiorini E, Benedito R, Besseyrias V, Schuster-Gossler K, Pierres M, Manley NR, Duarte A, Macdonald HR, Radtke F (2008) Delta-like 4 is the essential, nonredundant ligand for Notch1during thymic T cell lineage commitment. *J Exp Med* 205: 2515-23

Kokubo, H., Miyagawa-Tomita, S., Nakazawa, M., Saga, Y. and Johnson, R. L. (2005) 'Mouse hesr1 and hesr2 genes are redundantly required to mediate Notch signaling in the developing cardiovascular system', *Developmental Biology,* 278(2), 301-309.

Koo BK, Yoon MJ, Yoon KJ, Im SK, Kim YY, Kim CH, Suh PG, Jan YN, Kong YY (2007) An obligatory role of mind bomb-1 in notch signaling of mammalian development. *PLoS One* 2: e1221

Korn, C. & Augustin, H.G. Mechanisms of Vessel Pruning and Regression. *Dev Cell* 34, 5-17 (2015).

Kovall, R. A., Gebelein, B., Sprinzak, D. and Kopan, R. (2017) 'The Canonical Notch Signaling Pathway: Structural and Biochemical Insights into Shape, Sugar, and Force', *Dev Cell,* 41(3), 228-241.

Krantz, I. D., Smith, R., Colliton, R. P., Tinkel, H., Zackai, E. H., Piccoli, D. A., Goldmuntz, E. and Spinner, N. B. (1999) 'Jagged1 mutations in patients ascertained with isolated congenital heart defects', *American Journal of Medical Genetics,* 84(1), 56-60.

Krebs, L. T., Starling, C., Chervonsky, A. V. and Gridley, T. (2010) 'Notch1 activation in mice causes arteriovenous malformations phenocopied by ephrinB2 and EphB4 mutants', *Genesis (New York, N.Y. : 2000),* 48(3), 146-150.

Krebs, L.T. *et al.* Haploinsufficient lethality and formation of arteriovenous malformations in Notch pathway mutants. *Genes & development* **18**, 2469-2473 (2004).

Krebs, L. T., Xue, Y., Norton, C. R., Shutter, J. R., Maguire, M., Sundberg, J. P., Gallahan, D., Closson, V., Kitajewski, J., Callahan, R., Smith, G. H., Stark, K. L. and Gridley, T. (2000) 'Notch signaling is essential for vascular morphogenesis in mice', *Genes & Development,* 14(11), 1343-1352.

Krzywinski, M., Schein, J., Birol, İ., Connors, J., Gascoyne, R., Horsman, D., Jones, S. J. and Marra, M. A. (2009) 'Circos: An information aesthetic for comparative genomics', *Genome Research,* 19(9), 1639-1645.

Lagares, D., Ghassemi-Kakroodi, P., Tremblay, C., Santos, A., Probst, C. K., Franklin, A., Santos, D. M., Grasberger, P., Ahluwalia, N., Montesi, S. B., Shea, B. S., Black, K. E., Knipe, R., Blati, M., Baron, M., Wu, B., Fahmi, H., Gandhi, R., Pardo, A., Selman, M., Wu, J., Pelletier, J.-P., Martel-Pelletier, J., Tager, A. M. and Kapoor, M. (2017) 'ADAM10-mediated ephrin-B2 shedding promotes myofibroblast activation and organ fibrosis'.

Lawson, N. D., Scheer, N., Pham, V. N., Kim, C.-H., Chitnis, A. B., Campos-Ortega, J. A. and Weinstein, B. M. (2001) 'Notch signaling is required for arterial-venous differentiation during embryonic vascular development', *Development,* 128(19), 3675-3683.

Lewis, A. E., Hwa, J., Wang, R., Soriano, P. and Bush, J. O. (2015) 'Neural crest defects in ephrin-B2 mutant mice are non-autonomous and originate from defects in the vasculature', *Developmental Biology,* 406(2), 186-195.

Li, B. and Dewey, C. N. (2011) 'RSEM: accurate transcript quantification from RNA-Seq data with or without a reference genome', *BMC Bioinformatics,* 12(1), 323.

Li, L., Krantz, I. D., Deng, Y., Genin, A., Banta, A. B., Collins, C. C., Qi, M., Trask, B. J., Kuo, W. L., Cochran, J., Costa, T., Pierpont, M. E. M., Rand, E. B., Piccoli, D. A., Hood, L. and Spinner, N. B. (1997) 'Alagille syndrome is caused by mutations in human Jagged1, which encodes a ligand for Notch1', *Nat Genet,* 16(3), 243-251.

Liberthson, R. R., Sagar, K., Berkoben, J. P., Weintraub, R. M. and Levine, F. H. (1979) 'Congenital coronary arteriovenous fistula. Report of 13 patients, review of the literature and delineation of management', *Circulation,* 59(5), 849-854.

Liberzon, A. *et al.* The Molecular Signatures Database (MSigDB) hallmark gene set collection. *Cell Syst* **1**, 417-425 (2015).

Limbourg, A., Ploom, M., Elligsen, D., Sörensen, I., Ziegelhoeffer, T., Gossler, A., Drexler, H. and Limbourg, F. P. (2007) 'Notch Ligand Delta-Like 1 Is Essential for Postnatal Arteriogenesis', *Circ Res,* 100(3), 363-371.

Liu, H., Kennard, S., & Lilly, B. (2009). NOTCH3 expression is induced in mural cells through an autoregulatory loop that requires endothelial-expressed JAGGED1. *Circulatio Research*, *104*(4), 466–475. http://doi.org/10.1161/CIRCRESAHA.108.184846

Liu, H., Zhang, W., Kennard, S., Caldwell, R. B. and Lilly, B. (2010) 'Notch3 is critical for proper angiogenesis and mural cell investment', *Circ Res,* 107(7), 860-870.

Liu, Q., Hu, T., He, L., Huang, X., Tian, X., Zhang, H., He, L., Pu, W., Zhang, L., Sun, H., Fang, J., Yu, Y., Duan, S., Hu, C., Hui, L., Zhang, H., Quertermous, T., Xu, Q., Red-Horse, K., Wythe, J. D. and Zhou, B. (2015) 'Genetic targeting of sprouting angiogenesis using Apln-CreER', *Nature Communications,* 6, 6020.

Loomes, K. M., Underkoffler, L. A., Morabito, J., Gottlieb, S., Piccoli, D. A., Spinner, N. B., Scott Baldwin, H. and Oakey, R. J. (1999) 'The Expression of Jagged1 in the Developing Mammalian Heart Correlates With Cardiovascular Disease in Alagille Syndrome', *Human Molecular Genetics,* 8(13), 2443-2449.

Luca, V. C., Jude, K. M., Pierce, N. W., Nachury, M. V., Fischer, S. and Garcia, K. C. (2015) 'Structural basis for Notch1 engagement of Delta-like 4', *Science (New York, N.Y.),* 347(6224), 847-853.

Luca, V. C., Kim, B. C., Ge, C., Kakuda, S., Wu, D., Roein-Peikar, M., Haltiwanger, R. S., Zhu, C., Ha, T. and Garcia, K. C. (2017) 'Notch-Jagged complex structure implicates a catch bond in tuning ligand sensitivity', *Science,* 355(6331), 1320-1324.

Luna-Zurita, L., Prados, B., Grego-Bessa, J., Luxán, G., del Monte, G., Benguría, A., Adams, R. H., Pérez-Pomares, J. M. and de la Pompa, J. L. (2010) 'Integration of a Notch-dependent mesenchymal gene program and Bmp2-driven cell invasiveness regulates murine cardiac valve formation', *The Journal of Clinical Investigation,* 120(10), 3493-3507.

Luxán, G., Casanova, J. C., Martínez-Poveda, B., Prados, B., D'Amato, G., MacGrogan, D., Gonzalez-Rajal, A., Dobarro, D., Torroja, C., Martinez, F., Izquierdo-García, J. L., Fernández-Friera, L., Sabater-Molina, M., Kong, Y.-Y., Pizarro, G., Ibañez, B., Medrano, C., García-Pavía, P., Gimeno, J. R., Monserrat, L., Jiménez-Borreguero, L. J. and de la Pompa, J. L. (2013) 'Mutations in the NOTCH pathway regulator MIB1 cause left ventricular noncompaction cardiomyopathy', 19, 193.

MacGrogan, D., D'Amato, G., Travisano, S., Martinez-Poveda, B., Luxán, G., del Monte-Nieto, G., Papoutsi, T., Sbroggio, M., Bou, V., Gomez-del Arco, P., Gómez, M. J., Zhou, B., Redondo, J. M., Jiménez-Borreguero, L. J. and de la Pompa, J. L. (2016) Sequential Ligand-Dependent Notch Signaling Activation Regulates Valve Primordium Formation and Morphogenesis, *Circ Res,* 118(10), 1480-1497.

Mancini SJ, Mantei N, Dumortier A, Suter U, MacDonald HR, Radtke F (2005) Jagged1-dependentNotch signaling is dispensable for hematopoietic stem cell self-renewal and differentiation. *Blood* 105: 2340-2

Manderfield, L. J., High, F. A., Engleka, K. A., Liu, F., Li, L., Rentschler, S. and Epstein, J. A. (2012) 'Notch activation of Jagged1 contributes to the assembly of the arterial wall', *Circulation,* 125(2), 314-23.

Mangukia, C. V. (2012) 'Coronary Artery Fistula', *The Annals of Thoracic Surgery,* 93(6), 2084-2092.

Männer, J. (1999) 'Does the subepicardial mesenchyme contribute myocardioblasts to the myocardium of the chick embryo heart? A quail-chick chimera study tracing the fate of the epicardial primordium', *The Anatomical Record,* 255(2), 212-226.

Martin, M. (2011) 'Cutadapt removes adapter sequences from high-throughput sequencing reads', *2011,* 17(1).

Masumura, T., Yamamoto, K., Shimizu, N., Obi, S. and Ando, J. (2009) 'Shear Stress Increases Expression of the Arterial Endothelial Marker EphrinB2 in Murine ES Cells via the VEGF-Notch Signaling Pathways', *Arteriosclerosis, Thrombosis, and Vascular Biology,* 29(12), 2125-2131.

Matsuura, A., Ito, M., Sakaidani, Y., Kondo, T., Murakami, K., Furukawa, K., Nadano, D., Matsuda, T. and Okajima, T. (2008) 'O-Linked N-Acetylglucosamine Is Present on the Extracellular Domain of Notch Receptors', *Journal of Biological Chemistry,* 283(51), 35486-35495.

Menendez-Montes, I., Escobar, B., Palacios, B., Gómez, M. J., Izquierdo-Garcia, J. L., Flores, L., Jiménez-Borreguero, L. J., Aragones, J., Ruiz-Cabello, J., Torres, M. and Martin-Puig, S. (2016) 'Myocardial VHL-HIF Signaling Controls an Embryonic Metabolic Switch Essential for Cardiac Maturation', *Dev Cell,* 39(6), 724-739.

Meyer, D. and Birchmeier, C. (1995) 'Multiple essential functions of neuregulin in development', *Nature,* 378, 386.

Michael Schneider, V. K., Lars Ulrik Nordstrøm, Lei Feng , Hideyuki Takeuchi,, Huilin Hao, V. C. L., K Christopher Garcia, Pamela Stanley , Peng Wu and Haltiwanger, R. S. (2017) 'Inhibition of Delta-induced Notch signaling using fucose analogs', *Nature Chemical Biology*.

Mikawa, T. and Fischman, D. A. (1992) 'Retroviral analysis of cardiac morphogenesis: discontinuous formation of coronary vessels', *Proc Natl Acad Sci U S A,* 89(20), 9504-9508.

Moloney, D. J., Panin, V. M., Johnston, S. H., Chen, J., Shao, L., Wilson, R., Wang, Y., Stanley, P., Irvine, K. D., Haltiwanger, R. S. and Vogt, T. F. (2000) 'Fringe is a glycosyltransferase that modifies Notch', *Nature,* 406(6794), 369-375.

Moorman, A. F. M. and Christoffels, V. M. (2003) 'Cardiac Chamber Formation: Development, Genes, and Evolution', *Physiological Reviews,* 83(4), 1223-1267.

Mukouyama, Y.-s., James, J., Nam, J. and Uchida, Y. (2012) 'Whole-Mount Confocal Microscopy for Vascular Branching Morphogenesis', *Methods in molecular biology (Clifton, N.J.),* 843, 69-78.

Myocardial Infarction, G. and Investigators, C. A. E. C. (2016) 'Coding Variation in ANGPTL4, LPL, and SVEP1 and the Risk of Coronary Disease', *The New England journal of medicine,* 374(12), 1134-1144.

Nakayama, A., Nakayama, M., Turner, C. J., Höing, S., Lepore, J. J. and Adams, R. H. (2013) 'Ephrin-B2 controls PDGFRβ internalization and signaling', *Genes & Development,* 27(23), 2576-2589.

Nakayama, M., Nakayama, A., van Lessen, M., Yamamoto, H., Hoffmann, S., Drexler, H. C. A., Itoh, N., Hirose, T., Breier, G., Vestweber, D., Cooper, J. A., Ohno, S., Kaibuchi, K. and Adams, R. H. (2013) 'Spatial regulation of VEGF receptor endocytosis in angiogenesis', *Nat Cell Biol,* 15(3), 249-260.

Nam, J., Onitsuka, I., Hatch, J., Uchida, Y., Ray, S., Huang, S., Li, W., Zang, H., Ruiz-Lozano, P. and Mukouyama, Y. S. (2013) 'Coronary veins determine the pattern of sympathetic innervation in the developing heart', *Development,* 140(7), 1475-85.

Napp, L. C., Augustynik, M., Paesler, F., Krishnasamy, K., Woiterski, J., Limbourg, A., Bauersachs, J., Drexler, H., Le Noble, F. and Limbourg, F. P. (2012) 'Extrinsic Notch Ligand Delta-Like 1 Regulates Tip Cell Selection and Vascular Branching Morphogenesis', *Circ Res,* 110(4), 530-535.

Navarro-Lopez, F., Soler, J., Magriña, J., Esplugues, E., Carlos Pare, J., Sanz, G. and Betriu, A. (1986) 'Systolic compression of coronary artery in hypertrophic cardiomyopathy', *International Journal of Cardiology,* 12(3), 309-320.

Nesbitt, T., Lemley, A., Davis, J., Yost, M. J., Goodwin, R. L. and Potts, J. D. (2006) 'Epicardial Development in the Rat: A New Perspective', *Microscopy and Microanalysis,* 12(5), 390-398.

Nielsen, C. M., Cuervo, H., Ding, V. W., Kong, Y., Huang, E. J. and Wang, R. A. (2014) 'Deletion of Rbpj from postnatal endothelium leads to abnormal arteriovenous shunting in mice', *Development,* 141(19), 3782-92.

Niessen, K. and Karsan, A. (2008) 'Notch Signaling in Cardiac Development', *Circ Res,* 102(10), 1169-1181.

Noseda, M., McLean, G., Niessen, K., Chang, L., Pollet, I., Montpetit, R., Shahidi, R., Dorovini-Zis, K., Li, L., Beckstead, B., Durand, R. E., Hoodless, P. A. and Karsan, A. (2004) 'Notch Activation Results in Phenotypic and Functional Changes Consistent With Endothelial-to-Mesenchymal Transformation', *Circ Res,* 94(7), 910-917.

Nowotschin, S., Xenopoulos, P., Schrode, N. and Hadjantonakis, A.-K. (2013) 'A bright single-cell resolution live imaging reporter of Notch signaling in the mouse', *BMC Dev Biol,* 13, 15-15.

Oda, T., Elkahloun, A. G., Pike, B. L., Okajima, K., Krantz, I. D., Genin, A., Piccoli, D. A., Meltzer, P. S., Spinner, N. B., Collins, F. S. and Chandrasekharappa, S. C. (1997) 'Mutations in the human Jagged1 gene are responsible for Alagille syndrome', *Nat Genet,* 16(3), 235-242.

Ottone, C., Krusche, B., Whitby, A., Clements, M., Quadrato, G., Pitulescu, M. E., Adams, R. H. and Parrinello, S. (2014) 'Direct cell-cell contact with the vascular niche maintains quiescent neural stem cells', *Nat Cell Biol,* 16(11), 1045-56.

Palmquist-Gomes, P., Guadix, J. A. and Pérez-Pomares, J. M. 'Avian embryonic coronary arterio-venous pattering involves the contribution of different endothelial and endocardial cell populations', *Developmental Dynamics*, n/a-n/a.

Park-Windhol, C. & D'Amore, P.A. Disorders of Vascular Permeability. *Annu Rev Pathol* 11, 251-281 (2016).

Pedrosa, A.R. *et al.* Endothelial Jagged1 antagonizes Dll4 regulation of endothelial branching and promotes vascular maturation downstream of Dll4/Notch1. *Arterioscler Thromb Vasc Biol* 35, 1134-1146 (2015).

Pérez-Pomares, J. M. and de la Pompa, J. L. (2011) 'Signaling During Epicardium and Coronary Vessel Development', *Circ Res,* 109(12), 1429-1442.

Pérez-Pomares, J. M., de la Pompa, J. L., Franco, D., Henderson, D., Ho, S. Y., Houyel, L., Kelly, R. G., Sedmera, D., Sheppard, M., Sperling, S., Thiene, G., van den Hoff, M. and Basso, C. (2016) 'Congenital coronary artery anomalies: a bridge from embryology to anatomy and pathophysiology—a position statement of the development, anatomy, and pathology ESC Working Group', *Cardiovasc Res,* 109(2), 204-216.

Pérez-Pomares, J. M., Macías, D., García-Garrido, L. and Muñoz-Chápuli, R. (1998) 'The origin of the subepicardial mesenchyme in the avian embryo: an immunohistochemical and quail-chick chimera study', *Developmental Biology,* 200(1), 57-68.

Pitulescu, M. E. and Adams, R. H. (2010) 'Eph/ephrin molecules—a hub for signaling and endocytosis', *Genes & Development,* 24(22), 2480-2492.

Pitulescu, M. E., Schmidt, I., Giaimo, B. D., Antoine, T., Berkenfeld, F., Ferrante, F., Park, H., Ehling, M., Biljes, D., Rocha, S. F., Langen, U. H., Stehling, M., Nagasawa, T., Ferrara, N., Borggrefe, T. and Adams, R. H. (2017) 'Dll4 and Notch signalling couples sprouting angiogenesis and artery formation', *Nat Cell Biol,* 19(8), 915-927.

Poelmann, R. E., Gittenberger-de Groot, A. C., Mentink, M. M., Bökenkamp, R. and Hogers, B. (1993) 'Development of the cardiac coronary vascular endothelium, studied with antiendothelial antibodies, in chicken-quail chimeras', *Circ Res,* 73(3), 559-568.

Polacheck, W. J., Kutys, M. L., Yang, J., Eyckmans, J., Wu, Y., Vasavada, H., Hirschi, K. K. and Chen, C. S. (2017) 'A non-canonical Notch complex regulates adherens junctions and vascular barrier function', *Nature,* 552, 258.

Pompa de la, J. L., Wakeham, A., Correia, K. M., Samper, E., Brown, S., Aguilera, R. J., Nakano, T., Honjo, T., Mak, T. W., Rossant, J. and Conlon, R. A. (1997) 'Conservation of the Notch signalling pathway in mammalian neurogenesis', *Development,* 124(6), 1139-1148.

Potente, M. and Mäkinen, T. (2017) 'Vascular heterogeneity and specialization in development and disease', *Nature Reviews Molecular Cell Biology,* 18, 477.

Radtke F, Wilson A, Stark G, Bauer M, van Meerwijk J, MacDonald HR, Aguet M (1999) Deficient T cell fate specification in mice with an induced inactivation of Notch1. *Immunity* 10: 547-58

Ranger, A. M., Oukka, M., Rengarajan, J. and Glimcher, L. H. (1998) 'Inhibitory Function of Two NFAT Family Members in Lymphoid Homeostasis and Th2 Development', *Immunity,* 9(5), 627-635.

Red-Horse, K., Ueno, H., Weissman, I. L. and Krasnow, M. A. (2010) 'Coronary arteries form by developmental reprogramming of venous cells', *Nature,* 464(7288), 549-53.

Riley, P. R. and Smart, N. (2011) 'Vascularizing the heart', *Cardiovasc Res,* 91(2), 260-8.

Ritchie, M. E., Phipson, B., Wu, D., Hu, Y., Law, C. W., Shi, W. and Smyth, G. K. (2015) 'limma powers differential expression analyses for RNA-sequencing and microarray studies', *Nucleic Acids Research,* 43(7), e47-e47.

Robinson, M. D., McCarthy, D. J. and Smyth, G. K. (2010) 'edgeR: a Bioconductor package for differential expression analysis of digital gene expression data', *Bioinformatics,* 26(1), 139-140.

Roca, C. and Adams, R. H. (2007) 'Regulation of vascular morphogenesis by Notch signaling', *Genes & Development,* 21(20), 2511-2524.

Salvucci, O. and Tosato, G. (2012) 'Essential roles of EphB receptors and EphrinB ligands in endothelial cell function and angiogenesis', *Adv Cancer Res,* 114, 21-57.

Scehnet, J. S., Jiang, W., Ram Kumar, S., Krasnoperov, V., Trindade, A., Benedito, R., Djokovic, D., Borges, C., Ley, E. J., Duarte, A. and Gill, P. S. (2007) 'Inhibition of Dll4-mediated signaling induces proliferation of immature vessels and results in poor tissue perfusion', *Blood,* 109(11), 4753-4760.

Schneider, M., Kumar, V., Nordstrøm, L. U., Feng, L., Takeuchi, H., Hao, H., Luca, V. C., Garcia, K. C., Stanley, P., Wu, P. and Haltiwanger, R. S. (2018) 'Inhibition of Delta-induced Notch signaling using fucose analogs', *Nature Chemical Biology*.

Sedmera, D., Pexieder, T., Vuillemin, M., Thompson, R. P. and Anderson, R. H. (2000) 'Developmental patterning of the myocardium', *The Anatomical Record,* 258(4), 319-337.

Sedmera, D., Reckova, M., DeAlmeida, A., Coppen, S. R., Kubalak, S. W., Gourdie, R. G. and Thompson, R. P. (2003) 'Spatiotemporal pattern of commitment to slowed proliferation in the embryonic mouse heart indicates progressive differentiation of the cardiac conduction system', *The Anatomical Record Part A: Discoveries in Molecular, Cellular, and Evolutionary Biology,* 274A(1), 773-777.

Shah, A. V., Birdsey, G. M., Peghaire, C., Pitulescu, M. E., Dufton, N. P., Yang, Y., Weinberg, I., Osuna Almagro, L., Payne, L., Mason, J. C., Gerhardt, H., Adams, R. H. and Randi, A. M. (2017) 'The endothelial transcription factor ERG mediates Angiopoietin-1-dependent control of Notch signalling and vascular stability', *Nature Communications,* 8, 16002.

Shalaby, F., Rossant, J., Yamaguchi, T. P., Gertsenstein, M., Wu, X. F., Breitman, M. L. and Schuh, A. C. (1995) 'Failure of blood-island formation and vasculogenesis in Flk-1-deficient mice', *Nature,* 376(6535), 62-6.

Sharma, B., Chang, A. and Red-Horse, K. (2017a) 'Coronary Artery Development: Progenitor Cells and Differentiation Pathways', *Annual review of physiology,* 79, 1-19.

Sharma, B., Ho, L., Ford, G. H., Chen, H. I., Goldstone, A. B., Woo, Y. J., Quertermous, T., Reversade, B. and Red-Horse, K. (2017b) 'Alternative Progenitor Cells Compensate to Rebuild the Coronary Vasculature in Elabela- and Apj-Deficient Hearts', *Dev Cell,* 42(6), 655-666.e3.

Shi, S. and Stanley, P. (2003) 'Protein O-fucosyltransferase 1 is an essential component of Notch signaling pathways', *Proceedings of the National Academy of Sciences,* 100(9), 5234-5239.

Sjöqvist, M. and Andersson, E. R. (2017) 'Do as I say, Not(ch) as I do: lateral control of cell fate', *Developmental Biology*.

Sommer, R. J., Hijazi, Z. M. and Rhodes, J. F. (2008) 'Pathophysiology of Congenital Heart Disease in the Adult', *Part I: Shunt Lesions,* 117(8), 1090-1099.

Sörensen, I., Adams, R. H. and Gossler, A. (2009) 'DLL1-mediated Notch activation regulates endothelial identity in mouse fetal arteries', *Blood,* 113(22), 5680-5688.

Soriano, P. (1999) 'Generalized lacZ expression with the ROSA26 Cre reporter strain', *Nat Genet,* 21(1), 70-71.

Srinivas S, Watanabe T, Lin CS, William CM, Tanabe Y, Jessell TM, Costantini F (2001) Cre reporter strains produced by targeted insertion of EYFP and ECFP into the ROSA26 locus. *BMC developmental biology* 1: 4

Sturn, A., Quackenbush, J. and Trajanoski, Z. (2002) 'Genesis: cluster analysis of microarray data', *Bioinformatics,* 18(1), 207-208.

Su, S.-a., Yang, D., Wu, Y., Xie, Y., Zhu, W., Cai, Z., Shen, J., Fu, Z., Wang, Y., Jia, L., Wang, Y., Wang, J. a. and Xiang, M. (2017) 'EphrinB2 Regulates Cardiac Fibrosis Through Modulating the Interaction of Stat3 and TGF-β/Smad3 Signaling', *Circ Res*.

Subramanian, A., Tamayo, P., Mootha, V. K., Mukherjee, S., Ebert, B. L., Gillette, M. A., Paulovich, A., Pomeroy, S. L., Golub, T. R., Lander, E. S. and Mesirov, J. P. (2005) 'Gene set enrichment analysis: A knowledge-based approach for interpreting genome-wide expression profiles', *Proceedings of the National Academy of Sciences,* 102(43), 15545-15550.

Suchting, S., Freitas, C., le Noble, F., Benedito, R., Breant, C., Duarte, A. and Eichmann, A. (2007) 'The Notch ligand Delta-like 4 negatively regulates endothelial tip cell formation and vessel branching', *Proc Natl Acad Sci U S A,* 104(9), 3225-30.

Swift, M. R. and Weinstein, B. M. (2009) 'Arterial–Venous Specification During Development', *Circ Res,* 104(5), 576-588.

Tammela, T., Zarkada, G., Wallgard, E., Murtomäki, A., Suchting, S., Wirzenius, M., Waltari, M., Hellström, M., Schomber, T., Peltonen, R., Freitas, C., Duarte, A., Isoniemi, H., Laakkonen, P., Christofori, G., Ylä-Herttuala, S., Shibuya, M., Pytowski, B., Eichmann, A., Betsholtz, C. and Alitalo, K. (2008) 'Blocking VEGFR-3 suppresses angiogenic sprouting and vascular network formation', *Nature,* 454, 656.

Tatsuya I., Yasuo H. and Larry K. (2003) 'Notch Signaling in Vascular Development' *Arteriosclerosis, Thrombosis, and Vascular Biology*. 2003;23:543-553, originally https://doi.org/10.1161/01.ATV.0000060892.81529.8F

Taylor, P., Takeuchi, H., Sheppard, D., Chillakuri, C., Lea, S. M., Haltiwanger, R. S. and Handford, P. A. (2014) 'Fringe-mediated extension of O-linked fucose in the ligand-binding region of Notch1 increases binding to mammalian Notch ligands', *Proc Natl Acad Sci U S A,* 111(20), 7290-7295.

Tian, X., Hu, T., He, L., Zhang, H., Huang, X., Poelmann, R. E., Liu, W., Yang, Z., Yan, Y., Pu, W. T. and Zhou, B. (2013) 'Peritruncal coronary endothelial cells contribute to proximal coronary artery stems and their aortic orifices in the mouse heart', *PLoS One,* 8(11), e80857.

Tian, X., Hu, T., Zhang, H., He, L., Huang, X., Liu, Q., Yu, W., He, L., Yang, Z., Yan, Y., Yang, X., Zhong, T. P., Pu, W. T. and Zhou, B. (2014) 'Vessel formation. De novo formation of a distinct coronary vascular population in neonatal heart', *Science,* 345(6192), 90-4.

Tian, X., Hu, T., Zhang, H., He, L., Huang, X., Liu, Q., Yu, W., He, L., Yang, Z., Zhang, Z., Zhong, T. P., Yang, X., Yang, Z., Yan, Y., Baldini, A., Sun, Y., Lu, J., Schwartz, R. J., Evans, S. M., Gittenberger-de Groot, A. C., Red-Horse, K. and Zhou, B. (2013) 'Subepicardial endothelial cells invade the embryonic ventricle wall to form coronary arteries', *Cell Research,* 23(9), 1075-1090.

Tian, X., Li, Y., He, L., Zhang, H., Huang, X., Liu, Q., Pu, W., Zhang, L., Li, Y., Zhao, H., Wang, Z., Zhu, J., Nie, Y., Hu, S., Sedmera, D., Zhong, T. P., Yu, Y., Zhang, L., Yan, Y., Qiao, Z., Wang, Q.-D., Wu, S. M., Pu, W. T., Anderson, R. H. and Zhou, B. (2017) 'Identification of a hybrid myocardial zone in the mammalian heart after birth', *Nature Communications,* 8(1), 87.

Tian, X., Pu, W. T. and Zhou, B. (2015) 'Cellular Origin and Developmental Program of Coronary Angiogenesis', *Circ Res,* 116(3), 515-530.

Timmerman, L. A., Grego-Bessa, J., Raya, A., Bertrán, E., Pérez-Pomares, J. M., Díez, J., Aranda, S., Palomo, S., McCormick, F., Izpisúa-Belmonte, J. C. and de la Pompa, J. L. (2004) 'Notch promotes epithelial-mesenchymal transition during cardiac development and oncogenic transformation', *Genes & Development,* 18(1), 99-115.

Trindade, A., Ram Kumar, S., Scehnet, J. S., Lopes-da-Costa, L., Becker, J., Jiang, W., Liu, R., Gill, P. S. and Duarte, A. (2008) 'Overexpression of delta-like 4 induces arterialization and attenuates vessel formation in developing mouse embryos', *Blood,* 112(5), 1720-1729.

Uyttendaele, H., Ho, J., Rossant, J. & Kitajewski, J. Vascular patterning defects associated with expression of activated Notch4 in embryonic endothelium. *Proc Natl Acad Sci U S A* 98, 5643-5648. (2001).

van den Akker, N. M., Caolo, V., Wisse, L. J., Peters, P. P., Poelmann, R. E., Carmeliet, P., Molin, D. G. and Gittenberger-de Groot, A. C. (2008) 'Developmental coronary maturation is disturbed by aberrant cardiac vascular endothelial growth factor expression and Notch signalling', *Cardiovasc Res,* 78(2), 366-75.

VanDusen, N. J., Casanovas, J., Vincentz, J. W., Firulli, B. A., Osterwalder, M., Lopez-Rios, J., Zeller, R., Zhou, B., Grego-Bessa, J., De La Pompa, J. L., Shou, W. and Firulli, A. B. (2014) 'Hand2 is an Essential Regulator for Two Notch-Dependent Functions within the Embryonic Endocardium', *Cell reports,* 9(6), 2071-2083.

Villa, N., Walker, L., Lindsell, C. E., Gasson, J., Iruela-Arispe, M. L. and Weinmaster, G. (2001) 'Vascular expression of Notch pathway receptors and ligands is restricted to arterial vessels', *Mechanisms of Development,* 108(1), 161-164.

Viragh, S. and Challice, C. E. (1981) 'The origin of the epicardium and the embryonic myocardial circulation in the mouse', *The Anatomical Record,* 201(1), 157-168.

Volz, K. S., Jacobs, A. H., Chen, H. I., Poduri, A., McKay, A. S., Riordan, D. P., Kofler, N., Kitajewski, J., Weissman, I. and Red-Horse, K. (2015) 'Pericytes are progenitors for coronary artery smooth muscle', *eLife,* 4, e10036.

Vrancken Peeters, M.-P. F. M., Gittenberger-de Groot, A. C., Mentink, M. M. T., Hungerford, J. E., Little, C. D. and Poelmann, R. E. (1997) 'Differences in development of coronary arteries and veins', *Cardiovasc Res,* 36(1), 101-110.

Wagner, N., Wagner, K.-D., Theres, H., Englert, C., Schedl, A. and Scholz, H. (2005) 'Coronary vessel development requires activation of the TrkB neurotrophin receptor by the Wilms' tumor transcription factor Wt1', *Genes & Development,* 19(21), 2631-2642.

Walter, W., Sánchez-Cabo, F. and Ricote, M. (2015) 'GOplot: an R package for visually combining expression data with functional analysis', *Bioinformatics,* 31(17), 2912-2914.

Wang, H. U., Chen, Z.-F. and Anderson, D. J. (1998) 'Molecular Distinction and Angiogenic Interaction between Embryonic Arteries and Veins Revealed by ephrin-B2 and Its Receptor Eph-B4', *Cell,* 93(5), 741-753.

Wang, Y., Nakayama, M., Pitulescu, M. E., Schmidt, T. S., Bochenek, M. L., Sakakibara, A., Adams, S., Davy, A., Deutsch, U., Luthi, U., Barberis, A., Benjamin, L. E., Makinen, T., Nobes, C. D. and Adams, R. H. (2010) 'Ephrin-B2 controls VEGF-induced angiogenesis and lymphangiogenesis', *Nature,* 465(7297), 483-486.

Wang, Y., Wu, B., Chamberlain, A. A., Lui, W., Koirala, P., Susztak, K., Klein, D., Taylor, V. and Zhou, B. (2013) 'Endocardial to Myocardial Notch-Wnt-Bmp Axis Regulates Early Heart Valve Development', *PLoS One,* 8(4), e60244.

Wang, Y., Wu, B., Lu, P., Zhang, D., Wu, B., Varshney, S., del Monte-Nieto, G., Zhuang, Z., Charafeddine, R., Kramer, A. H., Sibinga, N. E., Frangogiannis, N. G., Kitsis, R. N., Adams, R. H., Alitalo, K., Sharp, D. J., Harvey, R. P., Stanley, P. and Zhou, B. (2017) 'Uncontrolled angiogenic precursor expansion causes coronary artery anomalies in mice lacking Pofut1', *Nature Communications,* 8(1), 578.

Wessels, A., van den Hoff, M. J. B., Adamo, R. F., Phelps, A. L., Lockhart, M. M., Sauls, K., Briggs, L. E., Norris, R. A., van Wijk, B., Perez-Pomares, J. M., Dettman, R. W. and Burch, J. B. E. (2012) 'Epicardially-derived Fibroblasts Preferentially Contribute to the Parietal Leaflets of the Atrioventricular Valves in the Murine Heart', *Developmental Biology,* 366(2), 111-124.

Wharton, K. A., Johansen, K. M., Xu, T. and Artavanis-Tsakonas, S. (1985) 'Nucleotide sequence from the neurogenic locus Notch implies a gene product that shares homology with proteins containing EGF-like repeats', *Cell,* 43(3, Part 2), 567-581.

Wu, B., Wang, Y., Lui, W., Langworthy, M., Tompkins, K. L., Hatzopoulos, A. K., Baldwin, H. S. and Zhou, B. (2011) 'Nfatc1 coordinates valve endocardial cell lineage development required for heart valve formation', *Circ Res,* 109(2), 183-92.

Wu, B., Zhang, Z., Lui, W., Chen, X., Wang, Y., Chamberlain, A. A., Moreno-Rodriguez, R. A., Markwald, R. R., O'Rourke, B. P., Sharp, D. J., Zheng, D., Lenz, J., Baldwin, H. S., Chang, C. P. and Zhou, B. (2012) 'Endocardial cells form the coronary arteries by angiogenesis through myocardial-endocardial VEGF signaling', *Cell,* 151(5), 1083-96.

Wu, S.-P., Kao, C.-Y., Wang, L., Creighton, C. J., Yang, J., Donti, T. R., Harmancey, R., Vasquez, H. G., Graham, B. H., Bellen, H. J., Taegtmeyer, H., Chang, C.-P., Tsai, M.-J. and Tsai, S. Y. (2015) 'Increased COUP-TFII expression in adult hearts induces mitochondrial dysfunction resulting in heart failure', *Nature Communications,* 6, 8245.

Wu, S. P., Cheng, C. M., Lanz, R. B., Wang, T., Respress, J. L., Ather, S., Chen, W., Tsai, S. J., Wehrens, X. H., Tsai, M. J. and Tsai, S. Y. (2013) 'Atrial identity is determined by a COUP-TFII regulatory network', *Dev Cell,* 25(4), 417-26.

Yamamoto, S., Charng, W.-L., Rana, N. A., Kakuda, S., Jaiswal, M., Bayat, V., Xiong, B., Zhang, K., Sandoval, H., David, G., Wang, H., Haltiwanger, R. S. and Bellen, H. J. (2012) 'A Mutation in EGF Repeat-8 of Notch Discriminates Between Serrate/Jagged and Delta Family Ligands', *Science,* 338(6111), 1229-1232.

Yang, L.-T., Nichols, J. T., Yao, C., Manilay, J. O., Robey, E. A. and Weinmaster, G. (2005) 'Fringe Glycosyltransferases Differentially Modulate Notch1 Proteolysis Induced by Delta1 and Jagged1', *Molecular Biology of the Cell,* 16(2), 927-942.

Yang J, Bucker S, Jungblut B, Bottger T, Cinnamon Y, Tchorz J, Muller M, Bettler B, Harvey R, Sun QY, Schneider A, Braun T (2012) Inhibition of Notch2 by Numb/Numblike controls myocardial compaction in the heart. *Cardiovasc Res* 96: 276-85

Yashiro, K., Shiratori, H. and Hamada, H. (2007) 'Haemodynamics determined by a genetic programme govern asymmetric development of the aortic arch', *Nature,* 450(7167), 285-288.

You, L.-R., Lin, F.-J., Lee, C. T., DeMayo, F. J., Tsai, M.-J. and Tsai, S. Y. (2005) 'Suppression of Notch signalling by the COUP-TFII transcription factor regulates vein identity', *Nature,* 435(7038), 98-104.

Zhang, H., Pu, W., Li, G., Huang, X., He, L., Tian, X., Liu, Q., Zhang, L., Wu, S. M., Sucov, H. M. and Zhou, B. (2016a) 'Endocardium Minimally Contributes to Coronary Endothelium in the Embryonic Ventricular Free Walls', *Circ Res*.

Zhang, H., Pu, W., Tian, X., Huang, X., He, L., Liu, Q., Li, Y., Zhang, L., He, L., Liu, K., Gillich, A. and Zhou, B. (2016b) 'Genetic lineage tracing identifies endocardial origin of liver vasculature', *Nat Genet,* 48(5), 537-543.

# Bibliography

Zhang, H., Lui, K. O. and Zhou, B. (2018) 'Endocardial Cell Plasticity in Cardiac Development, Diseases and Regeneration', *Circulation Research,* 122(5), 774-789.

Zhang, J., Chu, L.-F., Hou, Z., Schwartz, M. P., Hacker, T., Vickerman, V., Swanson, S., Leng, N., Nguyen, B. K., Elwell, A., Bolin, J., Brown, M. E., Stewart, R., Burlingham, W. J., Murphy, W. L. and Thomson, J. A. (2017) 'Functional characterization of human pluripotent stem cell-derived arterial endothelial cells', *Proceedings of the National Academy of Sciences,* 114(30), E6072-E6078.

Zhou, B., Ma, Q., Rajagopal, S., Wu, S. M., Domian, I., Rivera-Feliciano, J., Jiang, D., von Gise, A., Ikeda, S., Chien, K. R. and Pu, W. T. (2008) 'Epicardial progenitors contribute to the cardiomyocyte lineage in the developing heart', *Nature,* 454, 109.

Zhou, B. and Pu, W. T. (2012) 'Genetic Cre-loxP assessment of epicardial cell fate using Wt1-driven Cre Alleles', *Circ Res,* 111(11), e276-e280.

# Supplementary information

**Supplementary Table 1.** Word file containing the lethality phases of *Jagged1;Nfatc1-Cre, Dll4;Nfatc1-Cre, Dll4;Cdh5-Cre, ManicFringeGof;Tie2-Cre, Efnb2;Nfatc1-Cre* embryos.

**Supplementary Table 2.** Excel file containing lists of differentially expressed genes identified after analysis of RNA-seq data, for contrasts between E12.5 *Jag1$^{flox}$;Nfatc1--Cre* (Jag1Nfatc1 211Deg); E12.5 *Dll4$^{flox}$;Nfatc1-Cre* (Dll4Nfatc1 274Deg); E16..5 *Dll4$^{flox}$;Cdh5-Cre* (Dll4Cdh5 163Deg); E15.5 *MFng$^{GOF}$;Tie2–Cre* (MfngT2 536-1928Deg); and E16.5 *Efrnb2 $^{flox}$*; *Nfatc1-Cre* (Efnb2Nfatc1 5Deg), and their control counterparts. For the comparison involving *Mfng$^{GOF}$;Tie2-Cre.,* differentially expressed genes were further filtered by requiring abs(logFC) > 0.5. Upregulated genes appear in red background and downregulated genes in blue.

**Supplementary Table 3.** Excel file describing results obtained with IPA for the sets of genes detected as differentially expressed (adjusted p_value < 0.05) in contrasts between *Jag1$^{flox}$;Nfatc1-Cre* (JAG1NF), *Dll4$^{flox}$;Nfatc1-Cre* (Dll4NF), *Dll4$^{flox}$;Cdh5-Cre$^{ERT2}$* (Dll4Cdh5) and *Mfng$^{GOF}$;Tie2-Cre* (MFT2) and their control counterparts. For the comparison between *Mfng$^{GOF}$;Tie2-Cre* and its control counterpart, differentially expressed genes were further filtered by requiring abs(logFC) > 0.5. Upstream Regulator analyses results, in sheets labelled as "UpRegTransc", are restricted to molecules of type "transcription regulator". For each predicted upstream regulator, tables describe expression log ratio (when available), predicted activation state, activation z-score, enrichment p_value and the collection of differentially expressed genes that are targets of the regulator. Downstream Effect analyses results, in sheets labelled as "CardSystDevFunc", are restricted to functions of category "Cardiovascular System Development and Function". For each functional term, tables describe enrichment p_value, predicted activation state, activation z-score and the collection of differentially expressed genes associated to that particular function. Positive and negative z-score values suggest activation or inhibition of the corresponding upstream regulator or function in the mutant or control condition, respectively; abs(z-score) > 2 and p_value < 0.05 are considered significant.

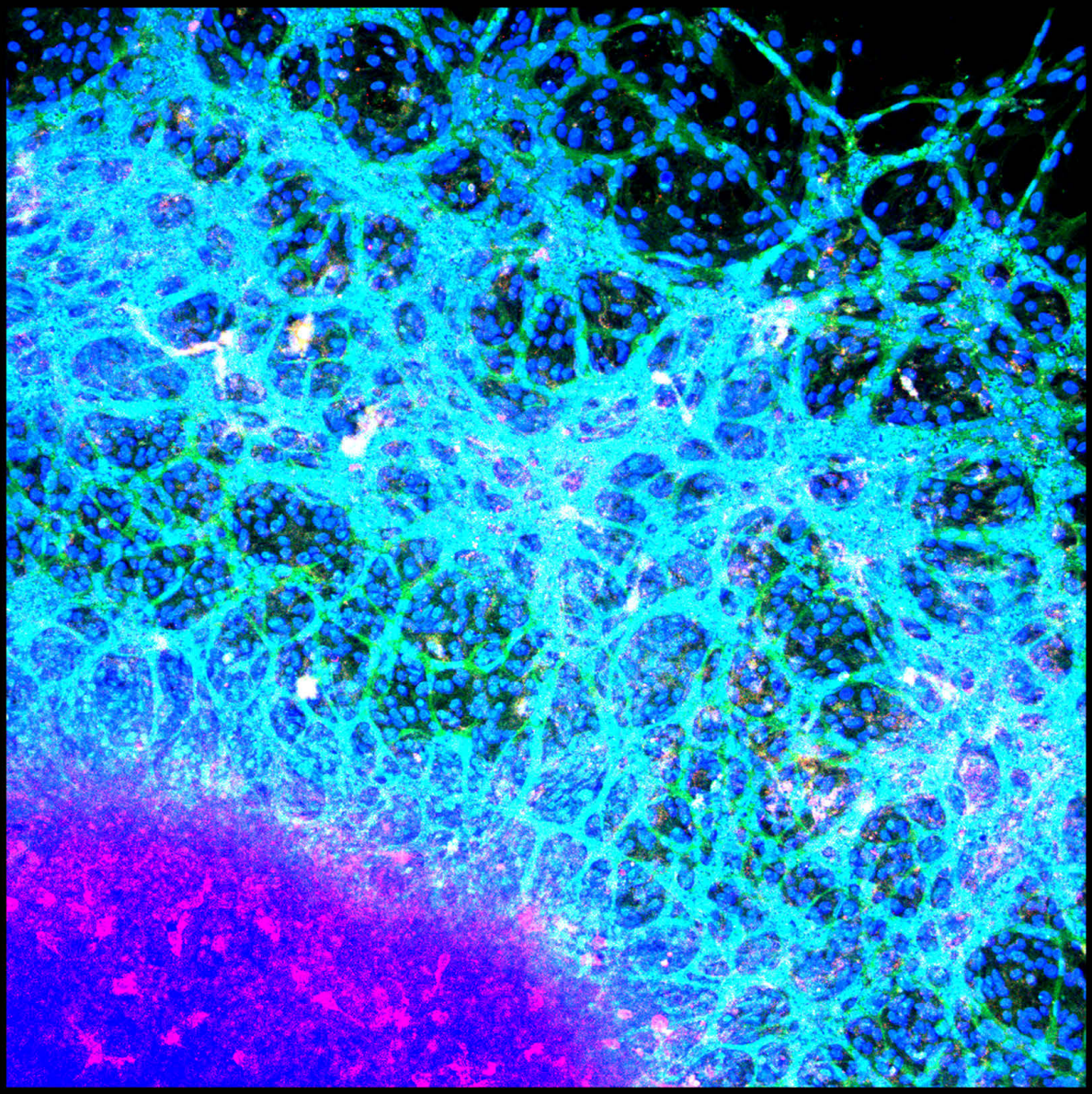
## Supplementary information

**Supplementary Table 4.** Excel file describing enriched gene sets identified with GSEA for the collections of genes detected as expressed in comparisons between *Jag1*$^{flox}$*;Nfatc1-Cre* (JAG1NF), *Dll4*$^{flox}$*;Nfatc1-Cre* (Dll4NF), *Dll4*$^{flox}$*;Cdh5-Cre*$^{ERT2}$ (Dll4Cdh5), *Mfng*$^{GOF}$*;Tie2-Cre* (MFT2), *Dll4*$^{GOF}$*;Tie2-Cre* (Dll4T2) and *Efnb2*$^{flox}$*;Nfatc1-Cre* (Efnb2NF) and their control counterparts. Analyses were performed against Hallmark (HM) and KEGG gene set databases. For each contrast and gene set, tables describe Normalized Enrichment Score (NES) and FDR q_value. Positive and negative NES values indicate congruent expression of gene set members in the mutant or control condition, respectively. FDR q_values < 0.25 are considered significant.

**Supplementary Table 5.** Excel file containing the statistics data source.

**Cover Page**. Whole-mount image of an E12.5 WT embryo showing N1ICD (red nuclei) expression in the Sinus Venosus subepicardial endothelial cells.

**Back Cover**. Mouse ventricular explant of a Dll4;Nfatc1mutant embryo showing increased number of transmural endothelial branches stained with Pecam1(green) and infected with a Lentivirus control (red).



UAM
UNIVERSIDAD AUTONOMA
DE MADRID

cnic